

Utah State University

DigitalCommons@USU

All Graduate Theses and Dissertations

Graduate Studies

8-2022

Pesticide-Leaf Interactions and Their Implications for Pesticide Fate Modeling

Ashlie Kinross
Utah State University

Follow this and additional works at: <https://digitalcommons.usu.edu/etd>



Part of the [Chemistry Commons](#)

Recommended Citation

Kinross, Ashlie, "Pesticide-Leaf Interactions and Their Implications for Pesticide Fate Modeling" (2022).
All Graduate Theses and Dissertations. 8597.
<https://digitalcommons.usu.edu/etd/8597>

This Dissertation is brought to you for free and open access by the Graduate Studies at DigitalCommons@USU. It has been accepted for inclusion in All Graduate Theses and Dissertations by an authorized administrator of DigitalCommons@USU. For more information, please contact digitalcommons@usu.edu.



PESTICIDE-LEAF INTERACTIONS AND THEIR IMPLICATIONS FOR PESTICIDE

FATE MODELING

by

Ashlie Kinross

A dissertation submitted in partial fulfillment
of the requirements for the degree

of

DOCTOR OF PHILOSOPHY

in

Chemistry

Approved:

Kimberly J. Hageman, Ph.D.
Major Professor

William J. Doucette, Ph.D.
Committee Member

Lisa M. Berreau, Ph.D.
Committee Member

Alvan C. Hengge, Ph.D.
Committee Member

Nicholas E. Dickenson, Ph.D.
Committee Member

D. Richard Cutler, Ph.D.
Vice Provost of Graduate Studies

UTAH STATE UNIVERSITY
Logan, Utah

2022

Copyright © Ashlie Kinross 2022

All Rights Reserved

ABSTRACT

Pesticide-Leaf Interactions and their Implications for Pesticide Fate Modeling

by

Ashlie Kinross, Doctor of Philosophy

Utah State University, 2022

Major Professor: Dr. Kimberly J. Hageman

Department: Chemistry and Biochemistry

Pesticides are often directly applied to plant material making it imperative that the interaction of the pesticide with the leaf is understood. Lab and field studies with pesticides applied to leaves can give insight into this interaction. The first analytical method necessary for either a lab or field study is the method for extracting pesticides from leaves.

This work introduces two extraction methods for two different instruments used to extract a suite of 20 pesticides from two different leaf types (alfalfa and citrus). Both extraction methods were shown to produce extracts that were colorless and had good recovery of pesticides.

After establishing a reliable extraction method, lab studies were conducted to investigate the equilibrium between the leaf surface and air for a pesticide after application. This equilibrium is described using the leaf-air partition coefficient ($K_{\text{leaf-air}}$). In this work, we used chlorpyrifos as both the active ingredient alone as well as in a formulation. The $K_{\text{leaf-air}}$ for the active ingredient decreased with temperature. The formulation showed the same behavior but was less sensitive to temperature changes.

Another process that was studied due to the impact it could have on volatilization was foliar penetration. Foliar penetration was shown to increase with temperature for both the active ingredient alone as well as the formulation. Therefore, temperature both increases the volatilization as well as the foliar penetration, but the extent to which each process was affected by temperature was different for the active ingredient alone compared to the formulation.

Using the newly measured $K_{\text{leaf-air}}$ values, a pesticide fate model was improved and used to predict pesticide behavior for six field dissipation studies conducted with chlorpyrifos and λ -cyhalothrin. Measured foliar photodegradation rates were also incorporated into the model to optimize the predicted pesticide concentration in leaves over longer periods of time after application compared to previous work. The optimized prediction of leaf concentration was used to conduct a risk assessment for honeybees for a seven-day period after pesticide application to determine when pesticide levels exposed honeybees to the concentration equivalent to the lethal dose to 50% of the population (LD_{50}).

PUBLIC ABSTRACT

Pesticide-Leaf Interactions and their Implications for Pesticide Fate Modeling

Ashlie Kinross, Doctor of Philosophy

The work described here provides measured data to improve the understanding of the interaction between a pesticide and leaf surface after application. Two methods were developed, one using a newly introduced instrument, for the extraction of pesticides from leaves. This is required to measure the concentration of pesticide in the leaves. Using one of the developed extraction methods, measurements were made to determine how a pesticide equilibrates between a leaf and the air above it. These measurements were incorporated into a pesticide fate model that predicts how a pesticide moves through the environment after application to an agricultural field. The updated fate model was used to predict the danger the pesticide posed to honeybees.

ACKNOWLEDGMENTS

First and foremost, I would like to thank Dr. Kimberly Hageman for her guidance, support, and enthusiasm throughout my PhD program. I don't know how I would have survived without your continuous encouragement. I couldn't have asked for a better supervisor, so thank you!

I would like to thank Dr. William Doucette for allowing me to use the EDGE in your lab as well as other equipment used in the fugacity meter setup. Thank you and your students for giving me instrument training and instrument use time.

To my other committee members, Dr. Lisa Berreau, Dr. Alvan Hengge, and Dr. Nicholas Dickenson, thank you for pushing me to be a better chemist throughout my degree. I would also like to thank you for the valuable feedback on projects during my PhD degree. Thank you to Dr. Randa Jabbour, Dr. Ricardo Ramirez, Dr. Scott Bernhardt, and Dr. Theresa Pitts-Singer for sharing your expertise in pesticide use, pests, toxicology, and bees. I also appreciate all the help with my last two projects, especially the insights you shared about how my work could be used by farmers and regulators. I truly appreciate your enthusiasm and support.

Thank you to the members of the Hageman lab group, Calvin, Sean, Jeffrey, Samantha, Alexandria, Anna, and Shan, for your friendship and assistance. All of you helped me keep my sanity throughout my PhD.

Thank you to Buckley Banham for being willing to take on any project I brought to you and going above and beyond to improve on the ideas. Thank you to Cindy Weatbrook in the Chemistry and Biochemistry department office for helping make sure I was completing all things necessary for my degree as well as for your friendship.

Thank you to Dr. Doug Harris, Dr. Shawn Miller, Rob Alumbaugh, and Dr. Bob Brown for your guidance and your shared insight about teaching while I was a teaching assistant. I loved my time teaching, which was largely due to your efforts.

To my family, thank you for the continuous support. Without all of you I wouldn't even have started this journey, let alone be finishing it now. To my husband Carson, thank you for your constant support throughout my PhD and for the confidence you had in me that I would be able to complete this, especially when I wasn't confident in myself. Thanks to all of you for listening to all my ramblings and frustrations about my projects and always offering encouragement.

Ashlie Kinross

CONTENTS

	Page
Abstract	iii
Public Abstract.....	v
Acknowledgments.....	vi
Contents	viii
List of Tables	xii
List of Figures.....	xiii
List of Abbreviations	xv
Chapter 1. Introduction	1
1.1 Introduction to Pesticides.....	1
1.2 Extraction Methods for Organic Contaminants in Environmental Matrices:	3
1.3 Leaf-Air Partitioning and Foliar Penetration	7
1.4 Environmental Modeling and Pollinator Risk Assessment	10
1.5 Project Objectives	12
Chapter 2. Comparison of Accelerated Solvent Extraction (ASE) and Energized Dispersive Guided Extraction (EDGE) for the Analysis of Pesticides in Leaves	14
2.1 Introduction:.....	15
2.2 Materials and Methods:.....	17
2.2.1 Strategy Overview	17

2.2.2 Materials, Chemicals, and Standards	18
2.2.3 Leaf Collection and Preparation	19
2.2.4 Lipid Mass Determination	20
2.2.5 UV-Visible Spectra of the Leaf Extracts	21
2.2.6 Spike and Recovery Experiments	22
2.2.7 ASE Methods	23
2.2.8 EDGE Methods	23
2.2.9 Comparison of Pesticide Concentrations in Field Samples	24
2.2.10 Quantification of Pesticides in Leaf Extracts by GC-MS/MS	24
2.2.11 Quality Assurance	26
2.2.12 Statistical Analysis	27
2.3 Results and Discussion:	27
2.3.1 Optimizing the Layered ASE Method	27
2.3.2 Extracted Lipid Masses and Extract Color	29
2.3.3 UV-Visible Spectra of the Leaf Extracts	31
2.3.4 Spike and Recovery Results	34
2.3.5 Pesticide Concentrations in Field Samples	38
2.3.6 Method Parameter Comparison	39
2.4 Conclusion	40

Chapter 3. Investigating the Effects of Temperature, Relative Humidity, Leaf Collection Date, and Foliar Penetration on Leaf-Air Partitioning.....	42
3.1 Introduction.....	43
3.2 Materials and Methods.....	46
3.2.1 Materials and Chemicals.....	46
3.2.2 Application of Chlorpyrifos to Leaves	48
3.2.3 Measurement of $K_{\text{leaf-air}}$ Values.....	51
3.2.4 Measuring Foliar Penetration.....	54
3.2.5 Chlorpyrifos Quantification.....	55
3.2.6 Statistical Methods.....	56
3.3 Results and Discussion	56
3.3.1 Influence of Temperature on $K_{\text{leaf-air}}$ Values	56
3.3.2 Influence of Temperature on Foliar Penetration.....	60
3.3.3 Influence of Relative Humidity on $K_{\text{leaf-air}}$ and Foliar Penetration	62
3.3.4 Influence of Leaf Collection Date on $K_{\text{leaf-air}}$ and Foliar Penetration	64
3.3.5 Comparison of Measured to Predicted $K_{\text{leaf-air}}$ Values.....	66
3.3.6 Influence of Foliar Penetration on $K_{\text{leaf-air}}$ Values.....	69
Chapter 4. Optimizing a Pesticide Fate Model Using Field Dissipation Studies to Predict Honeybee Exposure.....	71
4.1 Introduction.....	72

4.2 Materials and Methods.....	74
4.2.1 Materials	74
4.2.2 Foliar Photodegradation Studies	76
4.2.3 Field Dissipation Studies	83
4.2.4 Honeybee Risk Assessment	86
4.3 Results and Discussion	88
4.3.1 Foliar Photodegradation Studies	88
4.3.2 Field Dissipation Studies and Model Optimization	90
4.3.3 Honeybee Risk Quotients	98
Chapter 5. Conclusion.....	102
5.1 General Conclusions	102
5.2 Future Recommendations	107
References.....	110
Appendix.....	127
Curriculum Vitae	151

LIST OF TABLES

	Page
Table 2.1	List of the compound class of each pesticide studied.....19
Table 2.2	Target analyte retention times and selected reaction monitoring (SRM) transitions.....25
Table 2.3	Comparison of extraction parameters for both the ASE and the EDGE. Extraction data from the Layered ASE and Layered EDGE methods using alfalfa leaves were used for this comparison.....39
Table 3.1	Summary of predictive $K_{\text{leaf-air}}$ equations from previous studies.....44
Table 3.2	Chemical structure and properties of chlorpyrifos.....47
Table 3.3	GC-MS/MS SRM transition ions used for quantification of d10-chlorpyrifos and chlorpyrifos.....56
Table 3.4	Model inputs used to compare measured and predicted $K_{\text{leaf-air}}$ values...65
Table 4.1	Chemical properties of active ingredients used.....77
Table 4.2	Chemical structures of the active ingredients used.....78
Table 4.3	Pesticide formulation information.....78
Table 4.4	Foliar photodegradation application rates based on formulation label...80
Table 4.5	GC-MS/MS SIM and SRM transition ions.....84
Table 4.6	Details for the chlorpyrifos field dissipation trials and PeDAL model input values.....85
Table 4.7	Details for the λ -cyhalothrin field dissipation trials and PeDAL model input values.....86
Table 4.8	Leaf sampling times for each case study.....86
Table 4.9	Pseudo-first order foliar photodegradation rates for λ -cyhalothrin and indoxacarb on alfalfa leaves with 95% confidence intervals.....90
Table 4.10	CPL ₂₄ and DT ₅₀ calculated using both the predicted concentrations and the measured chlorpyrifos concentrations.....95
Table 4.11	CPL ₂₄ and DT ₅₀ calculated using both the predicted concentrations and the measured λ -cyhalothrin concentrations.....99
Table 4.12	Leaf concentration seven days after pesticide application and the time when the risk quotient equals one when using predicted leaf concentrations from the PeDAL model as well as the measured leaf concentrations.....101

LIST OF FIGURES

	Page
Figure 2.1	UV-Vis spectra for two different samples extracted the same way.....21
Figure 2.2	UV-Vis spectra for samples that were ran on different days to check the instrument consistency.....22
Figure 2.3	Photos of alfalfa extracts from the ASE.....27
Figure 2.4	Comparison of the lipid mass extracted for each step of the method development process for 0.5 g alfalfa leaves on the ASE.....27
Figure 2.5	Comparison of the percent recoveries from alfalfa leaves using both the Layered ASE and Layered EDGE methods.....29
Figure 2.6	Lipid mass and residual lipid mass extracted for each extraction method when using no sorbents and when using the Layered ASE, Mixed ASE, Layered EDGE, and Mixed EDGE methods.....30
Figure 2.7	UV-Vis absorbance spectra for extracts from each method.....33
Figure 2.8	Comparison of the average percent recoveries when taking all compounds into account when using the Layered ASE, Mixed ASE, Layered EDGE, and Mixed EDGE methods.....34
Figure 2.9	Comparison of the percent recoveries with each method.....36
Figure 2.10	Compounds that have a significantly different percent recovery when comparing different extraction methods and leaf types.....37
Figure 2.11	Pesticide field concentration for each extraction method38
Figure 3.1	Schematic diagram of the solid-phase fugacity meter.....50
Figure 3.2	Photograph of inside the solid-phase fugacity meter.....50
Figure 3.3	Equilibrium testing for chlorpyrifos using a flow rate of ~65 mL/min...51
Figure 3.4	Measured $\log K_{\text{leaf-air}}$ values over a range of temperatures.....57
Figure 3.5	Measured $\log K_{\text{leaf-air}}$ values over a range of temperatures.....58
Figure 3.6	Mean percent of insecticide measured in each of the three leaf layers extracted at the end of 16-h tests conducted at five temperatures.....60
Figure 3.7	Percent in the ethanol-extractable layer over a range of temperatures....60
Figure 3.8	Measured $\log K_{\text{leaf-air}}$ values at different relative humidity conditions....62
Figure 3.9	Mean percent of insecticide measured in each of the three leaf layers extracted at the end of 16-h tests conducted at four different relative humidity levels.....63
Figure 3.10	Measured $\log K_{\text{leaf-air}}$ values measured from leaves collected in different months in 2020 for experiments conducted at 10 and 25 °C.....63
Figure 3.11	Foliar penetration data from leaves collected in different months in 2020 with experiments conducted at 10 and 25 °C.....66

Figure 3.12	Comparison of our measured alfalfa $\log K_{\text{leaf-air}}$ values at 10 and 25 °C for chlorpyrifos compared to predicted $\log K_{\text{leaf-air}}$ values for other plant species.....	67
Figure 4.1	Alfalfa leaf setup for photodegradation experiments.....	79
Figure 4.2	Light spectrum produced by the Atlas SunTest CPS+ solar simulator...	81
Figure 4.3	Foliar photodegradation of each compound on alfalfa leaves.....	89
Figure 4.4	Predicted and measured chlorpyrifos concentrations in leaves for each trial.....	92
Figure 4.5	Predicted and measured chlorpyrifos concentrations in leaves for each trial after modifying the PeDAL model.....	94
Figure 4.6	Predicted and measured λ -cyhalothrin concentrations in leaves for each trial.....	96
Figure 4.7	Predicted and measured λ -cyhalothrin concentrations in leaves for each trial after modifying the PeDAL model.....	97
Figure 4.8	Risk quotients over time based on the predicted plant concentration...	100

LIST OF ABBREVIATIONS

Abbreviation	Definition
ASE	Accelerated Solvent Extraction
CPL ₂₄	Cumulative Percentage Lost in 24 Hours from Plants
DCM	Dichloromethane
DCPA	Dimethyl tetrachloroterephthalate
DE	Diatomaceous Earth
dSPE	Dispersive Solid Phase Extraction
DT ₅₀	Time to Reach 50% of the Initial Plant Concentration in Days
ECOTOX	Ecotoxicology Knowledgebase
EDGE	Energized Dispersive Guided Extraction
EI	Electron Ionization
GC	Gas Chromatography
GCB	Graphitized Carbon Black
$\Delta H_{i,\text{leaf-air}}$	Change in Enthalpy for the Transfer from Leaf to Gas Phase
HCH	Hexachlorohexane
$K_{\text{leaf-air}}$	Leaf-air Partition Coefficient
$K_{\text{octanol-air}}$	Octanol-air Partition Coefficient
$K_{\text{plant-air}}$	Plant-air Partition Coefficient
$K_{\text{soil-air}}$	Soil-air Partition Coefficient
$K_{\text{water-air}}$	Water-air Partition Coefficient
LD ₅₀	Lethal Dose for 50% of the Population
$\Delta_{\text{leaf-air}}U$	Change in Internal Energy for the Transfer from Leaf to Gas Phase
MS	Mass Spectrometer
MSPD	Matrix Solid-Phase Dispersion
<i>o,p'</i> -DDD and <i>p,p'</i> -DDD	Dichlorodiphenyldichloroethane
<i>o,p'</i> -DDE and <i>p,p'</i> -DDE	Dichlorodiphenyldichloroethylene
<i>o,p'</i> -DDT and <i>p,p'</i> -DDT	Dichlorodiphenyltrichloroethane
PCB	Polychlorinated biphenyl
PDMS	Polydimethylsiloxane
PeDAL	Pesticide Dissipation from Agricultural Lands
PLE	Pressurized Liquid Extraction
PLoVo	Pesticide Loss via Volatilization
PNA	<i>p</i> -nitroanisole
PPDB	Pesticide Properties Database
QuEChERS	Quick, Easy, Cheap, Effective, Rugged and Safe
RQ	Risk Quotient
SIM	Single Ion Monitoring
SPLE	Selective Pressurized Liquid Extraction
SRM	Selective Reaction Monitoring

Chapter 1. Introduction

1.1 Introduction to Pesticides

Pesticides (including insecticides, herbicides, fungicides, etc.) are classified as chemicals that either kill, obstruct, or manage the growth of an organism. Worldwide pesticide usage was estimated to be up to 3.5 million tons in 2020.¹ Pesticides are critical in the public health sector to help control infectious diseases such as dengue fever, yellow fever, zika, malaria, trypanosomiasis, and leishmaniasis, which are transmitted by insects.^{1,2} Due to the lack of efficient pharmacological treatments for these diseases, the most successful method in reducing the disease transmission is controlling the transmission vectors.³ Pesticides are also necessary for the agricultural industry. Because pesticides protect crops against weeds, insects, and disease they can help farmers increase the amount of harvestable produce. The estimated economic return of pesticide use in the USA was ~\$16 billion in 1992, and that value has likely increased since then.⁴ Herbicides are the most used type of pesticide (~50% of all crop protection chemicals) used throughout the world. Without herbicides, it is estimated that there would be a \$13-21 billion loss annually in farm income in the US.⁴

Pesticides can be classified based on their target organism, their modes of action, or their chemical structure.^{1,5,6} A common mode of action for insecticides is inhibiting cholinesterase enzymes such as acetylcholinesterase.^{1,5,7,8} The inhibition of acetylcholinesterase leads to an accumulation of acetylcholine. Because acetylcholine is found throughout the body in the neuromuscular and skeletal muscle intersections, a buildup can lead to the malfunction of respiration and muscle tissue of the heart, leading

to death.^{5,7} Many organisms can be affected by this mode of action including mammals, birds, fish and insects.⁵

While pesticide use is necessary, these compounds can be toxic to non-target organisms including beneficial insects such as pollinators.⁶ In honeybees, exposure to pesticides can happen at different times based on the bee's role in the hive. The forager bees, that collect pollen from a field, are exposed to pesticide through interacting with the plants when they collect pollen and nectar. Bees that remain in the hive, though, are exposed when contaminated pollen and nectar are brought back into the hive. This can cause mass death of the hive, referred to as "colony collapse disorder".⁶ While insect toxicity has been studied in the lab to find the lethal dose for 50% of the population (LD₅₀), more work is needed to determine the risk that bees pollinating a field are exposed to and how to minimize the exposure.

The first step to studying pesticides in the plant system is extraction. A high-recovery method is required to study pesticides at low concentrations in the environment. The development and comparison of two extraction methods, one method developed for a newly introduced extraction instrument, used to extract a suite of pesticides from two different leaf types are discussed in Chapter 2. Once the extraction method is developed, experiments can be conducted to understand environmental processes that pesticides experience after application to a field. Two important processes that influences pesticide fate after field application is volatilization and foliar penetration. Volatilization of a pesticide is affected by the intermolecular interactions of the pesticide with the leaf surface, which can be described using the leaf-air partition coefficient. If a pesticide penetrates the leaf, though, it is likely unavailable for partitioning between the air and

leaf surface. Chapter 3 discusses the measurement of both leaf-air partitioning and foliar penetration for the pesticide chlorpyrifos at different temperatures and humidities. Leaf-air partitioning is of importance because this is a parameter used in several pesticide fate models. One previously developed model is the Pesticide Dissipation from Agricultural Lands (PeDAL) model.⁹ In chapter 4, the PeDAL model was improved by incorporating the measured leaf-air partition coefficients model and evaluated with six field dissipation studies. Chapter 4 discusses the optimization of the model and how it was used to complete a risk assessment for honeybees for a week after pesticide application for the six field studies.

1.2 Extraction Methods for Organic Contaminants in Environmental

Matrices:

The first step in studying contaminants of interest in the environment is extraction of the contaminants from environmental matrices. Extraction is required to remove the compounds of interest from the environmental matrices of the sample. There are several different extraction methods previously developed for the extraction of pesticides from plants including Soxhlet,¹⁰⁻¹³ the Quick, Easy, Cheap, Effective, Rugged and Safe (QuEChERS) method,^{11,13-15} Matrix Solid-Phase Dispersion (MSPD),^{11,14,16,17} Pressurized Liquid Extraction (PLE),^{10-14,16,18} and Selective PLE (SPLE).^{16,18} However, these methods often have disadvantages.

Soxhlet extraction was introduced in the mid-nineteenth century and is still a benchmark method for extraction of solid samples. In this method a sample is placed in a thimble-holder that is filled with condensed solvent in a distillation flask. This solvent fills the thimble-holder until an overflow level is reached, at which point a siphon

aspirates the solute from the thimble-holder back into the bottom of a distillation flask, taking the extracted analytes with it into the bulk liquid. The bulk liquid is continually heated, leading to continuous evaporation, condensation, and extraction of the solvent.¹⁹ This is a simple technique to use, but the main disadvantages are that the extraction often takes a long time (minimum extraction time is generally 8 h) and it requires more solvent than other methods (50-300 mL).

QuEChERS is a sample preparation approach based on the dispersion of salts to extract (salting-out effect), isolate a wide range of analytes from complex matrices in addition to the cleanup of the extract. It was originally developed to extract pesticide residues from fruit and vegetables. This extraction method utilizes the salting-out effect, which promotes transfer of the analytes of interest out of the aqueous layer and into the organic layer. In this step a homogenized sample is added to a test tube along with salt and solvent. The test tube is then vortexed and centrifuged. Next, dispersive Solid Phase Extraction (dSPE) is used to further cleanup the extract. dSPE is carried out by adding sorbents and salts directly to the sample, vortexing the samples, and then centrifuging the sample to separate the analytes of interest and the matrix compounds that would interfere with the analysis.^{20,21} A downfall of this method is that the sample cleanup often requires several different sorbents, all completed in separate steps. This can increase the time and materials required for sample preparation.

MSPD extraction is a simple extraction/cleanup procedure. First, the sample matrix is mixed with sorbent material using a mortar and pestle. After thorough mixing, the sample/sorbent mixture is packed into a column, that is then eluted with a relatively small amount of the appropriate solvent. These columns can also have extra sorbents

packed at the bottom, below the sample/sorbent mixture, to better remove matrix interferences.¹¹ While this procedure is simple and uses small amounts of solvent, this process cannot be automated so it is still a time-consuming process to prepare samples for analysis.

PLE and SPLE are conducted using an instrument called an Accelerated Solvent Extractor (ASE), which has led to the using ASE and PLE synonymously, but it is important to note that PLE and SPLE refer to the method used. In PLE, solid samples are packed into stainless steel extraction cells. Cells are then transferred into an oven where solvent is pumped into the cell and the cell is heated (40-200 °C). Because the system is closed, the solvent remains in the liquid phase while the pressure is maintained at a set value (typically 1500 psi) using a pressure transducer and static valve. The elevated temperatures and pressures in the extraction cell help increase the efficiency of the extraction by causing the solvent to better penetrate the sample matrix. After a specified hold time the solvent and extracted analytes are transferred to a collection bottle. The difference between SPLE and PLE is that SPLE uses sorbents in the extraction cell to retain the matrix material, so no further sample cleanup is required after extraction.^{18,22} SPLE has several advantages compared to other methods. First, SPLE carries out extraction and sample cleanup in one step, reducing the steps required for sample preparation. This method also uses relatively small amounts of solvent (~30 mL), and it requires less time to extract samples (less than an hour per sample) than other methods. The ASE instrument is automated so it will extract one sample and continue to the next sample automatically, further simplifying this method.

Even with several extraction methods previously developed, sample preparation is still often the source of a bottleneck in sample analysis so new methods are still being developed. The Energized Dispersive Guided Extraction (EDGE) system was recently introduced (late 2017). This instrument was developed to combine PLE with dSPE. In EDGE, sample cells are packed with the sample matrix and sorbents. The instrument moves the sample cell into an oven that is sealed. Solvent is added to cell and is heated (creating a small buildup of pressure due to heating a sealed system). Heating the cell results in solvent being pumped into the extraction cell, mixing the sorbent and matrix together. The solvent is held in the cell for a specified hold time, allowing analytes to partition into the solvent. After this, solvent and extracted analytes are transferred to a collection bottle.^{23,24}

While the EDGE has several advantages (relatively small volume of solvent required, less time required to extract samples, and it is automated), this method has not been compared to previously used, trusted methods by anyone outside of CEM. A comparison is necessary to better understand the benefits as well as any disadvantages in using a new extraction instrument. It is also important to determine if the methods that were previously developed for use with other extraction methods are transferable for use with the EDGE or if new extraction parameters will need to be tested and verified.

Chapter 2 describes the comparison of a SPLE method using the ASE instrument to an extraction method using the EDGE instrument. This chapter is a modified version of my first-author publication in *Journal of Chromatography A*.²⁵ Modifications were made to include data from the Supplemental Information. This paper had three co-authors. Dr. Kimberly J. Hageman and Dr. William J. Doucette contributed by providing

feedback on experimental design and manuscript. Alexandria L. Foster contributed as a lab assistant.

1.3 Leaf-Air Partitioning and Foliar Penetration

For many pesticides, the main dissipation process is volatilization from the plant after application. If we hope to accurately predict how a pesticide is moving through an environment, understanding this process is critical. Pesticide volatilization from the leaf surface can be described using the leaf-air partition coefficient ($K_{\text{leaf-air}}$). The $K_{\text{leaf-air}}$ is the ratio of the concentration of the chemical of interest on the leaf to the concentration in the air at equilibrium. This property is dependent on the chemical properties as well as the intermolecular interactions of the chemical of interest with the leaf. There have been previous studies that have measured plant-air partition coefficients ($K_{\text{plant-air}}$) and $K_{\text{leaf-air}}$ values using a variety of methods.²⁶⁻³¹ We will refer to all of the measured values as $K_{\text{leaf-air}}$ values to simplify the discussion.

Nizzetto et al.²⁶ used field sampling of tree leaves and air to calculate the $K_{\text{leaf-air}}$ values. However, measuring an equilibrium value in the field is difficult because the conditions are not controlled and can change rapidly. In fact, Nizzetto et al.'s work shows that for large molecular weight compounds a leaf-air equilibrium was not reached during the growing season in which samples were collected.²⁶ Due to the complications of measuring $K_{\text{leaf-air}}$ values in the field, most studies are conducted in the lab. Bacci and Gaggi³¹ and Bacci et al.³⁰ measured $K_{\text{leaf-air}}$ values by placing potted azalea plants in a 200-L greenhouse along with trays of sand that had been contaminated with the compounds of interest. Air and plant samples were taken periodically and the concentration in each were used to calculate the $K_{\text{leaf-air}}$ during both an uptake of the

chemical of interest as well as a release phase. However, because this study used a whole plant there were other possible processes that could both increase and decrease the pesticide concentration in the leaf such as translocation through the plant as well as degradation of the compound by plant metabolism. Bolinius et al.²⁹ simplified the setup and measured $K_{\text{leaf-air}}$ values using small leaf disks (18 mm in diameter) that were sandwiched between polydimethylsiloxane (PDMS) disks that were contaminated with polychlorinated biphenyls (PCBs). The leaf-PDMS partition coefficient was calculated, and then using PDMS-air partition coefficients from the literature, this value was converted to $K_{\text{leaf-air}}$ values. The downfall of this study, however, is that it uses leaves that were cut. Cutting the leaves exposes the sides of the leaf so partitioning could occur through the sides rather than the cuticle of the plant, which is often considered the penetration barrier. This likely affected the measured leaf concentration, which would affect the calculated $K_{\text{leaf-air}}$ value. Kömp and McLachlan^{27,28} developed the solid-phase fugacity meter to use for measuring $K_{\text{leaf-air}}$ values. This setup starts with placing plant material in a glass column and then an air stream is passed over the plant material slowly to allow for an equilibrium between the vegetation and air to be reached. After passing through the glass column containing the plants the air travels through a sorbent trap to collect the air-phase contaminants. The plant and air concentrations were used to calculate $K_{\text{leaf-air}}$ values. Having the glass column containing all the vegetation allows for control of the temperature of the system so comparisons of $K_{\text{leaf-air}}$ values at different temperatures can be achieved. This method allows the use of whole leaves to get accurate $K_{\text{leaf-air}}$ values. Also, in this system equilibrium between the leaves and air can be

confirmed by repeating the experiments using different experiment run times or flow rates and comparing the results.

While $K_{\text{leaf-air}}$ values have been measured previously, much of the work considers whole leaf concentrations when calculating the $K_{\text{leaf-air}}$ values. While this approach likely gives the most useful values for environmental modeling because then the whole leaf can be described, which is what is present in the environment, it may not accurately be describing the mechanism for partitioning. This is because after pesticide application to a leaf, the pesticide can penetrate deeper into the leaf, making it unavailable for volatilization. Pesticide foliar penetration is thought to primarily be a diffusion process through the cuticular membrane. That leads to this process being molecule size dependent, with smaller compounds having higher diffusion rates.³²⁻³⁵ Foliar penetration also is affected by the cuticle waxes that make up the membrane, which makes this process plant-specific.^{32,33,36} Diffusion increases with temperature.^{32,34,35,37,38} The increase in diffusion with temperature is due to more movement of the cuticular waxes, which leads to more ‘holes’ that compounds can travel through to reach the deeper layers of the leaf. Because penetration is chemical-, plant-, and condition-specific more work is needed to understand this process and evaluate how this process affects volatilization of the compounds.

Chapter 3 describes the measurement of $K_{\text{leaf-air}}$ values and foliar penetration of the pesticide chlorpyrifos after application to alfalfa leaves at different temperatures and humidities using a solid-phase fugacity meter. Chlorpyrifos was studied as both the active ingredient alone as well as in the formulation mix. This chapter is modified from my first-author manuscript that has been submitted to the journal *Environmental Science &*

Technology. This manuscript has two co-authors. Dr. Kimberly J. Hageman contributed by providing feedback on experimental design and the manuscript. Calvin Luu contributed as a lab assistant.

1.4 Environmental Modeling and Pollinator Risk Assessment

After application of pesticide to an agricultural field, the pesticide goes through several processes to dissipate from the field. These processes include volatilization, photodegradation, microbial degradation, and water wash-off. Due to the concern of pesticide exposure to non-target organisms as well as a desire to predict effectiveness of a pesticide over time, predicting pesticide fate is an important area of research. Increasing the number of accurately modeled processes allows for not only a better mechanistic understanding of pesticide dissipation, but also more accurate predictions.

Several versions of a pesticide model have previously been developed in the Hageman lab including: a model predicting pesticide loss from bare soils,³⁹ the Pesticide Loss via Volatilization (PLoVo) model,⁴⁰ and the PeDAL model.⁹ The model predicting pesticide loss from bare soils predicted the volatilization from a system in which pesticide was applied to bare soil and compared different methods to predict loss. This study found that predicting loss through the soil-air and water-air partition coefficients ($K_{\text{soil-air}}$ and $K_{\text{water-air}}$) most accurately depicted the processes when comparing the results to literature-reported data. The PLoVo model improved on the bare soil model by considering pesticide volatilization from plant material as well. This model predicted pesticide fate based on volatilization from leaves and volatilization from soils. Volatilization from each matrix was predicted by the $K_{\text{water-air}}$, $K_{\text{soil-air}}$, and $K_{\text{leaf-air}}$. The $K_{\text{leaf-air}}$ values were calculated using an equation relating the octanol-air partition

coefficient ($K_{\text{octanol-air}}$) to the $K_{\text{leaf-air}}$ that had been previously developed from studies with PCBs. Because this equation was based on work conducted with PCBs instead of pesticides, it is unclear whether it accurately predicts the $K_{\text{leaf-air}}$ for pesticides.⁴⁰ The PeDAL model improved the PLoVo model by adding more processes to the model including foliar photodegradation and foliar penetration. However, the model only incorporated 15 foliar photodegradation rates for pesticides because these were the only available data in the literature. The penetration rate was set at a generic value of 0.002 h^{-1} , even though this process is likely chemical-, plant-, and condition specific. Therefore, more measured $K_{\text{leaf-air}}$ values using pesticides are needed along with more measured pesticide foliar photodegradation rates and more work investigating pesticide foliar penetration to improve the current model.

Pesticide fate modeling is critical to accurately assess risks to non-target organisms. Bees are of particular interest in risk assessment due to their critical role in pollinating crops. A specific pesticide is ranked as high, medium, or low concern to bees based on the toxicity threshold LD_{50} . However, this generic grouping does not consider bee behavior or difference in pesticide concentration in a field based on application details. In addition to this complication, the LD_{50} values are measured for two exposure routes: contact or oral. In a field, though, a bee that is pollinating flowers is exposed through both exposure routes simultaneously, so both need to be considered. Assessing risk to bees based on the actual field concentrations is of utmost importance, especially for farmers that manage bees and actively bring them to a field to pollinate their crops. If a farmer brings bees too early, not only will the bees die, but the crop will not be pollinated and there will be less harvestable crop.

Chapter 4 describes the measurement of foliar photodegradation rates and their incorporation into the PeDAL model along with the measured $K_{\text{leaf-air}}$ values from chapter 3. The PeDAL model was evaluated by comparing modeled to measured pesticide concentration in leaves for six field studies, optimized, and then this optimized model was used to predict the risk exposure for honeybees. This chapter is written in the format of a journal article that will be submitted to the journal *Agricultural Science & Technology*. This manuscript has four co-authors. Sean Lyons completed the photodegradation studies and some of the field work. Dr. Kimberly J. Hageman provided feedback on the experimental design and the manuscript. Micah McClure contributed by taking field samples in two of the dissipation studies. Dr. Randa Jabbour contributed by providing feedback on experimental design and the manuscript.

1.5 Project Objectives

The overall goal of this work was to gain a better understanding of pesticide interactions with leaves and then use this knowledge to improve modeling to allow for more accurate risk assessments to honeybees. The specific objectives for each project were:

- 1) Optimize and validate an SPLE method using the ASE instrument for the extraction of a suite of 20 semi-volatile pesticides from citrus and alfalfa leaves. Modify this optimized ASE method for use with the EDGE instrument and to compare the performance of the two instruments in terms of extract color and extracted lipid mass, recovery of spiked target pesticides, pesticide concentrations in field samples, and other extraction parameters. These comparisons were made for both instruments when sorbents were placed in the extraction cells in both a layered and mixed manner (Chapter 2).

- 2) Quantify the effects of formulation, temperature, humidity, and leaf collection date on leaf-air partitioning and foliar penetration for an example pesticide-plant combination. Use this data to better understand the link between foliar penetration and leaf-air partitioning (Chapter 3).
- 3) Obtain foliar photodegradation rates for three insecticides (as the active ingredient alone as well as in a formulation) commonly used with alfalfa. Conduct field studies designed to investigate effects of weather conditions and application timing on dissipation rates of chlorpyrifos and λ -cyhalothrin. Optimize the PeDAL model for predicting foliar pesticide concentrations during a one-week period following the pesticide application. Predict how field-based pesticide risk quotients change over time after pesticide application (Chapter 4).

Chapter 2. Comparison of Accelerated Solvent Extraction (ASE) and Energized Dispersive Guided Extraction (EDGE) for the Analysis of Pesticides in Leaves

The content of this chapter has been published in Journal of Chromatography A: Ashlie D. Kinross, Kimberly J. Hageman, William J. Doucette, Alexandria L. Foster.

Comparison of Accelerated Solvent Extraction (ASE) and Energized Dispersive Guided Extraction (EDGE) for the Analysis of Pesticides in Leaves. *J. Chromatogr. A*. 1627 (2020), <https://doi.org/10.1016/j.chroma.2020.461414>.

Kimberly J. Hageman contributed by providing feedback on experimental design and manuscript. William J. Doucette contributed by providing feedback on experimental design and manuscript. Alexandria L. Foster contributed as a lab assistant.

2.1 Introduction:

Pesticides (including herbicides, insecticides, and fungicides) are commonly used in agricultural systems worldwide; however, concerns about their negative impacts on human health and the environment⁴¹ require careful monitoring of their concentrations in plant tissues and other environmental matrices. The extraction step is a critical, but often challenging, step in the quantification of pesticides in plant materials. A number of approaches for extracting pesticides from plant materials have been used, including Pressurized Liquid Extraction (PLE),^{10-14,16,18} Selective PLE (SPLE),^{16,18} Quick, Easy, Cheap, Effective, Rugged, and Safe (QuEChERS),^{11,13-15} Matrix Solid-Phase Dispersion (MSPD),^{11,14,16,17} Soxhlet,¹⁰⁻¹³ and dispersive Solid Phase Extraction (dSPE).^{11,14,15,17}

The Energized Dispersive Guided Extraction (EDGE®) system was introduced by CEM Corporation in October 2017 and was developed to combine PLE with dSPE⁴² and is claimed to be ‘faster than Soxhlet, more automated than QuEChERS, and simpler than other solvent extraction systems.’²³ A brief description of the EDGE approach is included here; for further details, readers should consult the CEM website and EDGE manual. To perform an EDGE extraction, the sample and selected sorbents are added to an extraction cell that contains a filter at the bottom of the cell. The instrument transfers the cell into a sealed, sample chamber where specified volumes of solvents are added from the bottom to the gap between the cell and chamber walls (‘Bottom Volume’). A smaller amount of solvent is also added to the cell from the top (‘Top Volume’). The walls of the chamber are heated (25-200 °C), causing the solvent to expand and disperse into the sample through the holes in the bottom of the cell. Because the system is sealed, temperatures above the solvent boiling point at 1 atm can be used and the volatilized solvent will not

escape the cell (maximum pressure is 200 psi). Solvent is held in the cell for a selected amount of time, allowing analytes to partition into the solvent. The solvent and extracted analytes then drain through the filter into a collection vial. While a number of Application Notes for EDGE methods can be found on the CEM website,²⁴ to the best of our knowledge, no peer-reviewed publications exist that evaluate EDGE or compare its performance to that of any of the well-known, trusted extraction approaches.

To evaluate the performance of the EDGE, we compared it to an SPLE method designed for use with a Thermo Scientific Dionex Accelerated Solvent Extractor (ASE). We used the ASE for this comparison because of similarities between EDGE and ASE instrumentation. SPLE has been described in detail in Subedi et al.¹⁸ In brief, SPLE is conducted by packing the sample and a layer of selected sorbents into a stainless-steel extraction cell. The sorbents are included to retain compounds that interfere with instrument analysis of target compounds (i.e. in-cell cleanup). The extraction cells are transferred to an oven, solvent is added to the sealed cell, and the cell is heated (40-200 °C). Since the system is closed, the solvent remains in the liquid phase while the pressure is maintained at a specified level during heating (typically to 1500 psi) using a pressure transducer and static valve. Elevated temperatures and pressures help to increase the efficiency of the extraction process.²² After a selected hold time, the solvent and extracted analytes are transferred to a collection bottle. EDGE and ASE are similar in that they both use a robotic arm to move cells from a tray or rack of prepared cells, use elevated temperatures, and can perform in-cell cleanup by packing sorbents into the extraction cells. A critical difference is that the ASE instrument uses a much higher pressure in the cell. While the EDGE instrument does build up pressure (maximum 200

psi), the operating pressure is not set by the user. Instead, it is the result of the solvent expanding due to heat.

The first objective of this project was to optimize and validate an SPLE method using the ASE instrument for the extraction of a suite of 20 semi-volatile pesticides from citrus and alfalfa leaves. The second objective was to modify the optimized ASE method for use with the EDGE instrument and to compare the performance of the two instruments using various criteria. Because SPLE methods usually use layers of sorbent and sample in the extraction cell and because no investigations into the effects of layering versus mixing have been reported in the literature for either method, the third objective was to compare mixing and layering for each method. The four methods (Layered ASE, Mixed ASE, Layered EDGE, Mixed EDGE) were compared in terms of 1) extract color and extracted lipid mass, 2) lipid content analysis in extracts based on UV-Vis absorbance spectra, 3) recovery of spiked target pesticides, 4) pesticide concentrations in field samples, and 5) other extraction parameters.

2.2 Materials and Methods:

2.2.1 Strategy Overview

The first step was to optimize the in-cell cleanup of an ASE method for the extraction of pesticides in alfalfa leaves using a layered sorbent/leaf homogenate approach (the Layered ASE method). Optimization was achieved by determining the ideal masses of Florisil and graphitized carbon black (GCB) needed to obtain extracts that contained <10 mg of lipid and that were clear with minimal color. The 10 mg lipid threshold was selected based on the recommendation in Lavin et al.⁴³ Tests were then conducted to confirm that the Layered ASE method could also be used successfully with

citrus leaves. Next, tests were conducted in which the sorbents and leaf homogenate were mixed, instead of layered, in the ASE extraction cell (Mixed ASE method). Finally, the ASE methods were modified for use with the EDGE (Layered EDGE and Mixed EDGE methods), using many of the same extraction parameters as in the ASE methods. UV-Vis absorbance spectra were obtained to determine how well selected sorbents removed colored matrix compounds. Spike and recovery experiments were conducted for a suite of 20 pesticides. Finally, pesticides were quantified in alfalfa and citrus field samples to compare concentrations measured using both methods.

2.2.2 Materials, Chemicals, and Standards

The following materials and chemicals were purchased from Thermo Fisher Scientific (Massachusetts, USA) and subsidiary companies: optima-grade ethyl acetate, *n*-hexane, Florisil (60-100 mesh size), sea sand, cellulose filter papers for the extraction cells, and diatomaceous earth (DE). GCB (ENVI-Carb Packing) was purchased from Sigma-Aldrich, Inc. (Missouri, USA). C4 Q-Disks were purchased from CEM Corporation (North Carolina, USA). Before use, Florisil, sand, and DE were baked at 565 °C for 30 minutes to remove potential semi-volatile contaminants.

Twenty target pesticides were used in the spike and recovery experiments. Details about the pesticide classes investigated are provided in Table 2.1. Chlorpyrifos, *cis*-chlordane, dichlorodiphenyldichloroethane (*o,p'*-DDD and *p,p'*-DDD), dieldrin, endosulfan I, *s*-ethyl dipropylthiocarbamate (eptam), fenpropathrin, flupyradifurone, malathion, molinate, tolfenpyrad, triallate, and trifluralin were purchased from Sigma-Aldrich, Inc. (Missouri, USA). Dimethyl tetrachloroterephthalate (DCPA), dichlorodiphenyldichloroethylene (*o,p'*-DDE and *p,p'*-DDE),

dichlorodiphenyltrichloroethane (*o,p'*-DDT and *p,p'*-DDT), and endosulfan II were purchased from Thermo Fisher Scientific (Massachusetts, USA). Labeled standards d₁₄-trifluralin, d₆-*alpha*-HCH, d₈-*p,p'*-DDT and d₄-*alpha*-endosulfan were obtained from CDN Isotope Inc. (Quebec, Canada). d₁₀-chlorpyrifos was purchased from Sigma-Aldrich, Inc. (Missouri, USA).

Table 2.1 List of the compound class of each pesticide studied.

Pesticide	Compound Class
Chlorpyrifos	Chlorinated Organophosphate Pesticides
Cis-Chlordane	Organochlorines Pesticides and Metabolites
DCPA	Phthalate Pesticide
Dieldrin	Organochlorines Pesticides and Metabolites
Endosulfan I	Organochlorine Sulfide Pesticides and Metabolites
Endosulfan II	Organochlorine Sulfide Pesticides and Metabolites
Eptam	Thiocarbamate Pesticides
Fenprothrin	Pyrethroid Pesticides
Flupyradifurone	Butenolide Pesticides
Malathion	Organophosphate Pesticides
Molinate	Thiocarbamate Pesticides
<i>o,p'</i> -DDD	Organochlorines Pesticides and Metabolites
<i>o,p'</i> -DDE	Organochlorines Pesticides and Metabolites
<i>o,p'</i> -DDT	Organochlorines Pesticides and Metabolites
<i>p,p'</i> -DDD	Organochlorines Pesticides and Metabolites
<i>p,p'</i> -DDE	Organochlorines Pesticides and Metabolites
<i>p,p'</i> -DDT	Organochlorines Pesticides and Metabolites
Tolfenpyrad	Pyrazole Pesticides
Triallate	Thiocarbamate Pesticides
Trifluralin	Ditiroaniline Pesticides

2.2.3 Leaf Collection and Preparation

Alfalfa and citrus leaves were collected by hand from live plants growing in a hay-production farm in Utah and a grove in Florida, respectively. Leaf samples were homogenized and crushed into a powder using a mortar and pestle and ~400 mL of liquid nitrogen per sample. Crushed leaves were stored in glass jars at -20 °C until analysis.

Leaf homogenates (0.5 g) were mixed with 1.5 g DE to absorb moisture. When conducting the Layered ASE and Layered EDGE methods, extraction cells were packed (from bottom to top) with distinct layers of selected amounts of Florisil, GCB, and leaf/DE homogenate. When conducting Mixed ASE and Mixed EGDE methods, selected amounts of sorbents were mixed into the leaf/DE homogenate with a mortar and pestle before being packed into cells.

2.2.4 Lipid Mass Determination

The total extracted lipid masses in alfalfa and citrus leaves were determined by extracting them in the absence of sorbents using the solvents and parameters outlined in the ASE and EDGE Method sections. The mass of extracted lipids was determined gravimetrically by transferring the extract to a pre-weighed aluminum weigh boat and allowing the solvent to evaporate. The aluminum weigh boat was then placed in a 105 °C oven overnight and its mass was determined the next day.

Residual lipid masses were measured for each test conducted during the in-cell cleanup optimization procedure for the Layered ASE method with alfalfa leaves and eventually, for each leaf type with the Layered ASE, Mixed ASE, Layered EDGE, and Mixed EDGE methods. We note that non-volatile chemicals other than lipids may have also been extracted and measured during this procedure. Efforts were not made to determine the identity of extracted non-volatile chemicals since any of them can present problems during gas chromatography (GC) analysis.

2.2.5 UV-Visible Spectra of the Leaf Extracts

UV-Vis absorbance spectra were obtained using an Ocean Optics (Florida, USA) USB-ISS-UV/VIS. The absorbance spectra were collected from 200-890 nm using an integration time of 100 ms and 10-scan averaging. Instrument reproducibility was evaluated by analyzing an extract on two different days. To evaluate reproducibility of UV-Vis spectra for different extractions of the same leaf sample, two portions of a homogenized alfalfa sample were extracted separately and then analyzed. Good agreement was observed in both cases (Figure 2.1 and 2.2). UV-Vis spectra of extracts were obtained for each leaf type and on each instrument with (a) no sorbent, (b) with 5 g of Florisil, and (c) with 5 g of Florisil and 0.6 g of GCB added to the extraction cell.

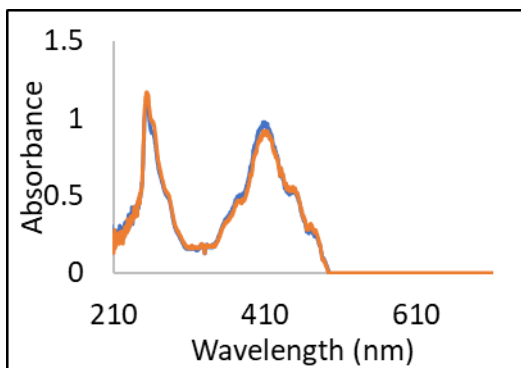


Figure 2.1. UV-Vis spectra for two different samples extracted the same way. This was used to test UV-Vis reproducibility between extracts.

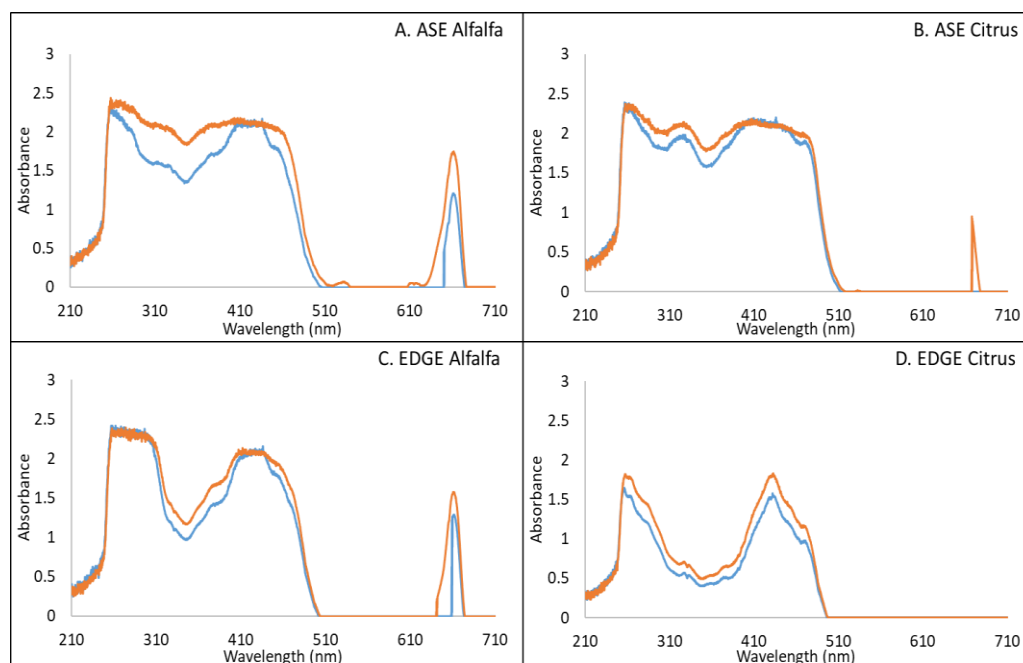


Figure 2.2 UV-Vis spectra for the same sample ran on different days to check the instrument consistency. A) UV-Vis spectra for alfalfa leaves extracted on the ASE with no sorbent. B) UV-Vis spectra for citrus leaves extracted on the ASE with no sorbent. C) UV-Vis spectra for alfalfa leaves extracted on the EDGE with no sorbent. D) UV-Vis spectra for citrus leaves extracted on the EDGE with no sorbent.

2.2.6 Spike and Recovery Experiments

Spike and recovery experiments were conducted by spiking 15 μL of a solution containing 8 $\text{ng}/\mu\text{L}$ of each target pesticide into extraction cells prepared according to the Layered ASE, Mixed ASE, Layered EDGE, and Mixed EDGE methods. The target pesticide solution was added directly to the sample after it was introduced into the extraction cells to minimize potential volatilization losses during the transfer. Each time that cells were spiked, a spike control was prepared by spiking the same volume of target pesticide solution into 300 μL of ethyl acetate. Extracts were blown down to 300 μL and placed in a GC vial containing a 400 μL insert. 15 μL of a solution containing 8 $\text{ng}/\mu\text{L}$ of each isotopically labelled compound was added to each extract and spike control. The isotopically labelled compounds were used as internal standards to account for instrument variability. All spike and recovery experiments were conducted in triplicate. Analyte

concentrations in leaf samples that had not been spiked were independently measured and subtracted before the percent recovery was calculated.

2.2.7 ASE Methods

All ASE experiments were conducted with an ASE-350 (Thermo Fisher Scientific, Massachusetts, USA) using 25:75 (v/v) ethyl acetate:*n*-hexane and the following parameters: 5 min heat time, 10 min static time, 50% solvent flush, 3 static cycles, 120 s purge, 80 °C and 1500 psi. This solvent combination and set of ASE parameters were based off those used by Perez et al.⁴⁴ but changes were made based on preliminary experiments.

In Test 1 of the Layered ASE method optimization procedure for alfalfa leaves, 34-mL ASE extraction cells were packed (from bottom to top) with a cellulose filter, 10 g of Florisil, the leaf/DE homogenate, sand to fill the pore space, and a second cellulose filter. In Test 2, cells were packed (from bottom to top) with a cellulose filter, 5 g of Florisil, 0.3 g of GCB, a second cellulose filter, the leaf/DE homogenate, sand to fill the pore space, and a third cellulose filter paper. In Test 3, the amount of GCB was increased to 0.6 g. The Layered ASE method was next tested with citrus leaves and then modified to produce the Mixed ASE method, which was tested on both alfalfa and citrus leaves.

2.2.8 EDGE Methods

An EDGE application note for pesticides suggests using acetonitrile as the extraction solvent, cellulose C4 Q-Disks, and the following parameters: 20 mL top volume, 10 mL bottom volume, 100 °C, a 1-min hold time, and two wash cycles (30 mL of water followed by 10 mL of acetonitrile).⁴⁵ To facilitate comparison of ASE and EDGE, we adapted this method such that it incorporated several of the parameters from

the Layered ASE method. Thus, our Layered EDGE method used 25:75 (v:v) ethyl acetate:*n*-hexane, C4 Q-Disks, and the following parameters: 20 mL top volume, 10 mL bottom volume, 80 °C, a 3-min hold time, and three wash cycles (10 mL of 25:75 (v:v) ethyl acetate:*n*-hexane in each cycle). In the Layered EDGE method, cells were packed with a C4 Q-Disk followed by a layer of 5 g of Florisil, a layer of 0.6 g of GCB, and a top layer of the leaf/DE homogenate. This method was tested with both alfalfa and citrus leaves and then modified to produce the Mixed EDGE method, which was also tested with both alfalfa and citrus leaves.

2.2.9 Comparison of Pesticide Concentrations in Field Samples

Pesticide concentrations obtained in alfalfa and citrus field samples using each of the four methods (Layered ASE, Mixed ASE, Layered EDGE, and Mixed EDGE) were compared. In these experiments, packed extraction cells were spiked with 15 µL of a solution containing 8 ng/µL of each isotopically labelled compound. In this case, labelled compounds were used as pesticide ‘surrogates’ since they underwent all sample preparation and analysis steps. All experiments were conducted in triplicate.

2.2.10 Quantification of Pesticides in Leaf Extracts by GC-MS/MS

All extracts were reduced in volume to 300 µL using a Turbovap II (Biotage, North Carolina, USA) with a water bath temperature of 35 °C and a starting flow rate of 3.0 L/min, ramp to 5 L/min over 10 minutes, ramp to 6.0 L/min over 5 minutes, hold at 6.0 L/min until extracts reached 300 µL. Extracts were then transferred to GC vials. Pesticides were quantified with a Thermo Fisher Scientific (Massachusetts, USA) Trace 1310 GC and TSQ 8000 Evo mass spectrometer (MS). Target analytes were separated with a 30 m x 0.25 mm x 0.25 µm ZB-5MSplus fused silica capillary column

(Phenomenex, California, USA) with a 10-m deactivated guard column (Thermo Fisher Scientific, Massachusetts, USA). The inlet temperature was 300 °C and injections were conducted in splitless mode. The oven temperature program was: 90 °C (hold 0.5 min), ramp to 170 °C at 15 °C/min, ramp to 210 °C at 1 °C/min, ramp to 300 °C at 5 °C/min (hold 10 min). The MS was operated in electron ionization-selective reaction monitoring (EI-SRM) mode using argon as the collision gas. Target analyte retention times and SRM transitions are provided in Table 2.2. Calibration curves were prepared using the ratio of the target analyte peak area to the corresponding surrogate peak area.

Table 2.2 Target analyte retention times and selected reaction monitoring (SRM) transitions.

Compound	Internal Standard	Retention Time (min)	MS Quantitation Peak	MS Confirming Peak 1	MS Confirming Peak 2
eptom	<i>d</i> ₆ - <i>alpha</i> -HCH	5.69	128.0 / 43.1	189.0 / 128.0	86.1 / 43.1
molinate	<i>d</i> ₆ - <i>alpha</i> -HCH	7.76	126.0 / 55.0	55.1 / 29.1	83.1 / 55.1
<i>d</i> ₁₄ -trifluralin		9.38	267.1 / 163.0	50.2 / 30.0	267.1 / 209.0
trifluralin	<i>d</i> ₁₄ -trifluralin	9.54	306.1 / 264.2	43.0 / 27.1	264.0 / 160.1
<i>d</i> ₆ - <i>alpha</i> -HCH		10.27	185.0 / 148.1	185.0 / 150.1	187.0 / 150.1
triallate	<i>d</i> ₁₀ -chlorpyrifos	13.30	86.1 / 43.1	43.0 / 41.1	268.0 / 184.0
malathion	<i>d</i> ₁₀ -chlorpyrifos	18.15	158.0 / 125.0	93.0 / 63.1	125.0 / 79.0
<i>d</i> ₁₀ -chlorpyrifos		18.24	324.0 / 259.9	326.0 / 196.9	326.0 / 262.0
chlorpyrifos	<i>d</i> ₁₀ -chlorpyrifos	18.56	314.0 / 258.0	286.0 / 257.9	316.0 / 259.9
DCPA	<i>d</i> ₁₀ -chlorpyrifos	18.83	299.0 / 221.0	301.0 / 222.9	301.0 / 273.0
<i>o,p'</i> -DDE	<i>d</i> ₈ - <i>p,p'</i> -DDT	24.62	246.0 / 176.1	176.1 / 150.1	248.0 / 176.1
flupyradifurone	<i>d</i> ₁₄ -trifluralin	24.70	282.0 / 247.1	212.1 / 175.0	212.1 / 174.0

d ₄ - <i>alpha</i> -endosulfan		24.89	207.0 / 171.9	172.0 / 137.0	235.0 / 140.7
endosulfan I	d ₄ - <i>alpha</i> -endosulfan	25.09	195.0 / 159.0	207.0 / 172.0	241.0 / 205.9
<i>cis</i> -chlordane	d ₈ - <i>p,p'</i> -DDT	25.20	373.0 / 265.9	236.8 / 119.0	377.0 / 266.1
dieldrin	d ₈ - <i>p,p'</i> -DDT	27.99	263.0 / 192.9	108.0 / 79.1	277.0 / 207.0
d ₈ - <i>p,p'</i> -DDT		28.15	184.0 / 156.1	326.0 / 254.0	254.0 / 219.2
<i>p,p'</i> -DDE	d ₈ - <i>p,p'</i> -DDT	28.35	246.0 / 176.1	176.1 / 150.1	318.0 / 246.1
<i>o,p'</i> -DDD	d ₈ - <i>p,p'</i> -DDT	29.01	199.1 / 164.2	235.0 / 165.1	237.0 / 165.1
endosulfan II	d ₄ - <i>alpha</i> -endosulfan	31.85	339.0 / 125.0	383.1 / 131.7	195.0 / 159.0
<i>o,p'</i> -DDT	d ₈ - <i>p,p'</i> -DDT	33.49	165.0 / 164.2	235.0 / 165.1	237.0 / 165.1
<i>p,p'</i> -DDD	d ₈ - <i>p,p'</i> -DDT	33.58	237.0 / 165.1	165.0 / 164.2	235.0 / 165.1
<i>p,p'</i> -DDT	d ₈ - <i>p,p'</i> -DDT	38.38	235.0 / 165.1	235.0 / 199.0	237.0 / 165.1
fenpropathrin	d ₆ - <i>alpha</i> -HCH	48.10	97.1 / 55.1	55.1 / 29.2	181.1 / 152.1
tolfenpyrad	d ₁₀ -chlorpyrifos	63.30	171.0 / 88.0	383.1 / 171.2	383.1 / 131.7

2.2.11 Quality Assurance

Sand blanks and empty cells were extracted on the ASE and EDGE, respectively, before every set of samples to minimize risk of carryover. Laboratory blanks, which were prepared by packing extraction cells with all components except leaf/DE homogenate, were processed using the same methods as samples and were extracted with every batch of ASE and EDGE samples. Target analyte concentrations were only reported if the concentrations were 2.5 times that in the laboratory blank. Additionally, a check standard was run after every 4–6 extracts on the GC-MS/MS to monitor the robustness of the calibration curve and instrument variability.

2.2.12 Statistical Analysis

Student t-tests were performed using Microsoft Excel 2016. ANOVA analyses were conducted using a Tukey Test using R version 3.6.0. Comparisons were considered significantly different if $p < 0.05$.

2.3 Results and Discussion:

2.3.1 Optimizing the Layered ASE Method

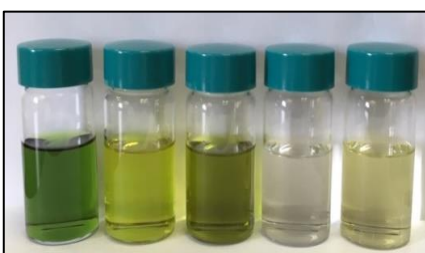


Figure 2.3 Photo of alfalfa extracts from the ASE (from left to right) using no sorbent, layered Florisil, mixed Florisil, layered Florisil and GCB, and mixed Florisil and GCB. Extractions of citrus leaves, and those performed with the EDGE instrument, showed similar results.

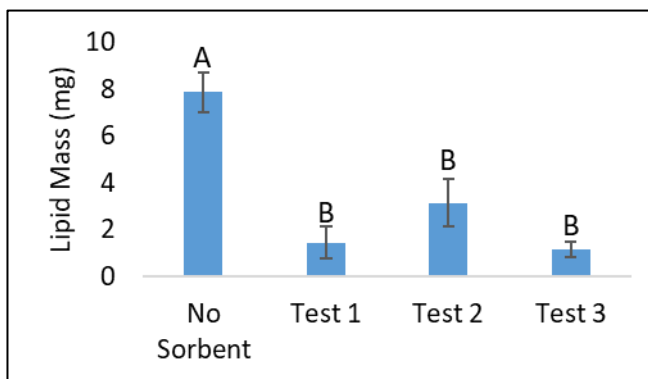


Figure 2.4 Comparison of the lipid mass extracted for each step of the method development process for 0.5 g alfalfa leaves on the ASE. Method development samples were packed in a layered manner. In addition to the 0.5 g alfalfa leaves, Test 1 cells contained 10 g of Florisil, Test 2 cells contained 5 g of Florisil and 0.3 g GCB, and Test 3 cells contained 5 g of Florisil and 0.6 g GCB. Each test was conducted in triplicate and error bars indicate standard deviation. Different letters above the bars indicate a significant difference.

The alfalfa extracted using the ASE parameters when no sorbent was included in the extraction cells produced extracts that were dark green (Figure 2.3) and resulted in 7.9 ± 0.8 (standard deviation) mg of total extracted lipid per 0.5-g leaf sample (Figure 2.4). Test 1, which incorporated 10 g of Florisil layered below the sample, resulted in six times less extracted lipid in the sample extract, or 1.4 ± 0.7 mg of residual lipid. Nonetheless, Test 1 extracts were still excessively colored for GC analysis (Figure 2.3). Thus, in Test 2 we incorporated 0.3 g GCB since GCB had previously been shown to remove colored plant pigments from extracts during SPLE⁴⁴. We also used less Florisil (5 g) in Test 2 because the residual lipid mass was already below our criterion of 10 mg per extract. Test 2 extracts were still colored and contained 3 ± 1 mg residual lipids. Increasing the GCB mass to 0.6 mg in Test 3 resulted in colorless extracts (Figure 2.3) and 1.1 ± 0.3 mg of residual lipid. The spike and recovery experiment conducted with alfalfa and the Test 3 method resulted in an average percent recovery for all tested pesticides of $62 \pm 15\%$ and average individual pesticide recoveries ranging from 37-96% (Figure 2.5). While optimization of the ASE parameters (for example, by changing the extraction solvents or % solvent flush) may have resulted in improved overall recovery, we adopted the Test 3 method as the optimized Layered ASE method. While high recoveries are ideal, the isotope dilution approach that uses labelled surrogates spiked into samples before extraction, corrects the reported concentrations for extraction inefficiencies and losses during sample preparation.

GCB has been used to reduce pigments in other extraction techniques and has commonly been used in QuEChERS.^{44,46-50} In a previous study, the removal of the pigment β -carotene was monitored using UV spectra and the GCB successfully removed

more than 90% of β -carotene from extracts.⁴⁶ However, other studies found that GCB does little to remove fatty acid matrix,⁵⁰ so other sorbents are required to produce extracts containing minimal matrix compounds. This was true for our work as well; Florisil was required along with GCB to produce extracts with little residual lipid mass. While pigments have a strong affinity for GCB, some common target analytes also have an affinity for GCB. Several studies have noted that the use of more GCB leads to a reduction in extraction efficiencies for certain analytes, but for other analytes the GCB has no effect.^{46,48,49,51}

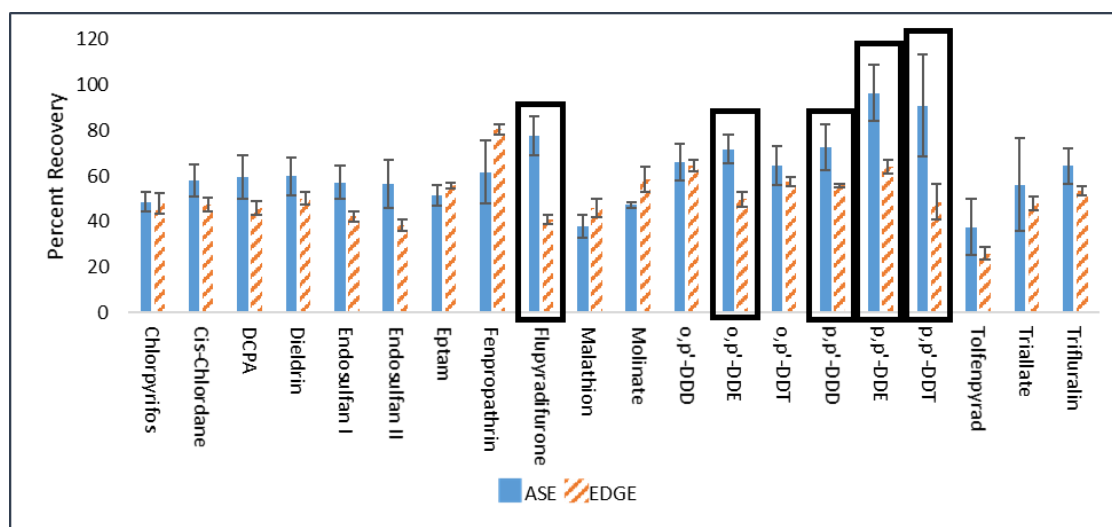


Figure 2.5 Comparison of the percent recoveries from alfalfa leaves using both the Layered ASE and Layered EDGE methods. The boxes surrounding compounds indicate that the percent recovery from the two methods are significantly different. Each test was conducted in triplicate and error bars indicate standard deviation.

2.3.2 Extracted Lipid Masses and Extract Color

Extracted lipid mass and extract color are two indicators of how successful the in-cell cleanup method is. While a low lipid mass and a colorless extract are desired, there is a tradeoff that may have to be made because the sorbents used for in-cell cleanup can also sorb the analytes of interest and cause a reduction in analyte recovery. Total lipid mass

extracted from alfalfa using the EDGE method with no sorbents was 7 ± 1 mg (Figure 2.6), which is lower than that extracted with the ASE method with no sorbents, but not significantly so ($p > 0.05$). The residual lipid mass obtained from alfalfa samples using the Layered ASE method was also compared to those obtained with the Mixed ASE, Layered EDGE, and Mixed EDGE methods (Figure 2.6). No significant differences in residual lipid masses were observed for these four methods. In all cases, extracts were colorless and residual lipid masses were below the 10 mg limit, indicating that extracts obtained from any of these methods are suitable for GC analysis.

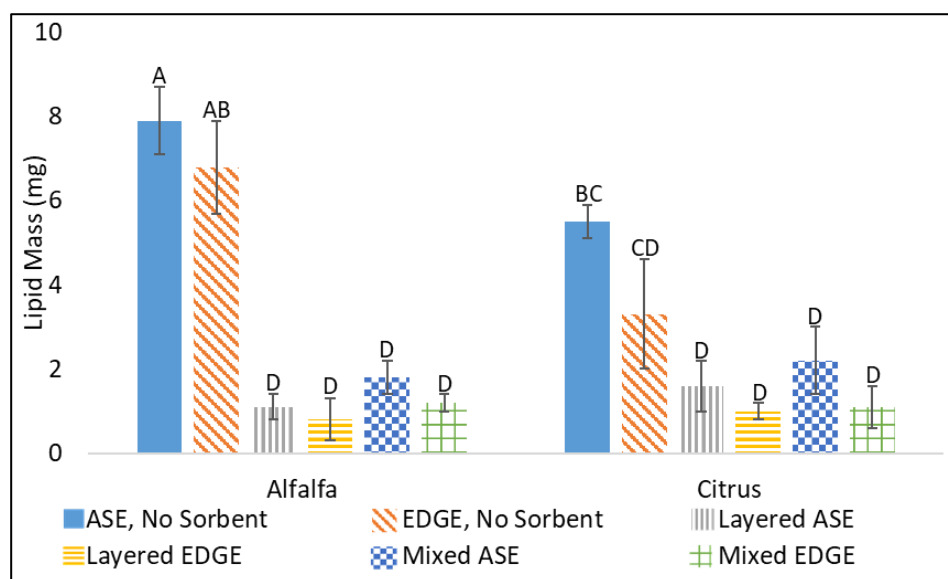


Figure 2.6 Lipid mass and residual lipid mass extracted for each extraction method when using no sorbents and when using the Layered ASE, Mixed ASE, Layered EDGE, and Mixed EDGE methods. Each test was conducted in triplicate and error bars indicate standard deviation. Different letters above the bars indicate a significant difference.

When extracting total lipids from citrus leaves using the ASE method with no sorbents, 5.5 ± 0.4 mg lipids per 0.5-g sample were extracted (Figure 2.6); this is significantly lower from that obtained with alfalfa leaves using the same method. When

extracting total lipids from citrus leaves using the EDGE method with no sorbents, 3 ± 1 mg of lipids per 0.5-g sample were extracted from citrus leaves, which is not significantly different from that obtained with ASE method. Interestingly, the reproducibility in extracted lipid quantities was worse for both alfalfa and citrus leaves when using EDGE; however, there was no indication that EDGE produced less reproducible results than ASE when all results from the study were considered.

No significant differences were observed in residual lipid masses extracted from citrus leaves when using the Layered ASE, Mixed ASE, Layered EDGE, or Mixed EDGE methods (Figure 2.6). The total mass extracted from the citrus with the EDGE method with no sorbents was also not significantly different from the residual masses; however, that extract was very colored (Figure 2.3) indicating that in-cell clean-up was needed. Extracts obtained from citrus leaves using the four in-cell clean-up methods were all colorless and contained less than 10 mg of lipids (Figure 2.6), indicating that any are suitable for GC analysis.

2.3.3 UV-Visible Spectra of the Leaf Extracts

A notable difference was observed in the UV-Vis spectra of extracts obtained using the ASE methods with no sorbents versus the EDGE method with no sorbents for both alfalfa (Figure 2.7B versus 2.7D) and citrus (Figure 2.7C versus 2.7E). The much stronger absorbance at ~ 350 nm in the ASE extracts indicates that the EDGE method did not extract leaf matrix compounds that absorb at this wavelength to the same extent that the ASE method did. This may be advantageous for EDGE users when pesticide analysis is the objective but could be problematic if using EDGE to investigate the chemical composition of leaves.

When extracting both alfalfa and citrus leaves using the ASE and EDGE methods, the absorbance from 210-510 nm were highest in extracts obtained when no sorbent was used, less when Florisil was included, and least when Florisil plus GCB were included (Figure 2.7B-E). Interestingly, the peaks associated with chlorophylls A and B at 600-700 nm (Figure 2.7A) were not observed when Florisil was included but those at the shorter wavelengths required GCB for removal, explaining why GCB is so effective at removing green and yellow colors from extracts. The spectra in Figure 2.7 also show that the Layered methods were consistently more effective at removing leaf matrix compounds than the Mixed methods (both with Florisil and Florisil plus GCB methods), which has important implications for in-cell clean-up design since the effects of layering versus mixing have not been compared before.

In sum, the Layered ASE, Mixed ASE, Layered EDGE, and Mixed EDGE methods all produced extracts with low UV-Vis absorbance, providing more evidence that these methods produce extracts that will have minimal matrix interference during GC analysis. These results also suggest that UV-Vis analysis could be an effective alternative, or addition, to lipid residual mass analysis when comparing and assessing the effectiveness of various extract clean-up methods. Advantages of the UV-Vis approach over the lipid residue approach are that it provides more specific information about the relative amounts of absorbing chemicals, is considerably faster, requires less steps, and does not destroy the extract.

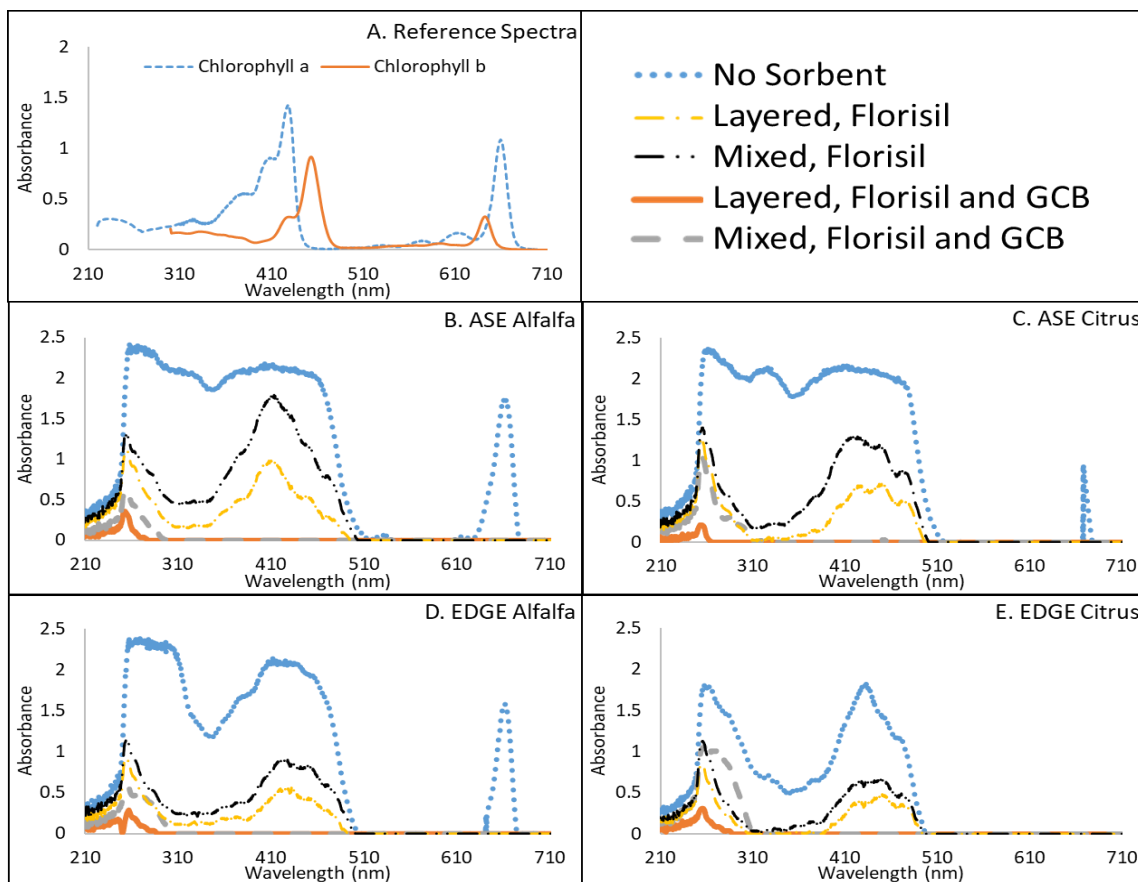


Figure 2.7 UV-Vis absorbance spectra for extracts from each method. A) Reference UV-Vis spectrum for a plant extract in diethyl ether showing expected absorbance for chlorophyll a and chlorophyll b.^{109,110} B) – E) UV-Vis spectra for alfalfa and citrus leaves extracted with no sorbent, only Florisil, and using the Layered ASE, Mixed ASE, Layered EDGE, and Mixed EDGE methods.

2.3.4 Spike and Recovery Results

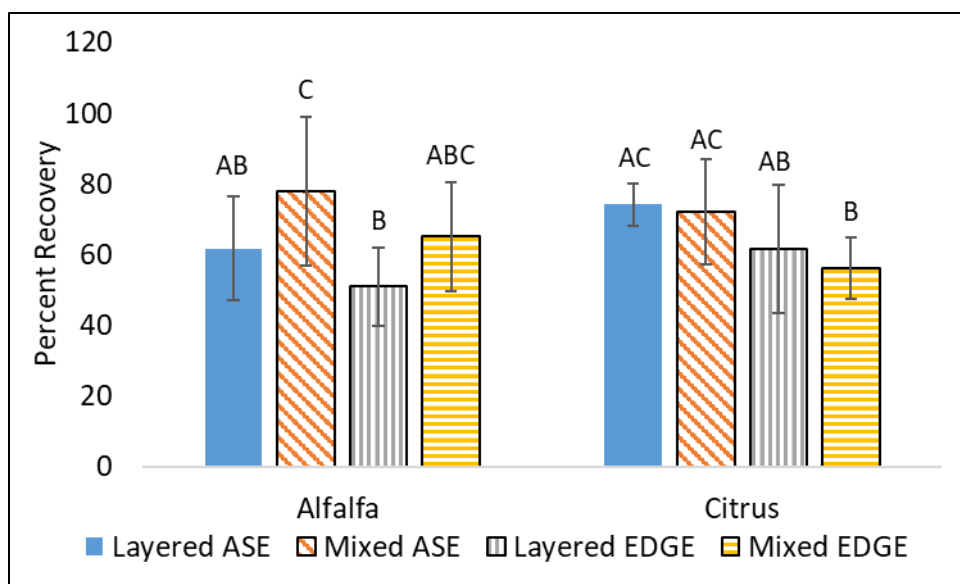


Figure 2.8 Comparison of the average percent recoveries when taking all compounds into account when using the Layered ASE, Mixed ASE, Layered EDGE, and Mixed EDGE methods. Each test was conducted in triplicate and error bars indicate standard deviation. Different letters above the bars indicate a significant difference.

Average recoveries for all pesticides for both types of leaves with all tested methods are shown in Figure 2.8. The spike and recovery results for each individual pesticide for alfalfa and citrus leaves with all tested methods are shown in Figures 2.5 and Figure 2.9, respectively. The key observations from Figure 2.8 are that average recoveries when all pesticides were included were significantly higher when using (a) the Layered ASE method compared to the Layered EDGE method for alfalfa and (b) the Mixed ASE method compared to the Mixed EDGE method for both alfalfa and citrus. These results suggest that overall, better recoveries of spiked pesticides can be expected with ASE compared to EDGE. The key observations from the figures showing results for individual pesticides (Figures 2.5 and 2.9) was that only a handful of the individual pesticides in each case had significantly higher recoveries with the ASE methods (Figure 2.10);

however, because *most* pesticides in each case had higher recoveries (even if not significantly higher) with the ASE methods, *average* recoveries calculated when all pesticides were included were higher with the ASE methods. For example, Figure 2.5 shows that with the Layered methods and alfalfa leaves, recoveries were significantly higher for only five of the 20 pesticides, but recoveries were higher (even if not significantly higher) for 16 of the 20 pesticides. The very large differences in recoveries for the pesticides with significant differences (for example, 78% versus 41% for flupyradifurone) also drove the differences in average recovery between the methods. Better recoveries of spiked pesticides with the EDGE methods may have been possible with further method development.

Significant differences in average pesticide extraction efficiencies for Layered versus Mixed methods were observed (Figure 2.8). Average recoveries when all pesticides were included were significantly higher when using (a) Mixed ASE method compared to the Layered ASE method for alfalfa and (b) the Layered EDGE method compared to the Mixed EDGE method for citrus leaves. These results suggest that both cell packing methods lead to similar recoveries for these pesticides. However, some compounds did show a significant difference in percent recovery (Figure 2.10). When there was a significant difference in recovery, the recovery was usually higher for the Mixed method. Recoveries may have been higher in some cases with the Mixed methods because extracted analytes did not travel through the all the sorbent, meaning less analyte-sorbent interaction. This hypothesis is supported by the observation that the Mixed methods also generally had higher extracted lipids than the Layered method (Figure 2.6).

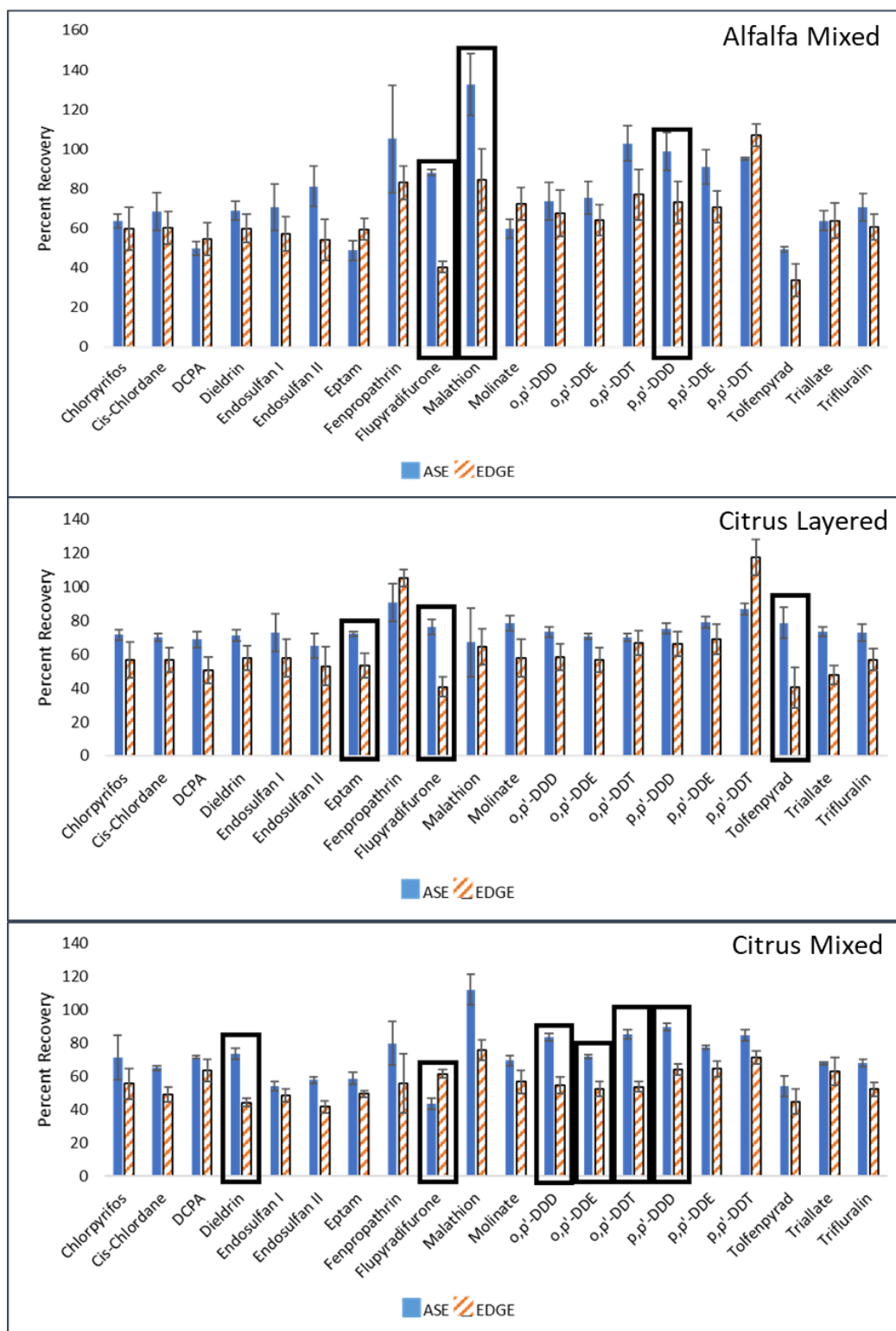


Figure 2.9 Comparison of the percent recoveries. The boxes surrounding compounds indicate that the percent recovery from the two methods are significantly different. Each sample was performed in triplicate and error bars indicate standard deviation.

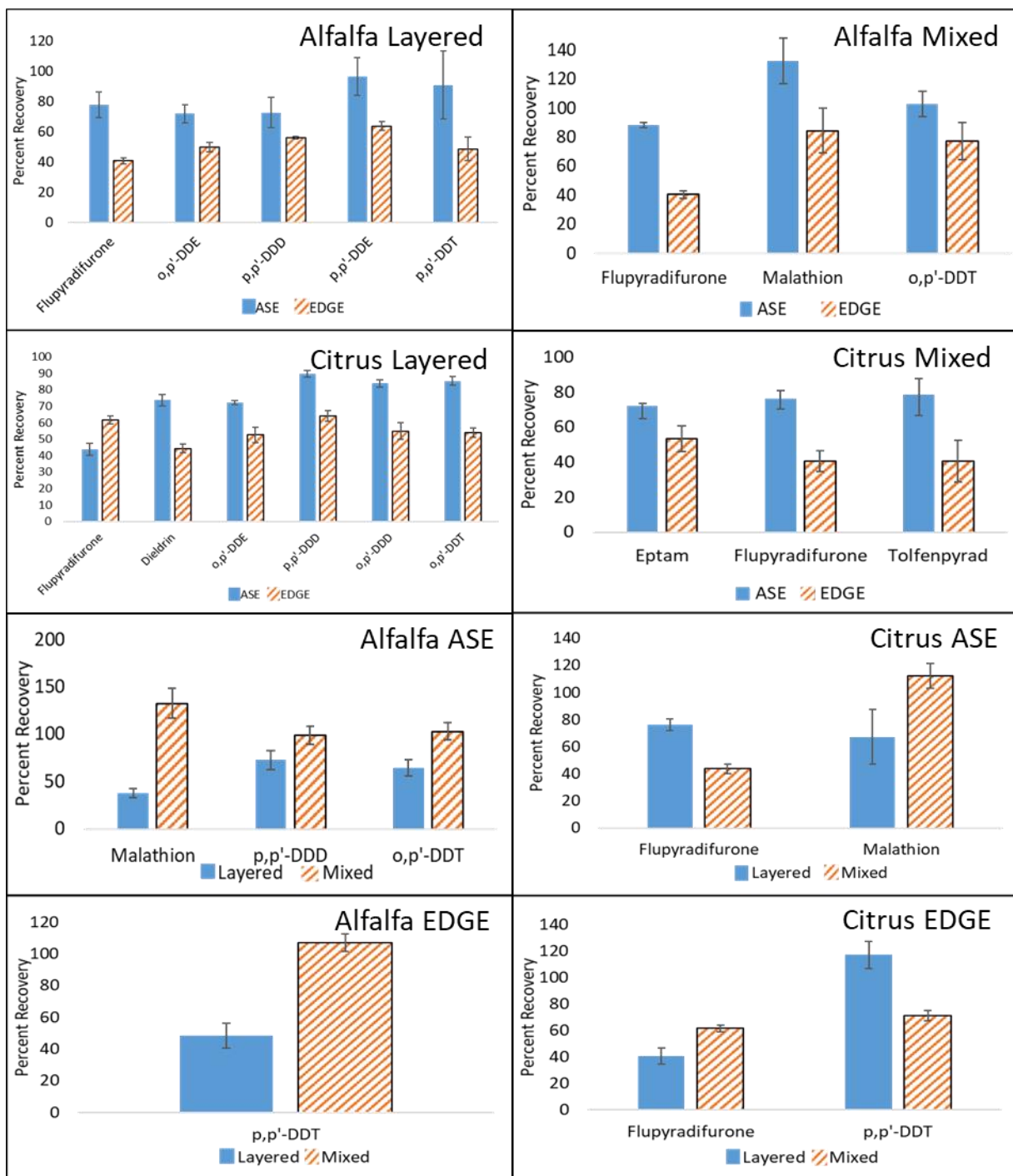


Figure 2.10 Compounds that have a significantly different percent recovery when extracting with different methods and leaves. Each sample was run in triplicate and error bars indicate standard deviation.

2.3.5 Pesticide Concentrations in Field Samples

The only target pesticide detected in field samples of alfalfa leaves was the pyrethroid insecticide, fenpropathrin. Its average concentration was 640 ± 90 ng/g when all four extraction methods were considered (Figure 2.11). The organophosphate insecticide malathion and the pyrazole insecticide tolfenpyrad were detected in field samples of citrus leaves at average concentrations of 1290 ± 270 ng malathion/g citrus leaf and

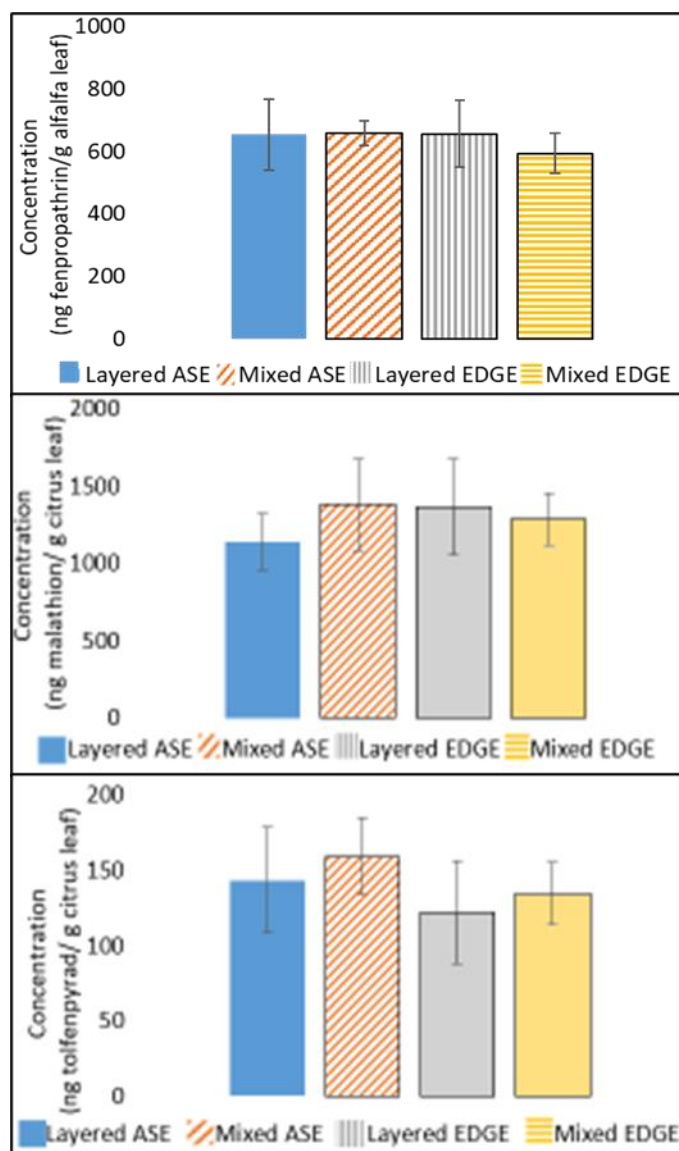


Figure 2.11 Pesticide concentration in alfalfa and citrus leaves for each extraction method. Each sample was run in triplicate and error bars indicate standard deviation.

140±30 ng tolfenpyrad/g citrus leaf when all extraction methods were considered (Figure 2.11). No significant differences in reported concentrations for any of these pesticides were observed for the four different extraction methods. More data is needed to make a broader conclusion; however, the lack of significant differences observed here suggests that ASE and EDGE methods are likely to produce similar pesticide concentrations in leaf extracts. The use of labelled surrogates increases the likelihood of this since they correct for extraction inefficiencies and losses during sample preparation.

2.3.6 Method Parameter Comparison

Table 2.3 Comparison of extraction parameters for both the ASE and the EDGE. Extraction data from the Layered ASE and Layered EDGE methods using alfalfa leaves were used for this comparison.

Parameter	ASE	EDGE
Lipid Weight Extracted (mg)	7.9±0.8	7±1
Residual Lipid Weight Extracted (mg)	1.1±0.3	0.8±0.5
Time Required for Extraction (minutes)	~45	~10
Amount of Solvent Used (mL)	~25	~35
Average Percent Recovery	60±20%	50±10%
Percent Recovery Range	37.5-96.4%	25.9-80.5%

Several extraction parameters were compared for Layered ASE and Layered EDGE methods using alfalfa leaves (Table 2.3). For the lipid mass extracted, the ASE extracted more than the EDGE. This, along with the UV-Vis spectra, shows that this EDGE method did not extract as much of the leaf matrix components as the ASE did. This indicates that for the methods used in this work the EDGE has better selectivity than the ASE. This can be viewed as an advantage or disadvantage for the EDGE, depending on the goal of extraction. If the goal is to produce extracts that require less clean-up using the methods from this work, the EDGE is a better choice, but if the goal is to extract total

lipids from samples the ASE is better suited. The residual lipid mass was similar for both the Layered ASE and Layered EDGE methods, showing that when sorbents were used for in-cell clean-up, similar amounts of leaf matrix were extracted. The average percent recovery, as well as the range, of spiked pesticides was higher with the Layered ASE method than the Layered EDGE method.

Extraction with the ASE method used in this work took ~4.5 times longer than the EDGE method. The ASE used slightly less solvent per extraction compared to the EDGE, but the amounts were similar. The ASE takes up more bench space, being almost 2 times wider than the EDGE. We also observed differences in ease of use between the instruments. The ASE methods required more time to pack the extraction cells compared to the EDGE methods. This is due to ASE cells requiring the dead space filled as well as requiring extra filters to allow for the extraction cells to be better sealed.

2.4 Conclusion

An SPLE method for extracting pesticides from leaves using the ASE was developed. The method developed led to clear colorless extracts with low residual lipid weight. An EDGE method based on the ASE method parameters was then developed. Extractions were performed for both alfalfa and citrus leaves and used sorbents in both a layered and mixed manner. The UV-Vis spectra of the Layered ASE, Mixed ASE, Layered EDGE, and Mixed EDGE methods were similar. For spike and recovery experiments, when there was a significant difference in the percent recovery, the ASE generally had the higher percent recovery. However, when extracting pesticides from field samples of alfalfa and citrus, there was no significant difference between extraction methods. The EDGE is faster than the ASE but does use slightly more solvent. These

results show that the higher pressures employed by the ASE system resulted in better extraction efficiencies of both pesticides and leaf matrix compounds; however, the use of surrogates means that results in reported pesticide concentrations in field samples were very similar. It is possible that the higher pressures employed by ASE are needed for extracting more-tightly bound analytes in more complex matrices, such as fish or soil.

Chapter 3. Investigating the Effects of Temperature, Relative Humidity, Leaf Collection Date, and Foliar Penetration on Leaf-Air Partitioning

The content of this chapter has been submitted to Environmental Science and Technology with the author list: Ashlie D. Kinross, Kimberly J. Hageman, and Calvin Luu.

Kimberly J. Hageman contributed by providing feedback on experimental design and manuscript. Calvin Luu contributed as a lab assistant.

3.1 Introduction

Volatilization from foliage is a key component of the dissipation process for many pesticides from agricultural fields. Volatilized pesticides are susceptible to atmospheric transport and can move off-site from an area of application, leading to non-target organism and human exposure.^{52,53} Leaf-air ($K_{\text{leaf-air}}$) and plant-air ($K_{\text{plant-air}}$) partition coefficients are used in chemical fate models to understand the behavior of pesticides and other organic contaminants in the environment. These partition coefficients represent the ratio of the concentration of the chemical of interest in the leaf or plant tissue, respectively, to that in air at equilibrium. Measured $K_{\text{plant-air}}$ and $K_{\text{leaf-air}}$ values have been previously reported for several chemical classes and plant species combinations. For the sake of simplicity, we will refer to all of these as $K_{\text{leaf-air}}$ values herein although strictly speaking, the difference is that the $K_{\text{plant-air}}$ also includes partitioning to stems and flowers or fruit, if present.

The chemicals for which measured $K_{\text{leaf-air}}$ values exist in the literature include polychlorinated biphenyls (PCBs), several historic-use pesticides (hexachlorohexanes (HCHs), *p,p*-dichlorodiphenyltrichloroethane (DDT), hexachlorobenzene, mirex, and thionazin), a degradation product of DDT (*p,p*-dichlorodiphenyldichloroethylene (DDE)), and two current-use pesticides (sulfotep and trifluralin) (Table 3.1).²⁶⁻³¹ To the best of our knowledge, no $K_{\text{leaf-air}}$ values for current-use pesticides other than sulfotep and trifluralin have been reported. Many of these reported $K_{\text{leaf-air}}$ values were measured in a volatilization chamber with low enough air flow over the leaf surface to allow equilibration and a system to trap gas-phase chemicals since their concentration is often too low for direct detection.^{27,28} While $K_{\text{leaf-air}}$ values can be measured in this type of

Table 3.1 Summary of predictive $K_{\text{leaf-air}}$ equations from previous studies. Most equations follow the form: $\text{Log } K_{\text{leaf-air}} = M (\text{log } K_{\text{octanol-air}}) + B$, and the values for M and B are listed. When in a different form, a full equation is given. All equations are to calculate the $\text{log } K_{\text{leaf-air}}$ at 25 °C.

Reference	Chemicals Studied	Plant Species	M	B
Nizzetto et al. ²⁶	PCBs	Chestnut	0.46	-2.83
		White Ash	0.49	-3.10
		Hazelnut	0.38	-2.12
		Mountain Ash	0.37	-1.94
		Maple	0.49	-3.08
		Beech	0.45	-2.60
		Larch	0.48	-2.99
		Spruce	0.33	-1.75
Kömp and McLachlan ²⁷	PCBs	Ryegrass (1)	1.09	-2.53
Kömp and McLachlan ²⁸	PCBs	Ryegrass (2)	1.15	-3.56
		Clover	0.70	0.15
		Plantain	0.87	-1.30
		Hawk's Beard	0.74	-0.07
		Yarrow	0.57	1.80
Bolinus et al. ²⁹	PCBs	Rhododendron	0.86	-0.51
Bacci et al. ^{30,31}	Nine Pesticides, PCBs	Azalea	$\text{Log } K_{\text{leaf-air}} = 1.14 \text{ log } K_{\text{ow}} - 0.92$	

laboratory experiment, the distribution of a chemical between the atmosphere and vegetation in the environment is often kinetically controlled by transfer across the air boundary layer surrounding the plant, or that above the surface of a densely planted field.⁵⁴ In particular, the less volatile chemicals (i.e. those with log octanol-air partition coefficient ($K_{\text{octanol-air}}$) values less than ~8) generally do not reach equilibrium during the lifetime of a plant due to slow transfer across the air boundary layer combined with high storage capacity of the leaves.⁵⁴

A common approach for modelling pesticide volatilization following application to plants is to calculate the equilibrium pesticide concentration in the air boundary layer

and to then use the diffusion rate across this boundary layer to calculate flux to the turbulent air.⁵⁵⁻⁵⁷ In the Pesticide Dissipation from Agricultural Land (PeDAL) model, pesticide concentrations in the boundary layer around plant surfaces are calculated with a multiphase partitioning equation that uses the $K_{\text{leaf-air}}$ and water-air partition coefficient ($K_{\text{water-air}}$) of the pesticide.^{9,39,40} However, $K_{\text{leaf-air}}$ values must be estimated with predictive equations generated previously from $K_{\text{leaf-air}}$ data for other chemical classes and plant species (Table 3.1) when measured values are not available. The appropriateness of using these equations to predict $K_{\text{leaf-air}}$ values for other chemical-plant combinations has not been fully investigated. Several other important questions about $K_{\text{leaf-air}}$ values for current-use pesticides have also not been addressed. For example, the effects of adjuvants need to be assessed since most pesticides are applied as formulations (*i.e.*, not pure active ingredients) and adjuvants are likely to affect the volatilization process. There is also currently no information about how relative humidity affects $K_{\text{leaf-air}}$ values; this could be important since relative humidity affects leaf structure and permeability⁵⁸⁻⁶⁰ and these properties may affect the strength and type of molecular interactions between pesticides and leaves. More information is also needed about how $K_{\text{leaf-air}}$ values change with plant growth stage since several leaf properties change during aging.^{61,62}

In evaluating pesticide volatilization from the leaf surface, it is also important to consider that penetration into inner leaf layers is also a possible fate processes.^{33-35,37,63,64} While leaf penetration likely has an effect on the amount of chemical available for volatilization, the interplay of these processes have not been directly investigated. Also of interest is the effect of temperature on pesticide behavior on the leaf surface since increasing temperatures are expected to increase volatilization from surfaces; however,

increasing temperature can also lead to increased diffusion into inner leaf layers.^{33,35,64}

Pesticide penetration into leaf layers for up to 24 h after application has been previously measured;⁶⁵ however, the effects of penetration on the volatilization of pesticides from leaf surfaces at different temperatures has not been investigated.

The primary objective of this work was to quantify the effects of temperature, formulation, relative humidity, and leaf collection date on leaf-air partitioning and foliar penetration for an example pesticide-plant combination. We then used this data to improve understanding of the link between foliar penetration and leaf-air partitioning. In this case study, the selected pesticide was the organophosphate insecticide, chlorpyrifos (CAS 2921-88-2), which we studied as an active ingredient alone and in a formulation mixture, and the selected plant was alfalfa (*Medicago sativa*, also known as lucerne). Chlorpyrifos has had traditional widespread use on alfalfa and many other crops, and has been measured in air near application sites.⁶⁶⁻⁶⁸ Chlorpyrifos use in agriculture has been prohibited in the United States⁶⁹ and Europe;^{70,71} however, it is still currently used in many other countries (*e.g.* New Zealand,^{71,72} China,^{71,73} and Brazil^{71,74}) and it is a good candidate for this study since its properties are similar to other organophosphate insecticides still in widespread use. While measured $K_{\text{leaf-air}}$ values are also needed for a larger set of current-use pesticides, we used this case study to identify key questions to direct future research in this area.

3.2 Materials and Methods

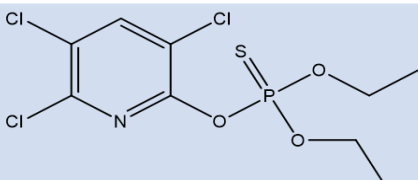
3.2.1 Materials and Chemicals

The following materials and chemicals were purchased from ThermoFisher Scientific (Massachusetts, USA) and subsidiary companies: Optima-grade acetone, ethyl

acetate, methylene chloride (DCM), *n*-hexane, HPLC-grade ethanol, Florisil (60-100 mesh size), sea sand, glass fiber and cellulose filter papers, diatomaceous earth (DE), and Amberlite XAD-2. Graphitized carbon black (GCB) was purchased from Sigma-Aldrich, Inc. (Missouri, USA) as ENVI™-Carb packing. Deactivated glass wool was purchased from Restek (Pennsylvania, USA).

Prior to use, XAD-2 was pre-cleaned with pressurized liquid extraction (PLE) using an ASE-350 (ThermoFisher Scientific, Massachusetts, USA). Separate extractions were performed using DCM and ethyl acetate. Both extractions were conducted with the following conditions: 5-min heat time, 5-min static time, 1 static cycle, 100% flush volume, 240-s purge time, 1500 psi, and 75 °C. The XAD-2 was left in a fume hood overnight to allow residual solvent to evaporate and was then stored in a pre-baked glass jar until use. One portion of XAD-2 was extracted and analyzed after the pre-cleaning procedure to ensure no chlorpyrifos was present. All Florisil, diatomaceous earth, sea sand, and glassware were pre-cleaned by baking at 565 °C for 30 minutes prior to use.

Table 3.2 Chemical structure and properties of chlorpyrifos. Structure drawn using ChemDraw. Log $K_{\text{octanol-air}}$, log $K_{\text{octanol-water}}$ and vapor pressure from EpiSuite.⁷⁵ Log $K_{\text{octanol-water}}$ and vapor pressures for each compound were from an experimental database, but the log $K_{\text{octanol-air}}$ values were calculated from the $K_{\text{octanol-water}}$ values and $K_{\text{air-water}}$ values from EpiSuite's experimental database.

Property	Chlorpyrifos
Structure	
Molecular Weight	350.6 g mol ⁻¹
Log $K_{\text{octanol-air}}$	8.88
Log $K_{\text{octanol-water}}$	4.96
Vapor Pressure	2.0 x 10 ⁻⁵ mm Hg

Chlorpyrifos active ingredient was purchased from Sigma-Aldrich, Inc. (Missouri, USA). The chemical structure and select properties of chlorpyrifos are shown in Table 3.2. The formulation containing chlorpyrifos, Drexel Chlorpyrifos 4E-AG, was purchased from a local farm store. This formulation contains 45% chlorpyrifos active ingredient and the remaining 55% is listed as “Other Ingredients.” The formulation specifies that it contains petroleum distillates, but no other information is given about other formulation components. The labeled standard d10-chlorpyrifos was purchased from Sigma-Aldrich, Inc. (Missouri, USA).

The alfalfa leaves used for measurements were collected from a research field in Logan, Utah, USA. Fresh leaves were collected each day that experiments were conducted. Stems were removed for all experiments. The experiments investigating temperature effects for both the active ingredient and formulation were conducted in May 2020 while those investigating relative humidity effects were conducted in July for the active ingredient and in August for the formulation. Additional experiments designed to investigate leaf age were completed with leaves collected between May and August 2020. Leaf area and thickness were measured each week that experiments were conducted, but no significant changes in these parameters were observed over time.

3.2.2 Application of Chlorpyrifos to Leaves

For all experiments, including the formulation experiments, the mass of active ingredient applied to leaves was 1 mg per ~40 g of leaves, resulting in a mass of active ingredient per leaf area similar to that applied to alfalfa plants in an agricultural field. The suggested application rate for the formulation containing chlorpyrifos (Drexel

Chlorpyrifos 4E-AG) is 1-2 pints/acre. Based on the size of the sample chamber (13.5 in x 9.75 in), alfalfa field leaf area index of 5.25, and the percent chlorpyrifos in the formulation (45%), this equates to 0.8-2 mg of chlorpyrifos active ingredient applied to the dish. To apply chlorpyrifos to leaves, 20 mL of a solution of 0.05 mg/mL of chlorpyrifos in hexane was mixed with ~40 g of whole alfalfa leaves in a glass dish until an even coating of the solution covered the leaves. This process did not result in the leaves being completely submerged in solvent. After mixing, the hexane was allowed to evaporate, which took ~15 min. Some chlorpyrifos may have volatilized during the solvent evaporation step, but that would not affect measured $K_{\text{leaf-air}}$ values since they are calculated from a concentration ratio.

We selected this pesticide application approach with the aim of creating a thin layer of chlorpyrifos (or chlorpyrifos plus non-volatile adjuvants, in the case of formulation experiments) on leaf surfaces. Hexane was used as the carrier instead of water since it volatilized quickly and a water layer on the leaf surface would interfere with leaf-air partitioning. Pesticide formulations often contain organic solvents to improve active ingredient solubility and other pesticide functions (*e.g.* the formulation we used in our experiment contained petroleum distillates, which generally include hexane as a component).⁷⁵ We observed no visual damage or changes in leaf mass during our chlorpyrifos application procedure; nonetheless, the hexane application could have affected the leaf surface chemistry and we did not conduct tests to monitor this.

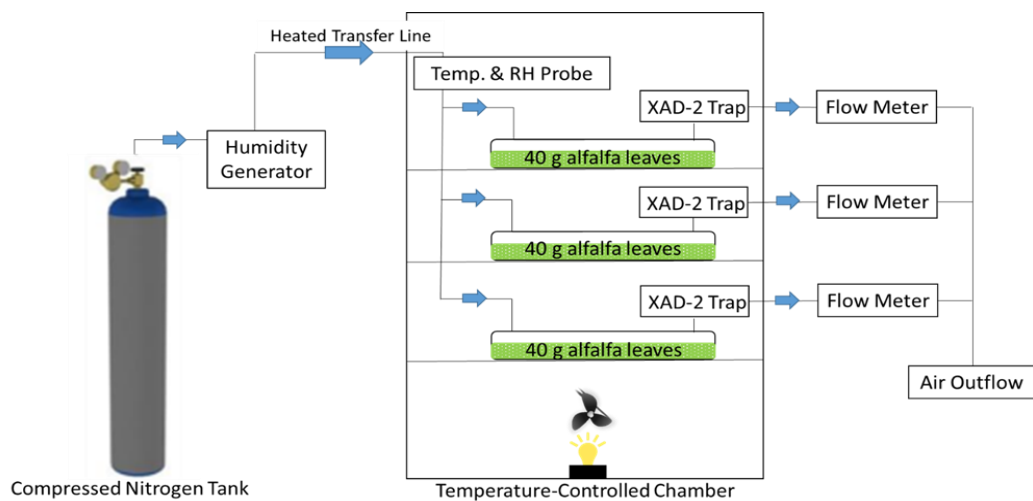


Figure 3.1 Schematic diagram of the solid-phase fugacity meter.



Figure 3.2 Photograph of inside the solid-phase fugacity meter.

3.2.3 Measurement of $K_{\text{leaf-air}}$ Values

$K_{\text{leaf-air}}$ values were measured using a solid-phase fugacity meter similar to that described previously.⁷⁶ A schematic and a photograph of the fugacity meter are provided in Figures 3.1 and 3.2, respectively. The same setup was used for all parameters tested.

After chlorpyrifos application, leaves were transferred into a flat glass sample chamber and spread evenly, resulting in complete coverage of the bottom of the sample chamber with one to two layers of leaves. The sample chamber was then covered with a sheet of aluminum metal and putty was used to create a seal. Two other sample chambers were assembled at the same time to allow for triplicate measurements. Sample chambers were placed in a temperature-controlled chamber and blocked from light sources to avoid possible photodegradation.

Nitrogen (used as a proxy for air) was directed into a humidity generator (Roscid Technologies, Massachusetts, USA) to adjust the relative humidity. This humidified nitrogen then flowed into the temperature-controlled chamber where sensor probes were used to log the temperature and relative humidity once per minute during experiments. The nitrogen was then split into three paths, each with a flow rate of ~65 mL/min. This

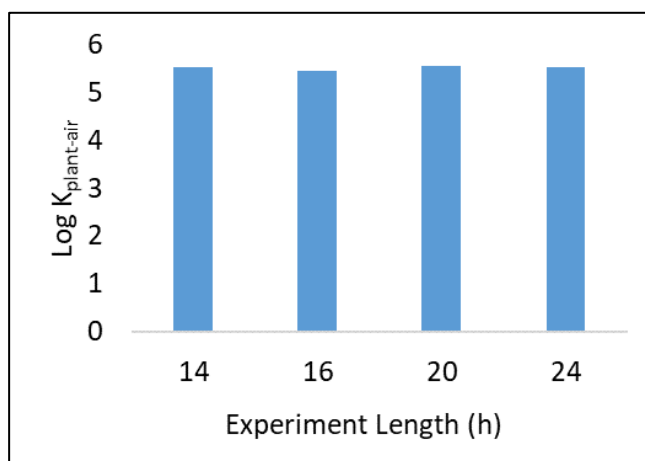


Figure 3.3 Equilibrium testing for chlorpyrifos using a flow rate of ~65 mL/min.

flow rate was selected based on preliminary tests showing that equilibrium was established under these conditions (Figure 3.3). To confirm that the selected flow rate was low enough to establish equilibrium between the leaves and air, tests (set up the same way the rest of experiments) were ran over different time spans. The measured $K_{\text{leaf-air}}$ values were unchanged between each experiment, showing that a flow rate of 65 mL/min was low enough to establish equilibrium for chlorpyrifos between the leaves and air. Flow rate was measured using mass flow meters capable of measuring flow rates of 0-500 mL/min (Aalborg, New York, USA) that were calibrated before use. Each stream of gas was directed into a sample chamber, where it flowed over the contaminated leaves. The nitrogen, containing volatilized chlorpyrifos, then exited the sample chambers and passed through sorbent traps filled with ~12 g of XAD-2. XAD-2 sorbent traps were prepared by packing them from bottom to top (opposite to the extraction solvent flow direction) with a cellulose filter, XAD-2 beads, and a glass fiber filter to hold the XAD-2 in place. Preliminary experiments to test for breakthrough of the XAD-2 sorbent trap was conducted to ensure that 12 g of XAD-2 was enough to collect all gas-phase insecticide. This test was conducted by running a chlorpyrifos active ingredient fugacity experiment at 30 °C and 100% humidity and adding a second sorbent trap after the original one. The second sorbent trap was extracted with the same procedure for XAD-2 extraction described in the main text. There was no chlorpyrifos detected in the second sorbent trap, showing that 12 g of XAD-2 was enough to collect all gas-phase insecticide. Experiments ran for 16 h (passing ~60 L of nitrogen through the system) to ensure enough chlorpyrifos was collected in the XAD-2 for quantification. There was no visual evidence of leaf drying over the experimental period and the leaf mass did not change.

Chlorpyrifos was extracted and quantified in the XAD-2 and whole leaves at the end of the experiments.

Chlorpyrifos was extracted from the XAD-2 sorbent traps using PLE. An isotopically labeled surrogate (d10-chlorpyrifos) was spiked into PLE cells before extraction to account for target analyte loss during sample workup. Chlorpyrifos was extracted from the XAD-2 cells using two separate extraction runs; the first extraction used DCM and the second used ethyl acetate. The following conditions were used for each extraction: 5-min heat time, 10-min static time, 1 static cycle, 50% flush volume, 240-s purge, 1500 psi, and 75 °C. Preliminary experiments showed that the percent recovery of chlorpyrifos was $80 \pm 2\%$ with this method. The chlorpyrifos mass extracted from the XAD-2 and the volume of air that passed through the sample chamber were used to calculate the chlorpyrifos concentration in air.

Chlorpyrifos was extracted from whole leaves following the PLE procedure described by Kinross et al.²⁵ First, all leaves from the sample chamber, except those set aside for foliar penetration studies, were crushed in liquid nitrogen. A portion of the crushed leaf sample was weighed and homogenized with DE to absorb moisture. The PLE cells were packed from bottom to top with a cellulose filter, 5 g of Florisil, 0.6 g of GCB, a cellulose filter, leaf (0.5 g) and DE (1.5 g) homogenate, sand (to remove dead space in the cell), and a glass fiber filter. d10-chlorpyrifos surrogate was spiked into PLE cells before extraction. Chlorpyrifos was extracted from leaves using 25:75 (v/v) ethyl acetate:*n*-hexane and the following PLE parameters: 5-min heat time, 10-min static time, 3 static cycles, 50% flush volume, 120-s purge, 1500 psi, and 80 °C. Preliminary

experiments showed that the percent recovery of chlorpyrifos was $79 \pm 5\%$ with this method.

Unitless $K_{\text{leaf-air}}$ values were calculated as the ratio of the concentrations in leaves to air, with concentrations expressed as mass per mass in both cases. All measured concentrations were above the limit of detection and the total concentration in the leaf and air system had a percent relative standard deviation of less than 15% between replicates for each test. All tests conducted over a range of temperatures (10-30 °C) were performed during a single week. Since fresh leaves were collected each morning of an experiment, we assumed that leaf properties were very similar for all temperature experiments. The experiments conducted over a range of relative humidity levels (40-100%) were also conducted during a single week.

3.2.4 Measuring Foliar Penetration

Following the 16-h experiments, three portions of leaves from one of the sample chambers were reserved for foliar penetration experiments, resulting in triplicate results for these experiments. These leaf samples underwent a sequential extraction scheme based on that previously described by Lichiheb et al.⁶⁵ with the objective of producing extracts containing pesticide that was unbound or loosely adsorbed to the leaf surface (ethanol extraction), pesticide that had penetrated into the cuticular layer of the leaf (hexane extraction), and bound pesticide not extracted by the other two steps (PLE). Although this and similar methods⁷⁷⁻⁷⁹ for extracting chemicals from different leaf layers have been described previously, the correlation between extraction step and pesticide position within the leaf layers has not been validated experimentally. Nonetheless, it is safe to presume that each of the extraction steps removed pesticide that was more tightly

bound to the leaves and had likely undergone deeper foliar penetration. Thus, comparison of the fraction of pesticide in the ethanol-, hexane-, and PLE-extractable fractions provides useful insight about foliar penetration even though these terms are operationally defined.

The ethanol-extractable fraction of chlorpyrifos was obtained by adding 15 mL of ethanol to a vial containing 0.5 g of whole leaves. The vial was hand-shaken for 60 s and the solvent was collected. The hexane-extractable fraction was obtained from the same set of leaves by adding 15 mL of hexane to the vial. After 20 s of shaking, the hexane was removed. The hexane rinse was repeated twice more, and the three hexane rinses were combined. Finally, the same leaves underwent PLE to remove remaining pesticide. The ethanol- and hexane-extractable fractions required external cleanup. Before external cleanup, d10-chlorpyrifos was added to extracts as a surrogate. External cleanup was performed with columns made in-house by packing glass pipettes (bottom to top) with glass wool, 0.6 g Florisil, and 0.1 g GCB. Columns were conditioned with 5 mL of hexane followed by 5 mL of 20:80 acetone:*n*-hexane. The extract was then added to the column and eluted with 15 mL of 20:80 acetone: *n*-hexane.

3.2.5 Chlorpyrifos Quantification

All extracts were concentrated to a volume of 300 μ L using a Turbovap II (Biotage, North Carolina, USA) with a water bath temperature of 35 $^{\circ}$ C and a constant flow of nitrogen at a rate of 6 L/min. Chlorpyrifos and d10-chlorpyrifos were quantified using a ThermoFisher Scientific (Massachusetts, USA) Trace 1310 gas chromatograph (GC) and TSQ 8000 Evo triple quadrupole mass spectrometer (MS). The target analyte was separated on a 30 m x 0.25 mm x 0.25 μ m ZB-5MSplus fused silica capillary column

(Phenomenex, California, USA) with a 10-m deactivated guard column. The inlet temperature was 300 °C and injections were made in splitless mode. The oven temperature program was 90 °C (hold for 0.5 min), ramp to 170 °C at 15 °C/min, ramp to 184 °C at 1 °C/min, ramp to 300 °C at 15 °C/min (hold for 10 min). The MS was used in selected reaction monitoring mode and transition ions are provided in Table 3.3.

Table 3.3 GC-MS/MS SRM transition ions used for quantification of d10-chlorpyrifos and chlorpyrifos.

Compound	MS Quantitation Peak	MS Confirming Peak 1	MS Confirming Peak 2
d10-Chlorpyrifos	324/260	326/197	326/262
Chlorpyrifos	314/258	286/258	316/260

3.2.6 Statistical Methods

Statistical analysis was performed using Jamovi 1.2.27. Post-hoc Tukey tests were used for significant difference testing.

3.3 Results and Discussion

3.3.1 Influence of Temperature on $K_{\text{leaf-air}}$ Values

The measured $\log K_{\text{leaf-air}}$ values for chlorpyrifos applied as the active ingredient ($\log K_{\text{leaf-air,AI}}$) and in a formulation ($\log K_{\text{leaf-air,formulation}}$) are shown in Figure 3.4. The mean $\log K_{\text{leaf-air,AI}}$ values ranged from 5.1 to 5.7 for the tested temperatures. These values are lower than the $\log K_{\text{soil-air,AI}}$ values (~6-9) and $\log K_{\text{soil-air,formulation}}$ values (~7) measured for chlorpyrifos previously using a similar experimental setup.⁷⁶ These results align well with those from field studies indicating that pesticide volatilization from plants is generally higher than from soil.⁸⁰ The $K_{\text{leaf-air,AI}}$ values for chlorpyrifos decreased with temperature, indicating increasing volatility with temperature (Figure 3.4). A decreasing

$K_{\text{leaf-air,AI}}$ with temperature was also previously observed for PCBs, HCHs, and PAHs on leaf surfaces.^{26–28} Our measured $K_{\text{leaf-air,AI}}$ values for chlorpyrifos decreased by ~ 0.7 log units over the 20 °C temperature range. For comparison, Kömp and McLachlan²⁷ reported a decrease of ~ 1 -2 log units for $K_{\text{leaf-air}}$ values of PCBs with ryegrass over the

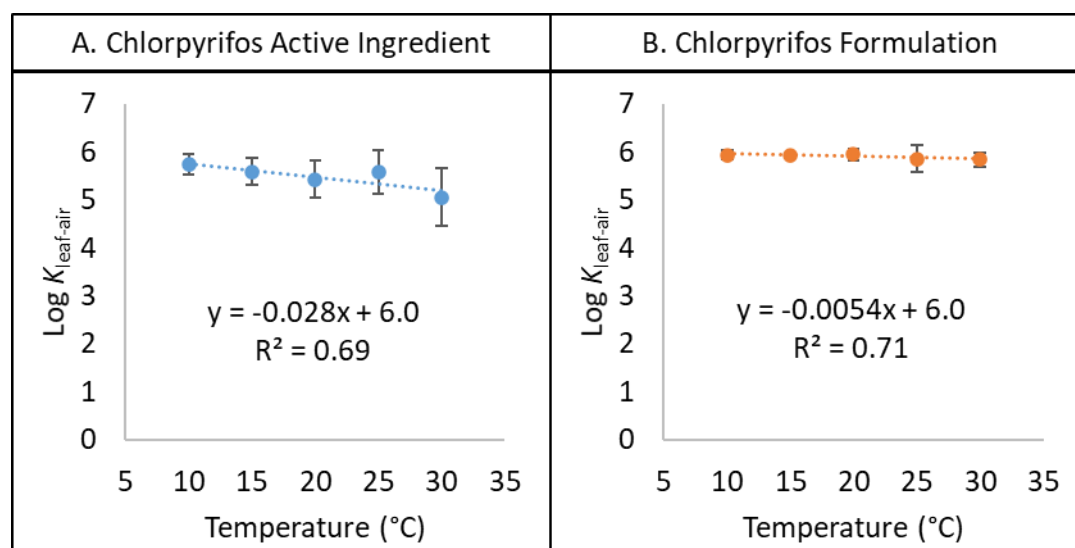


Figure 3.4 Measured log $K_{\text{leaf-air}}$ values over a range of temperatures. All tests were conducted at 100% relative humidity. Error bars indicate standard deviation ($n = 3$).

same temperature range.

The mean chlorpyrifos $K_{\text{leaf-air,formulation}}$ values also decreased with temperature; however, the change was ~ 0.09 log units over the tested temperature range and was thus much smaller than that for the $K_{\text{leaf-air,AI}}$ values. The mean log $K_{\text{leaf-air,formulation}}$ value was ~ 5.9 over the tested temperature range, indicating that the adjuvants significantly affected chlorpyrifos interactions with leaves in a way that decreased volatilization, especially at higher temperatures. It is logical that the $K_{\text{leaf-air,formulation}}$ values were higher than the $K_{\text{leaf-air,AI}}$ values because the purpose of many adjuvants in pesticide formulations is to decrease volatilization of the active ingredient.^{81,82} Nonetheless, the effects of adjuvants on $K_{\text{leaf-air}}$ values have not been quantified before and although $K_{\text{leaf-air}}$ measurements need

to be made for other pesticides, this observation has major implications for pesticide fate modelling in agroecosystems.

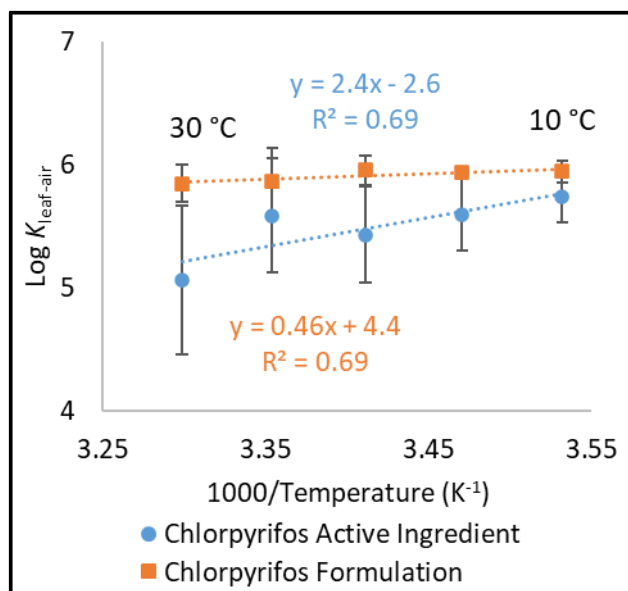


Figure 3.5 Measured $\log K_{\text{leaf-air}}$ values over a range of temperatures. All tests were conducted at 100% relative humidity. Error bars indicate standard deviation ($n = 3$).

We also calculated the change in internal energy for the phase transfer of chlorpyrifos from the leaf to gas phase ($\Delta_{\text{leaf-air}}U$) from the slope of the linear regression of $\log K_{\text{leaf-air}}$ versus $1/T$ (Figure 3.5) using equation 3.1.^{27,83}

$$\Delta_{\text{leaf-air}}U = 2.303 \cdot A \cdot R \quad (3.1)$$

where A is the slope, R is the ideal gas constant ($0.008314 \text{ kJ mol}^{-1} \text{ K}$), and 2.303 is the multiplication factor to convert from the common to the natural logarithm. The chlorpyrifos $\Delta_{\text{leaf-air}}U_{\text{AI}}$ and $\Delta_{\text{leaf-air}}U_{\text{formulation}}$ values were 45 and 9 kJ mol^{-1} , respectively. The ΔU is usually used to express the energy required to break intermolecular attractive forces between the chemical of interest and matrix compounds. However, in the case of leaf-air transfer, the ΔU is likely affected by the competing effects of temperature on the processes taking place on the leaf surface (i.e. volatilization versus diffusion to interior

leaf layers). Nonetheless, the $\Delta_{\text{leaf-air}}U$ values do indicate the sensitivity of the partition coefficient to temperature and thus can be used in the van't Hoff equation to calculate partition coefficients at temperatures other than the measured ones.⁸³ Most previous studies measured $K_{\text{leaf-air}}$ values at 25 °C. For our comparisons, we used the van't Hoff equation (3.2) to adjust predicted $K_{\text{leaf-air}}$ values (from Table 3.1) to other temperatures (T). We used the equation reported previously by Kömp and McLachlan.²⁷

$$K_{\text{leaf-air}}(T) = K_{\text{leaf-air}}(T_{\text{ref}}) * e^{[(\frac{\Delta H_{i,\text{leaf-air}}}{R})(\frac{1}{T} - \frac{1}{T_{\text{ref}}})]} \quad (3.2)$$

where $\Delta H_{i,\text{leaf-air}}$ is the enthalpy associated with the transfer of chemical, *i*, from the plant phase to air. To obtain $\Delta H_{i,\text{leaf-air}}$ values for our chemicals, we used the predictive equation reported by Taylor et al.⁴⁰ This equation (3.3) relates $\Delta H_{i,\text{leaf-air}}$ and $K_{\text{octanol-air}}$ values.

$$\Delta H_{i,\text{leaf-air}} = (1.4 \log K_{\text{octanol-air}}(298\text{ K})^2 - 0.24 \log K_{\text{octanol-air}}(298\text{ K}) - 0.55) \quad (3.3)$$

The $\Delta_{\text{leaf-air}}U$ values we measured are significantly lower than those predicted from the $\Delta_{\text{leaf-air}}H$ estimation equation presented in Taylor et al.⁴⁰ followed by conversion to $\Delta_{\text{leaf-air}}U$ (103 kJ/mol). The Taylor equation was derived from the relationship between $K_{\text{leaf-air}}$ and $K_{\text{octanol-air}}$ values for PCBs with ryegrass that were reported by Kömp and McLachlan.²⁷ This highlights the need to experimentally measure $\Delta_{\text{leaf-air}}U$ values for more compounds of interest and to not rely on predictions from PCB data. Our $\Delta_{\text{leaf-air}}U$ values were also substantially lower than the chlorpyrifos $\Delta_{\text{soil-air}}U_{\text{AI}}$ and $\Delta_{\text{soil-air}}U_{\text{formulation}}$ values (328 and 90 kJ mol⁻¹, respectively) reported previously,⁷⁶ indicating that the $K_{\text{leaf-air}}$ values are less sensitive to temperature changes than $K_{\text{soil-air}}$ values.

3.3.2 Influence of Temperature on Foliar Penetration

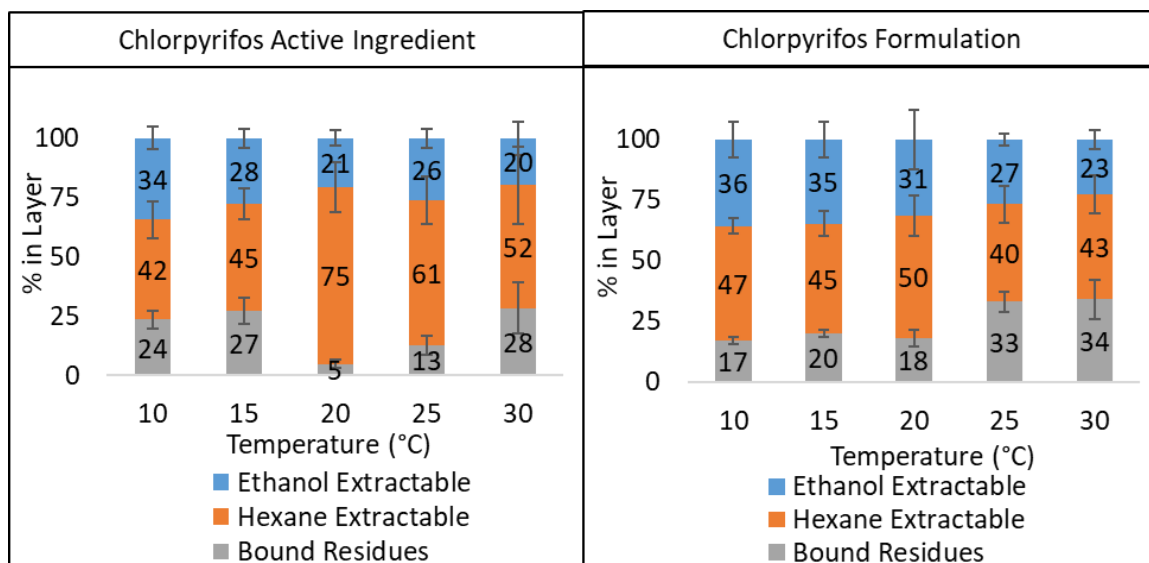


Figure 3.6 Mean percent of insecticide measured in each of the three leaf layers extracted at the end of 16-h tests conducted at five temperatures. All tests were conducted at 100% relative humidity. Error bars indicate standard deviation ($n=3$).

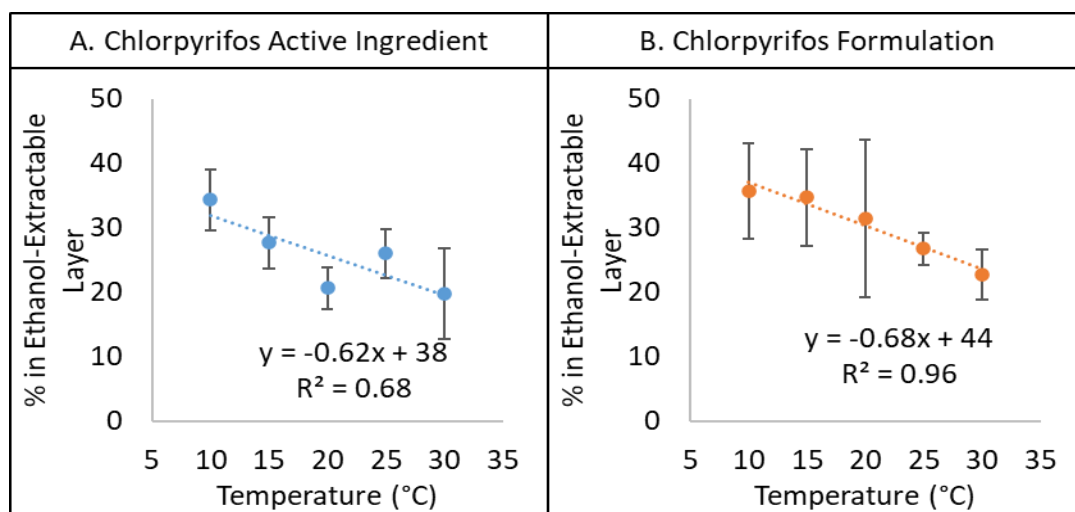


Figure 3.7 Percent in the ethanol-extractable layer over a range of temperatures. All tests were conducted at 100% relative humidity. Error bars indicate standard deviation ($n = 3$).

The distribution of chlorpyrifos in the three leaf extracts (i.e., mass in each extract divided by the total mass recovered in the three leaf extracts) was measured at the end of each of the 16-h tests conducted at five temperatures (Figure 3.6). The percent in air was

not included in these calculations since the mass measured in air was several orders of magnitude lower than in the leaf layers. Depending on the temperature, 20-34% of chlorpyrifos active ingredient (Figure 3.7A) was found in the ethanol-extractable layer; we assume that this portion was either unbound or sorbed to the leaf surface while most of the remaining mass had undergone penetration to deeper layers. For these tests, the mean percent in the ethanol-extractable layer decreased with temperature; however, the correlation was not significant ($p > 0.05$). Increasing foliar penetration with temperature can be attributed to increasing molecular diffusion with temperature.³⁴ No meaningful trends were observed for the percent of chlorpyrifos in either the hexane-extractable or bound-residue layers (Figure 3.6).

For tests conducted with chlorpyrifos formulation, the percent in the ethanol-extractable layer also decreased with temperature and in this case, the correlation was significant ($p < 0.05$) (Figure 3.7B). Previously, Lichiheb et al.⁶⁵ measured the foliar penetration rates of two fungicides in wheat leaves over 24 h; tests were conducted with chlorothalonil active ingredient alone and epoxiconazole as both active ingredient and in a formulation. Lichiheb et al.⁶⁵ noted that the influence of formulation additives on foliar penetration are specific to the mode of action of the pesticide: contact pesticide formulation additives promote surface adsorption while systemic pesticide formulation additives promote foliar penetration. A minor version of this effect was observed for chlorpyrifos (a contact insecticide⁸⁴) since the mean percent of formulated chlorpyrifos in the ethanol-extractable fraction was several percentage points higher than that of the chlorpyrifos active ingredient at every temperature; however, these differences were not statistically significant.

3.3.3 Influence of Relative Humidity on $K_{\text{leaf-air}}$ and Foliar Penetration

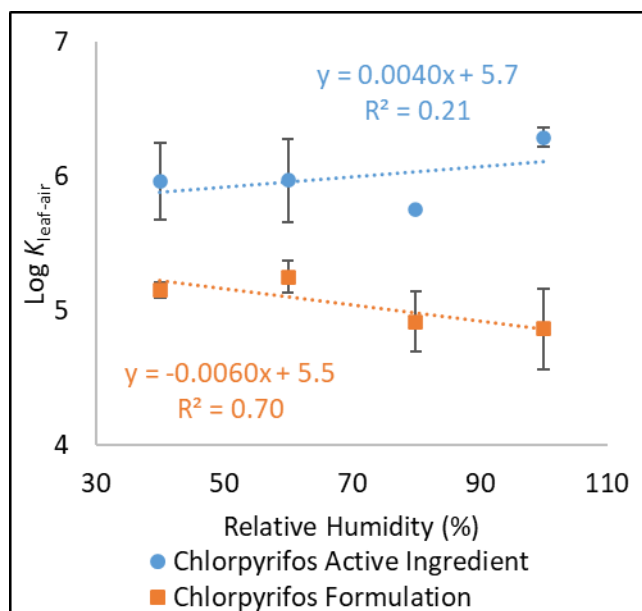


Figure 3.8 Measured $\log K_{\text{leaf-air}}$ values at different relative humidity conditions. All tests were conducted at 25 °C. Error bars indicate standard deviation (n = 3).

Relative humidity did not significantly affect any of the sets of measured $K_{\text{leaf-air}}$ values (the absolute value of all slopes was less than 0.01) (Figure 3.8). This is an interesting result because previous studies have shown that relative humidity significantly affects soil-air partitioning of pesticides⁸⁵ and PCBs,⁸⁶ mineral-air partitioning of organic substances,⁸⁷ and leaf cuticle penetration rates.⁶⁰ The lack of sensitivity to humidity may have occurred because leaves already contain water internally and thus, changes in air humidity did not significantly affect leaf properties. Additionally, the waxy leaf cuticle may have created a barrier preventing water from influencing the leaf properties, in contrast to behavior of water with soil and mineral surfaces.

The distribution of chlorpyrifos among extracts was also measured at the end of the 16-h tests at four relative humidity levels (Figure 3.9). The percent in the different layers were relatively consistent for tests conducted with both chlorpyrifos active

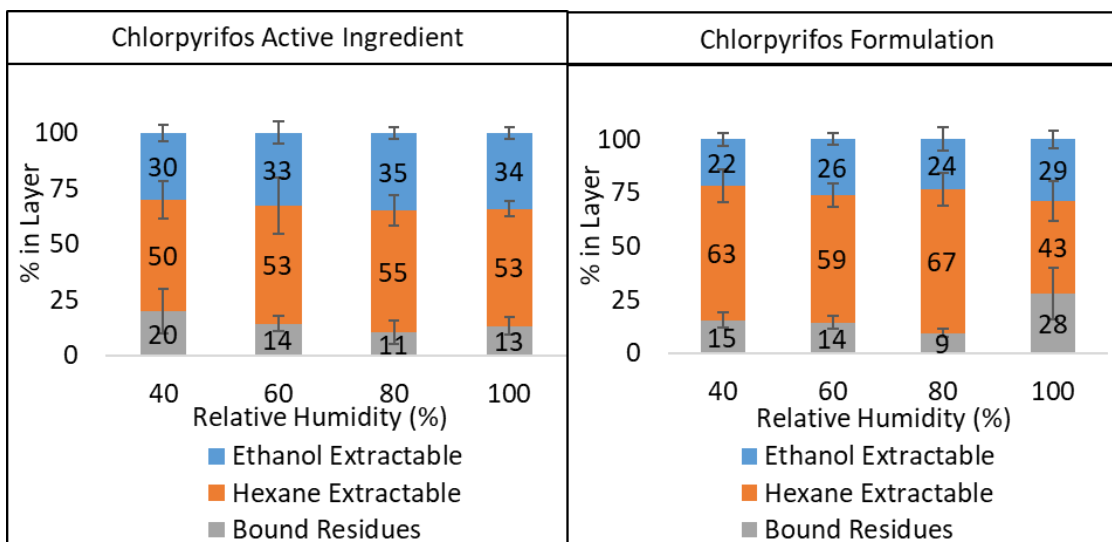


Figure 3.9 Mean percent of insecticide measured in each of the three leaf layers extracted at the end of 16-h tests conducted at four different relative humidity levels. All tests were conducted at 25 °C. Error bars indicate standard deviation (n=3).

ingredient alone and in the formulation at different humidity levels. This led us to conclude that relative humidity does not strongly affect foliar penetration for these systems. This is likely due to the same reasons that relative humidity did not affect our $K_{\text{leaf-air}}$ values as discussed previously.

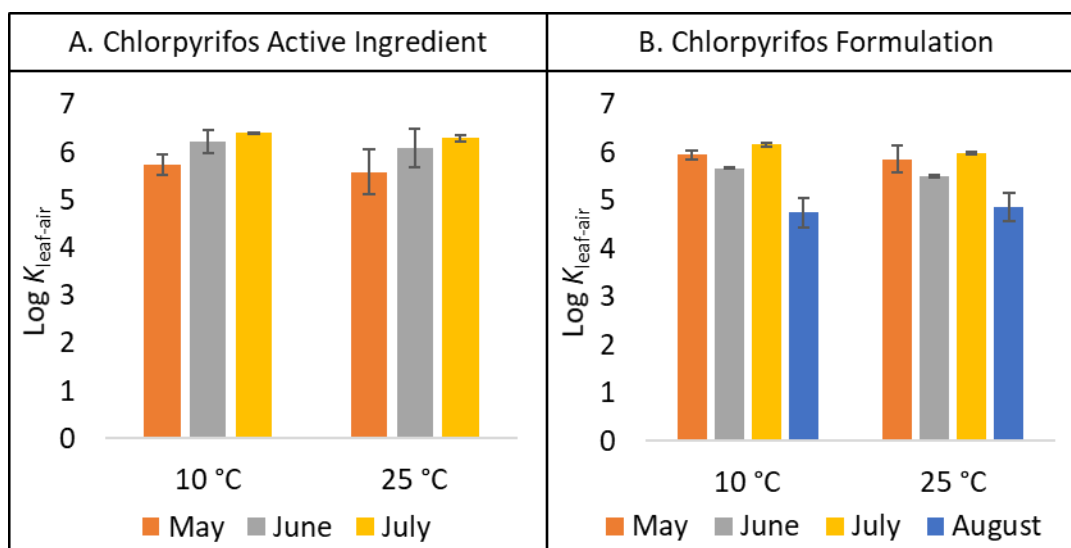


Figure 3.10 Measured log $K_{\text{leaf-air}}$ values measured from leaves collected in different months in 2020 for experiments conducted at 10 °C and 25 °C. All tests were conducted at 100% relative humidity. Error bars indicate standard deviation (n=3).

3.3.4 Influence of Leaf Collection Date on $K_{\text{leaf-air}}$ and Foliar Penetration

Chlorpyrifos $K_{\text{leaf-air,AI}}$ and $K_{\text{leaf-air,formulation}}$ values were measured separately using leaves collected during different months of summer 2020 (May-July for chlorpyrifos active ingredient and May-August for the formulation) at 10 and 25 °C (both at 100% relative humidity). The mean $K_{\text{leaf-air,AI}}$ and $\log K_{\text{leaf-air,formulation}}$ values varied by 1.4 log units (4.8-6.2 for the formulation at 10 °C) for leaves collected in different months in summer 2020 (Figure 3.10). To illustrate how this range in $K_{\text{leaf-air}}$ values could affect pesticide fate modeling outputs, we used the low and high mean measured $K_{\text{leaf-air}}$ value from the monthly tests at 25 °C as inputs in the PeDAL model⁹ and obtained predicted dissipation rates after 24 h. The dissipation rate was defined as the percent of pesticide lost from the field due to a combination of foliar photodegradation and volatilization from both soil and leaf compartments. Default input values used in the model are shown in Table 3.4. The predicted dissipation rates were 28 and 81% for chlorpyrifos active ingredient with the high and low-end $K_{\text{leaf-air}}$ values, respectively, while they were 48 and 99% for chlorpyrifos in the formulation. These results show that predicted pesticide dissipation is very sensitive to the $K_{\text{leaf-air}}$ value used in the model and therefore the role of factors that could affect $K_{\text{leaf-air}}$ values in the field deserve more investigation.

The observed variability in $K_{\text{leaf-air}}$ could be due to differences in plant growth stage (which can impact leaf size, thickness, and accumulation of different foliar tissues) or environmental conditions. The alfalfa in our research field was cut several times during the summer, which confounded our ability to quantitatively assess effects of leaf age in this study. Thus, an in-depth study on the effects of parameters associated with leaf collection date on $K_{\text{leaf-air}}$ should be conducted in future studies. Foliar penetration results

also varied among tests conducted with leaves from different months (Figure 3.11), but with no observable trends.

Table 3.4 Model inputs used to compare measured and predicted $K_{\text{leaf-air}}$ values.

Month	April	
Day of Month	5	
Temperature	25	°C
Wind speed	2.3	m/s
Cloud coverage	10	%
Relative Humidity	100	%
Latitude	41.76	° (N is +)
Longitude	-111.81	° (W is -)
Time Zone	-7	(- for W of Greenwich)
Elevation	1412	m
Field area	10000	m ²
spray time	12	0-23
Mass applied	100	g
%I	100	on plants
K_{pa} equation	generic	
LAI	4	
leaf length	0.1	m
leaf thickness	0.0002	m
soil density	2.4	kg/L
f_{oc}	0.0174	g/g

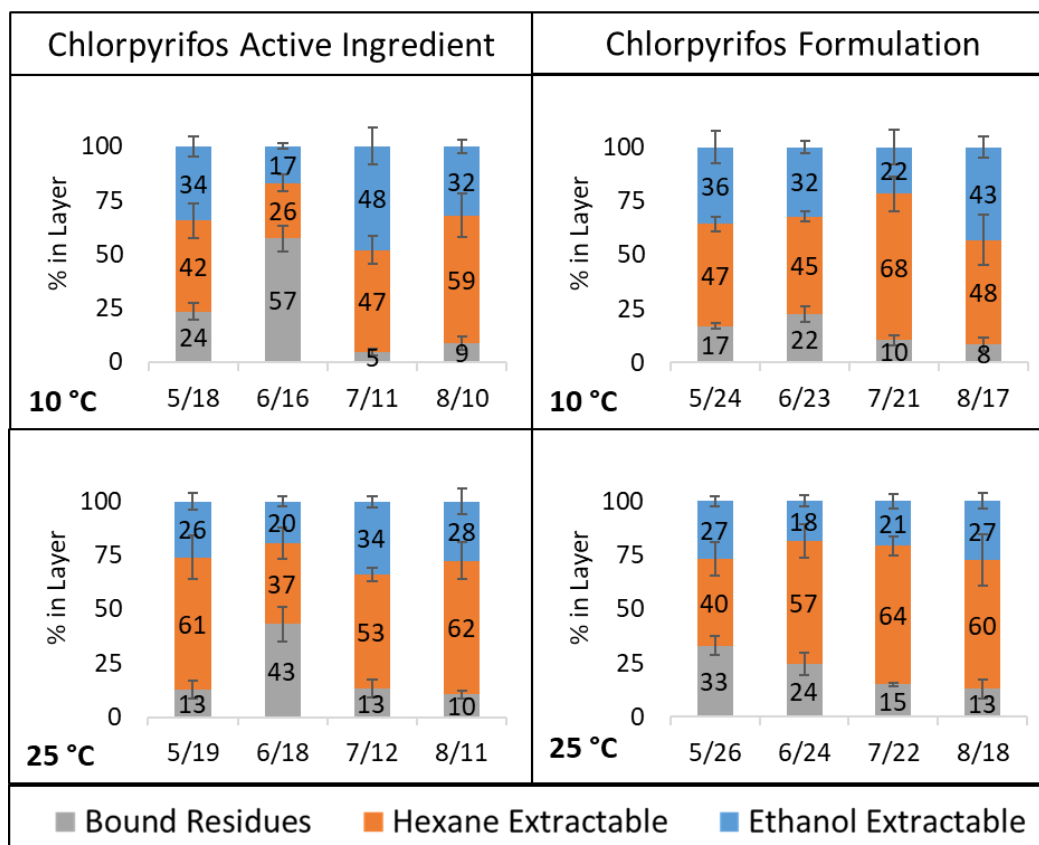


Figure 3.11. Foliar penetration data from leaves collected in different months in 2020 with experiments conducted at 10 °C and 25 °C and 100% relative humidity. Error bars indicate standard deviation ($n=3$).

3.3.5 Comparison of Measured to Predicted $K_{\text{leaf-air}}$ Values

We compared the mean measured chlorpyrifos $K_{\text{leaf-air}}$ values when using data from all months to the $K_{\text{leaf-air}}$ values calculated using the previously reported predictive equations (Table 3.1) as a way of assessing the validity of using such equations when measured $K_{\text{leaf-air}}$ are not available for specific plant-chemical combinations. This comparison at 10 °C and 25 °C is shown in Figure 3.12; note that we converted the $K_{\text{leaf-air}}$ values calculated using the predictive equation previously reported by Nizzetto et al.²⁶ to dimensionless ones for this exercise using the density of air at 10 °C and 25 °C (1.246 kg m⁻³, 1.184 kg m⁻³, respectively). Since the equations predict the $K_{\text{leaf-air}}$ at 25 °C, we

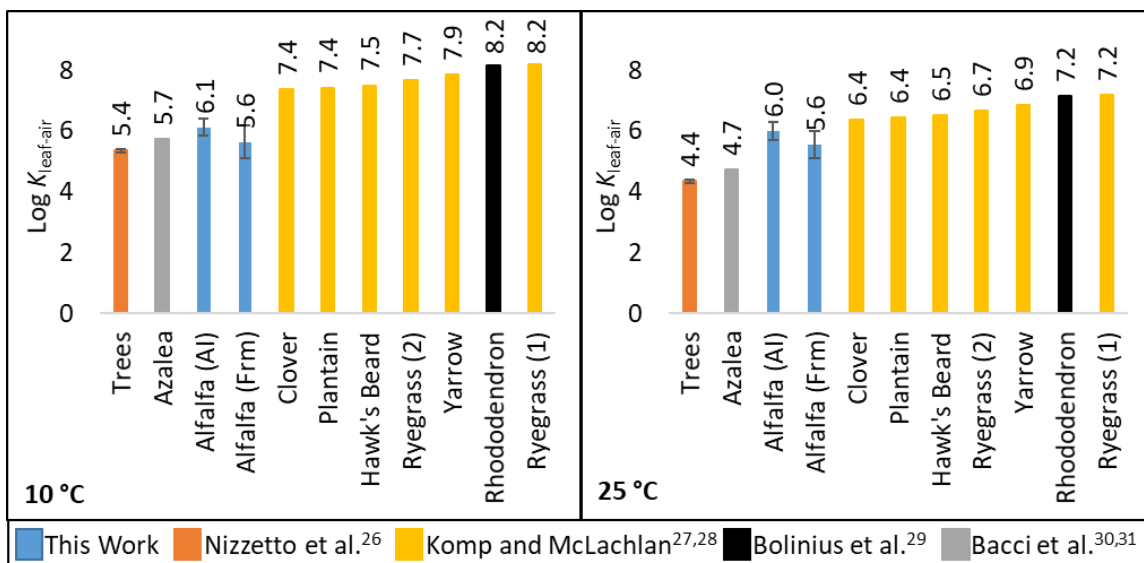


Figure 3.12 Comparison of our measured alfalfa log $K_{\text{leaf-air}}$ values at 10 and 25 °C for chlorpyrifos (as active ingredient (AI) and in formulation (Frm)), compared to predicted log $K_{\text{leaf-air}}$ values for other plant species determined using equations in Table 3.1. The mean and standard deviation shown for alfalfa was calculated from values measured in all months of the study (see Figure 3.10). The log $K_{\text{leaf-air}}$ values shown for trees is the mean for eight tree species as determined from field measurements.²⁶ The van't Hoff equation was used to adjust predicted $K_{\text{leaf-air}}$ values for temperature.^{27,85} Error bars represent standard deviation ($n=3$ for alfalfa (AI), $n=4$ for alfalfa (Frm), $n=8$ for trees.).

calculated the $K_{\text{leaf-air}}$ values at 10 °C using the van't Hoff equation and the $\Delta U_{\text{plant-air}}$ estimated with the Taylor et al. equation⁴⁰ since this is the approach we would have taken before measuring $K_{\text{leaf-air}}$ values for chlorpyrifos. Figure 3.12 shows that at 25 °C, the clover equation produces the best matched results (0.4 log units different from our measured $K_{\text{leaf-air,AI}}$), which is likely due to similarities between clover and alfalfa leaves. At 10 °C, the azalea predictive equation produces the best match; however, the difference is due to our measured values being less sensitive to temperature than predicted.

The relatively large range of measured $K_{\text{leaf-air}}$ values for both the active ingredient and the formulation depending on leaf collection date shown in Figure 3.10 may, in part, explain the range of $K_{\text{leaf-air}}$ values calculated using the different predictive equations

(Figure 3.12). The predicted $K_{\text{leaf-air}}$ values shown in Figure 3.12 span a range of 2.8 log units at both 10 and 25 °C. It is important to note, though, that leaf age is not the only factor leading to the range of predicted values in Figure 3.12, because different plant species used for measurements, different compounds used to create the predictive equations, and a difference in methods used for each study also is expected to produce a range in predicted $K_{\text{leaf-air}}$ values for chlorpyrifos.

In our previous work,^{9,40} we selected clover as a ‘generic plant’ and used Kömp and McLachlan’s²⁸ clover predictive equation to predict $K_{\text{leaf-air}}$ values when plant-specific equations were not available. While Figure 3.12 shows that the $K_{\text{leaf-air}}$ values for clover are closest to those for alfalfa at 25 °C, the difference between our measured $K_{\text{leaf-air,formulation}}$ and the predicted value is still 0.8 log units. We used our measured $K_{\text{leaf-air}}$ values and those from predictive equations as inputs in the PeDAL model to compare results.⁹ Default input values used in the model are shown in Table 3.4. When using the chlorpyrifos $K_{\text{leaf-air}}$ values predicted using the Kömp and McLachlan clover equation and the van’t Hoff equation for temperature adjustment using the Taylor et al. equation to calculate the $\Delta_{\text{leaf-air}}H$,⁴⁰ the modeled dissipation rates were 3% and 25% at 10 and 25 °C, respectively. In contrast, when we used the mean measured $K_{\text{leaf-air}}$ values for all months (6.1 and 6.0 at 10 and 25 °C for the active ingredient and 5.6 at both temperatures for the formulation), the modeled dissipation rate was 38% and 48% for chlorpyrifos active ingredient and 77% and 81% for chlorpyrifos in the formulation at 10 and 25 °C, respectively. This shows significant underestimation of the dissipation loss when using the Kömp and McLachlan clover equation, even at 25 °C, which only had a difference in $K_{\text{leaf-air}}$ values of 0.4 and 0.8 log units for the active ingredient and formulation,

respectively. These results further emphasize the need for improved tools to predict plant- and chemical-specific $K_{\text{leaf-air}}$ measurements.

3.3.6 Influence of Foliar Penetration on $K_{\text{leaf-air}}$ Values

The final objective of this work was to investigate the relationship between leaf-air partitioning and foliar penetration. To do this, we considered possible links between the observed temperature effects observed on $K_{\text{leaf-air}}$ (Figure 3.4) and foliar penetration (Figure 3.7). With regards to chlorpyrifos active ingredient, we observed that the $K_{\text{leaf-air}}$ values decreased with temperature, but that the sensitivity to temperature was rather weak. Our results suggest that the sensitivity of chlorpyrifos $K_{\text{leaf-air}}$ to temperature was not as strong as expected due to foliar penetration removing pesticide available for volatilization from the leaf surface. This volatilization-penetration link has important implications for pesticide behavior modeling and highlights the importance of directing future research towards measuring more $\Delta_{\text{leaf-air}}U$ and foliar penetration rates for current-use pesticides.

With regards to the chlorpyrifos formulation, we observed that temperature had a marginal effect on $K_{\text{leaf-air}}$ while at the same time, the effect of temperature on foliar penetration was similar to that for the active ingredient only. This observation is interesting because we can assume that the amount of pesticide available for volatilization was decreasing with temperature due to foliar penetration in the same way as was observed for the active ingredient, but that the more extreme loss in sensitivity to temperature was caused pesticide-adjuvant-leaf interactions on the leaf surface in the formulation experiments. In other words, in the formulation experiments, both foliar penetration and adjuvant interactions were working in concert to reduce volatility from

the leaf surface. Again, these observations have significant implications for pesticide modeling, highlighting the need for more measurements of pesticide physicochemical properties in the presence of adjuvants. Overall, our results indicate that there are several processes that affect $K_{\text{leaf-air}}$ values, and more work is needed to gain a better understanding of these processes.

Chapter 4. Optimizing a Pesticide Fate Model Using Field Dissipation Studies to Predict Honeybee Exposure

The content of this chapter has been written as a journal article that will be submitted to *Agricultural Science & Technology* with the author list: Ashlie D. Kinross, Sean Lyons, Kimberly J. Hageman, Micah McClure, and Randa Jabbour.

Sean Lyons contributed by completing the photodegradation studies and some of the field work. Dr. Kimberly J. Hageman contributed by providing feedback on the experimental design and the manuscript. Micah McClure contributed by taking field samples in two of the dissipation studies. Dr. Randa Jabbour contributed by providing feedback on experimental design and the manuscript.

4.1 Introduction

Pesticides are used in agriculture to protect crops and increase yields.⁴ However, this usage negatively impacts organisms and the environment when pesticides reach non-target areas. These negative effects can be minimized with a more complete understanding of the processes that control pesticide dissipation following application.² Dissipation is the total loss of pesticide from a field due to any process (including volatilization, photodegradation, and wash-off). Several models have been developed to predict pesticide dissipation from plants and/or soil and these models could be used by applicators to make more informed pesticide management decisions.^{56,88-90}

One such model is the Pesticide Dissipation from Agricultural Land (PeDAL) model.⁹ The PeDAL model includes components for simulating pesticide volatilization from soil and plant compartments, penetration into leaves, and photodegradation on leaves. The PeDAL model can be used to predict pesticide concentration in plants and soil over time after application. Two outputs that are useful when comparing application scenarios are the cumulative percentage lost in 24 hours from plants (CPL₂₄) and the time required for the pesticide concentration to dissipate to half of the original concentration following application (DT₅₀). Previously, the PeDAL model was evaluated by comparing DT₅₀ values for dissipation studies reported in the literature with predicted DT₅₀ for those same scenarios.⁹

While the model evaluation showed that the PeDAL model was capable of accurately predicting pesticide dissipation from leaves provided the necessary inputs were available, very few pesticide-plant specific foliar photodegradation rates have been measured. For pesticide foliar photodegradation, all but two rates^{91,92} we found in the

literature were measured on a “leaf proxy” (e.g. carnauba, paraffin, extracted leaf wax) instead of an intact leaf despite evidence suggesting these waxes don’t effectively mimic a leaf surface.⁹³⁻⁹⁶ Similarly, pesticide photodegradation on different fruit waxes have shown to vary by as much as a factor of five.⁹⁷ While the PeDAL model evaluation suggested that use of photodegradation data from a leaf type different from that being studied is not a large source of error, using pesticide-plant specific foliar photodegradation rates could enhance model performance.⁹ More photodegradation rates for pesticides on plant surfaces are needed to expand the applicability of the model.

Pesticide fate models can serve several purposes, with one of those being to provide inputs for pollinator risk assessment based on changing pesticide concentration in a field. Pesticide risk assessments usually rely on calculation of risk quotients (RQs), which indicate the ratio of the exposure concentration to a selected effect level, with the threshold of concern indicated by an RQ of 1. The method used herein to predict risk exposure for honeybees (*Apis mellifera*) is similar to that used previously;⁹⁸ however, the previous work focused on pesticide drift as the main exposure route to bees rather than the sprayed field itself. Risk assessments based on pesticide concentrations in sprayed fields are also clearly needed since agricultural fields can be a major source of pesticide exposure for both native bees and managed bees (e.g. honeybees and alfalfa leaf cutting bees) introduced to fields after pesticide application. Moreover, approaches for incorporating the effects of meteorology, field conditions, and application timing on pesticide concentrations, and therefore RQs, are needed in risk assessments.

The first objective of this work was to obtain foliar photodegradation rates for three insecticides (as the active ingredient alone as well as in a formulation) commonly

used on alfalfa (*Medicago sativa*, also known as lucerne). The selected insecticides were chlorpyrifos (CAS 2921-88-2), λ -cyhalothrin (CAS 91465-08-6), and indoxacarb (CAS 144171-61-9) due to their common application to alfalfa fields and their potential risk to honeybees. The second objective was to conduct field studies designed to investigate the effects of weather and crop conditions and application timing (specifically morning versus evening) on dissipation rates of chlorpyrifos and λ -cyhalothrin. The third objective was to use the results from the field studies to optimize the PeDAL model for predicting foliar pesticide concentrations during the week following pesticide application. The last objective was to use the optimized PeDAL model to determine how field-based pesticide RQs change over time following pesticide application and calculate the time to reach a specified RQ of one.

4.2 Materials and Methods

4.2.1 Materials

The following materials and chemicals were purchased from ThermoFisher Scientific (Massachusetts, USA) and subsidiary companies: acetone, acetonitrile, ethanol, ethyl acetate, *n*-hexane, Florisil (60-100 mesh size), sea sand, glass fiber and cellulose filter papers for the extraction cells, and diatomaceous earth (DE). Graphitized carbon black (GCB) was purchased from Sigma-Aldrich, Inc. (Missouri, USA) as ENVITM-Carb packing. All Florisil, diatomaceous earth, sea sand, and glassware were pre-cleaned by baking at 565 °C for 30 minutes prior to use.

The standards λ -cyhalothrin (99.5% purity), d10-chlorpyrifos (>97.5%), *p*-nitroanisole (>98%), and pyridine (99%) were purchased from ThermoFisher Scientific (Massachusetts, USA). The standard chlorpyrifos (98%) was purchased from Sigma-

Aldrich, Inc. (Missouri, USA), indoxacarb (97.9%) was purchased from LGC Dr. Ehrenstorfer (New Hampshire, USA), and d5-tertbutylazine (99.5%) was purchased from CDN Isotope Inc. (Quebec, Canada).

Commercial formulations containing the active ingredients chlorpyrifos, λ -cyhalothrin, and indoxacarb were obtained from local agricultural stores. The chlorpyrifos formulation was Drexel® Chlorpyrifos 4E-AG, the λ -cyhalothrin formulation was Warrior II with Zeon Technology®, and the indoxacarb formulation used was Steward® EC. Chemical properties and structures of the active ingredients are given in Tables 4.1-4.2 and information about the pesticide formulation are given in Table 4.3.

Table 4.1 Chemical properties of active ingredients used. Values were found using US EPA EpiSuite.¹¹¹

Property	Chlorpyrifos	λ -Cyhalothrin	Indoxacarb
Molecular Weight (g mol ⁻¹)	350.6	449.9	527.8
Log $K_{air-water}$	-3.92	-4.22	-10.95
Log $K_{octanol-water}$	4.96	7.00	4.65
Vapor Pressure (mm Hg)	2.0×10^{-5}	1.5×10^{-9}	1.2×10^{-10}
Water Solubility (mg L ⁻¹)	1.1	0.0050	0.20

Table 4.2 Chemical structures of the active ingredients used.

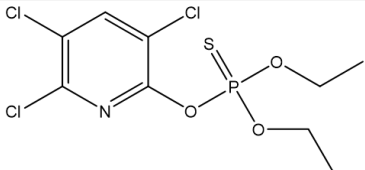
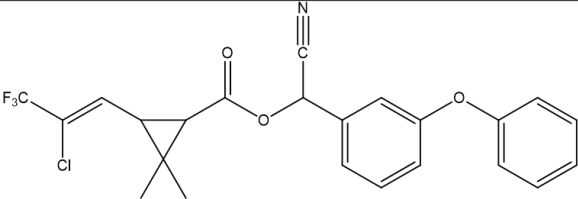
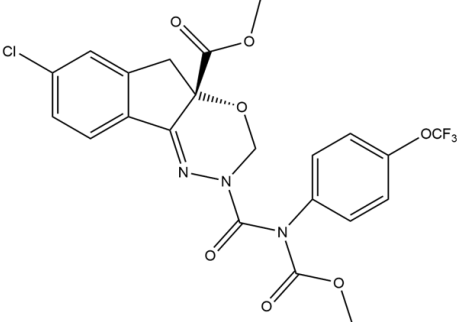
	Active Ingredient Structure
Chlorpyrifos	
λ-Cyhalothrin	
Indoxacarb	

Table 4.3 Pesticide formulation information.

	Chlorpyrifos	λ-Cyhalothrin	Indoxacarb
Formulation Name	Drexel® Chlorpyrifos 4E-AG	Warrior II with Zeon Technology®	Steward® EC
Pesticide Class	Insecticide	Insecticide	Insecticide
% Active Ingredient	44.9%	22.8%	15.84%
Other Ingredients	Petroleum distillates (concentration unavailable)	Titanium dioxide, petroleum solvent, other (concentration unavailable)	Octanol (1-5%), alkyl sulfonate salt (5-10%), other (69.16-78.16%)

4.2.2 Foliar Photodegradation Studies

4.2.2.1 Leaves

Alfalfa leaves were obtained from a research field near Logan, Utah on the same day they were used for each experiment. Experiments were performed in August and

September 2020 with leaves from fully grown alfalfa plants. The stems of individual leaves were threaded through a slit in polytetrafluoroethylene septa of gas chromatography (GC) vial caps, which were attached to GC vials containing deionized water (Figure 4.1). This setup aided in preserving leaf condition for the length of the experiment and in positioning the samples in the irradiation chamber. During trial runs, leaves became dried and discolored without the presence of water. GC vials were taped to the solar simulator sample tray in such a way that the alfalfa leaves were parallel to the tray surface and thus, each leaf received direct light exposure. Extra leaves were collected each day that an experiment was conducted for use in determining concentrations of pesticide present in leaves prior to their collection.



Figure 4.1 Alfalfa leaf setup for photodegradation experiments. For actual experimental samples, the leaf stem was pushed deeper into the vial so the leaf was positioned closer to the cap of the vial. This ensured a stable positioning of the leaves for the duration of the experiment.

4.2.2.2 Pesticide Application

Application solutions were prepared by dissolving the pure active ingredient or commercial formulation in ethyl acetate. In typical field applications, formulations are usually dissolved in water prior to application; however, we used ethyl acetate for these experiments since the selected pesticides were readily soluble in it and it evaporated quickly. We observed no visual damage to the leaf during our application procedure;

nonetheless, it is important to note that the ethyl acetate could have affected the leaf surface chemistry and we did not conduct tests to monitor this. The average surface area of an alfalfa leaf was determined to be 2.2 cm² and that area was used to calculate the pesticide mass needed to achieve the recommended application rates based on the commercial formulation labels (Table 4.4). Representing field conditions is important due to previous evidence suggesting that extremely high application rates can result in increased rates of photodegradation.^{99,100} After threading the leaves through the GC vial cap and positioning the leaves on the sample tray, a Hamilton syringe was used to apply 2800 ng/cm², 336 ng/cm², and 1230 ng/cm² of chlorpyrifos, λ -cyhalothrin, and indoxacarb to separate sets of leaves, respectively. The same mass of active ingredient was applied for both active ingredient and formulation studies.

Table 4.4 Foliar photodegradation application rates based on formulation label.

Pesticide Formulation	Active Ingredient Concentration (g L⁻¹)	Formulation Application Rate (L acre⁻¹)	Experimental Application Rate (ng cm⁻²)
Drexel® Chlorpyrifos 4E-AG	479	0.24	2800
Warrior II with Zeon Technology®	249	0.06	336
Steward® EC	150	0.33	1230

Following application to each leaf, solvent was evaporated in the dark prior to irradiation for 15 minutes. Application reproducibility was measured and found to be consistent (chlorpyrifos, λ -cyhalothrin, and indoxacarb had relative standard deviation percentages of 5.1%, 10.0%, and 12.6%, respectively ($n=3$)).

4.2.2.3 Irradiation

The spectrum of light produced by the SunTest CPS+, shown in Figure 4.2, was obtained using an Apogee PS-300 Spectroradiometer. Filters were used to cutoff wavelengths <280 nm to mimic the spectrum of sunlight observed at the surface of the Earth.¹⁰¹ The SunTest has previously been shown to effectively mimic natural sunlight.¹⁰² A cooler was attached to the SunTest to reduce volatilization of the studied compounds.

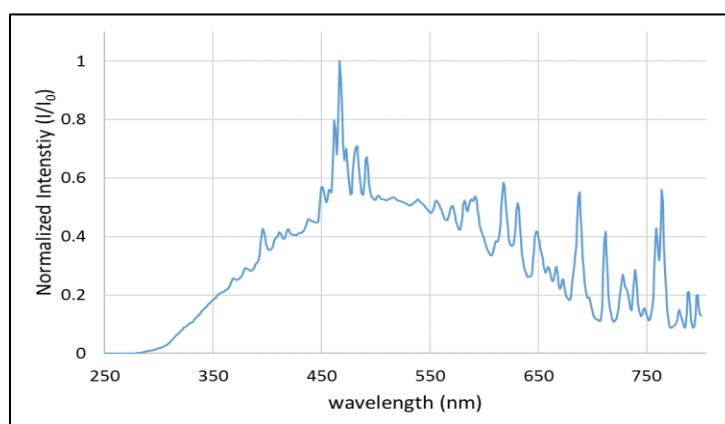


Figure 4.2 Spectrum of light produced by the Atlas SunTest CPS+ solar simulator.

Following solvent evaporation from leaves, the sample tray was placed into the solar simulator, which was set to irradiate samples at 550 W m^{-2} . Samples were irradiated for up to 8 h with samples being removed from the solar simulator at $t=0, 1, 2, 4, 6,$ and 8 h. When samples were removed from the solar simulator, individual leaves were stored in glass vials at $-20 \text{ }^{\circ}\text{C}$ until analysis. Dark controls were used to account for losses due to volatilization. The dark controls were placed in the solar simulator during experiments but were covered by aluminum foil to prevent light exposure. Similarly, to ensure that there was no transfer of pesticide from one leaf to another within the solar simulator, a leaf that received no pesticide was placed in the sample area and served as a blank. Cross-contamination in the solar simulator was not observed during any experiments.

4.2.2.4 Actinometry

The p-nitroanisole/pyridine (PNA/pyridine) chemical actinometer was used to account for possible fluctuations in light intensity during experiments.¹⁰³ Stock solutions of PNA in acetonitrile (10 mM) and pyridine in Milli-Q water (1 M) were prepared. In a dark environment prior to each experiment, these stock solutions were used to make a solution containing 10 μ M PNA and 1 mM pyridine. This solution was placed in quartz cuvettes, which were placed in the solar simulator. An actinometry sample was removed from the solar simulator each time leaf samples were removed. A dark control was used for the actinometry samples by covering one cuvette in aluminum foil for the duration of irradiation.

PNA and pyridine were quantified with a Shimadzu Prominence-i LC-2030C 3D with a UV detector and Agilent Poroshell 120 EC-C18 column (4.6 mm x 100 mm x 2.7 μ m). The mobile phase was 50:50 acetonitrile:water with a flow rate of 0.75mL/min. Peak areas were measured at 314 nm and the decrease in peak area with respect to irradiation times was used to monitor the intensity of light. The PNA/pyridine actinometer indicated that the light intensity was consistent throughout all experiments at 550 W m⁻². The equations used for these calculations can be found in Laszakovits et al.¹⁰³

4.2.2.5 Extraction and Analysis

Prior to extraction, a solution containing isotope-labelled surrogate compounds was spiked onto each leaf at a concentration equal to the initial pesticide application concentration to account for any losses during sample workup. d10-chlorpyrifos was used as the surrogate for chlorpyrifos and d5-tertbutylazine was used as the surrogate for λ -cyhalothrin and indoxacarb. 10 mL of ethanol was then added to each glass vial and the

vials were sonicated for 15 min using a Branson 1510 Ultrasonic Cleaner (New York, USA). The extracts were then concentrated to 1-2 mL under a gentle stream of nitrogen using a Biotage TurboVap II (North Carolina, USA).

The extracts were a dark green color and required additional cleanup. 15-cm glass pipettes were packed with glass wool followed by 0.6 g of Florisil and 0.1 g of GCB. The packed columns were conditioned with 5 mL of hexane and then 5 mL of 4:1 hexane:acetone immediately prior to their use. The concentrated extracts were then added and eluted with an additional 15 mL of 4:1 hexane:acetone. Eluent was concentrated to ~300 μ L using the Biotage TurboVap II. Preliminary spike and recovery experiments showed that the chlorpyrifos, λ -cyhalothrin, and indoxacarb recoveries were $79\pm 4\%$, $86\pm 9\%$, and $97\pm 12\%$, respectively, for the total extraction and cleanup process.

Pesticides were quantified using a ThermoFisher Scientific (Massachusetts, USA) Trace 1310 Gas Chromatograph (GC) coupled to a TSQ 8000 Evo triple quadrupole mass spectrometer (MS). Target analytes were separated with a 30 m x 0.25 mm x 0.25 μ m ZB-5MSplus fused silica capillary column (Phenomenex, California, USA) with a 10-m deactivated guard column. The inlet temperature was 300 °C and injections were conducted in splitless mode. The oven temperature program for chlorpyrifos was 90°C (hold 0.5 min), ramp to 300°C at 15°C/min, hold at 300°C for 10 minutes. For λ -cyhalothrin and indoxacarb, the oven temperature program was 90°C (hold 0.5 min), ramp to 170°C at 15°C/min, ramp to 300°C at 9°C/min (hold 10 min). The MS was operated with electron ionization and selective reaction monitoring (EI-SRM) for chlorpyrifos and indoxacarb and with single ion monitoring (EI-SIM) for λ -cyhalothrin. Target analyte SIM and SRM ions are provided in Table 4.5. An eight-point calibration

curve was prepared from the peak area ratios of the target analyte to the corresponding surrogate for each pesticide. There were no non-detects in this work. Characterization of the degradation products was not conducted and considered beyond the scope of this work. There is little known about photodegradation products of pesticides and their toxicity so this should be considered in future studies.

4.2.2.6 Calculating photodegradation rates

Table 4.5 GC-MS/MS SIM and SRM transition ions.

Compound	MS Quantitation Peak	MS Confirming Peak 1	MS Confirming Peak 2
d5-Terbuthylazine	178/143	219/137	219/76
λ-Cyhalothrin	197	181	208
Chlorpyrifos	314/258	286/258	316/260
Indoxacarb	218/203	264/176	203/134
d10-Chlorpyrifos	324/260	236/197	326/262

The concentration of pesticide present on leaves, normalized against the initial concentration, with respect to irradiation time was graphed and fit with an exponential line of the form in equation 4.1.

$$c_t = c_0 e^{-k_{\text{photo}} t} \quad (4.1)$$

where c_t is the pesticide concentration at time t , c_0 is the initial pesticide concentration, k_{photo} is the pseudo-first order photodegradation rate constant, and t is irradiation time.

We use the term ‘pseudo-first order’ when describing the rates because the nature of the decay depends on the reaction conditions.¹⁰⁴ After calculating these pseudo-first order rates, t-tests were conducted using Microsoft Excel to determine if the rates for the active ingredient and formulation of each pesticide were statistically different (with 95% confidence intervals).

4.2.3 Field Dissipation Studies

4.2.3.1 Field and Pesticide Application

Six field dissipation studies were performed: four on seed alfalfa plots in Logan, Utah, during the spring and summer of 2020 and two on hay alfalfa plots in Lingle, Wyoming during the spring of 2021. For each dissipation study, pesticide was applied to 0.1 acre of alfalfa for the Utah studies and to 0.04 acre of alfalfa for the Wyoming studies. Three of the studies performed in Utah were designed to measure the dissipation of chlorpyrifos when applied as the commercial formulation. These were conducted in three different months so that the effect of different weather conditions on chlorpyrifos concentrations in the field could be observed. The fourth study in Utah and the two studies in Wyoming were designed to measure the dissipation of the λ -cyhalothrin when applied as the commercial formulation. These studies were conducted to observe differences in λ -cyhalothrin behavior in seed versus hay fields and with different application timings (one morning and one evening). Additional details about applications are in Tables 4.6-4.7.

Table 4.6 Details for the chlorpyrifos field dissipation trials and PeDAL model input values.

	Chlorpyrifos Trial #1	Chlorpyrifos Trial #2	Chlorpyrifos Trial #3
Month	July	August	September
Day of Month	13	11	25
Application time (24 h clock)	9	9	10
Latitude	41.76°N	41.76°N	41.76°N
Longitude	111.81°W	111.81°W	111.81°W
Elevation (m)	1413	1413	1413
Leaf Area Index	5	6.5	5.5
Leaf length (m)	0.018	0.021	0.022
Leaf thickness (m)	0.000211	0.000195	0.000208
Drexel® Chlorpyrifos 4E-AG Application Rate (g a.i. / acre)	226	226	226

Table 4.7 Details for the λ -cyhalothrin field dissipation trials and PeDAL model input values.

	λ -Cyhalothrin Trial #1	λ -Cyhalothrin Trial #2	λ -Cyhalothrin Trial #3
Month	May	May	May
Day of Month	18	25	25
Application time (24 h clock)	9	10	20
Latitude	41.76°N	42.14°N	42.14°N
Longitude	111.81°W	104.35°W	104.35°W
Elevation (m)	1413	1272	1272
Leaf Area Index	6	5.25	5.25
Leaf length (m)	0.026	0.022	0.022
Leaf thickness (m)	0.000230	0.000211	0.000211
Warrior II with Zeon Technology® Application Rate (g a.i. / acre)	14	14	14

Hourly meteorological conditions were recorded throughout the experiments and are available in the appendix. Data includes air temperature, wind speed, and solar radiation intensity. No precipitation occurred during the field studies.

4.2.3.2 Sampling Protocol

Table 4.8 Leaf sampling times for each case study.

Trial	Sampling Times (h)
Chlorpyrifos Trials #1-3	0.5, 2, 4, 8, 12, 16, 24, 48, 96, 168
λ-Cyhalothrin Trial #1	0.5, 2, 4, 8, 12, 16, 24, 48, 96, 168
λ-Cyhalothrin Trial #2	1, 4, 7, 10, 22, 28, 34, 46, 58, 70, 82, 100, 124, 148, 172
λ-Cyhalothrin Trial #3	1, 6, 12, 18, 24, 36, 48, 60, 72, 90, 138, 162

Leaf sampling times for each case study can be found in Table 4.8. Sampling was conducted for ~7 days past the application day and each study included 10-15 sampling times. At each sampling time, samples were collected from three separate parts of the field and stored individually to determine the spatial variability of the insecticide

concentration within the field. All leaf samples were collected from the upper portion of the alfalfa plant (top 10 cm). After collection, leaf samples were placed in pre-baked aluminum foil packets and stored on ice until transport to the laboratory where they were then placed in a freezer at -20 °C until analysis. Baked foil packets were prepared for field sampling. Leaf samples were collected and placed into the foil packets which were then placed into individual plastic, sealable bags. All samples from a single time point were then placed into the same larger plastic, sealable bag. Latex gloves were changed in between each sample to ensure no cross-contamination. Field blanks were collected at the first and final time points by holding a bag open in the field for one minute so that the packets were open to the atmosphere. Background samples were also collected the same way one day prior to application. To ensure no contamination in the laboratory during extraction/analysis, laboratory blanks were run at the start and end of all extraction sequences. All field and laboratory blanks indicated that contamination did not occur.

4.2.3.3 Extraction and Analysis

Analytes were extracted from leaf samples following the extraction procedure used by Kinross et al.²⁵ First, leaf samples were crushed in liquid nitrogen using a mortar and pestle. A portion of the crushed leaf sample was weighed and homogenized with DE to absorb moisture. Pressurized liquid extraction (PLE) using an ASE-350 (ThermoFisher Scientific, Massachusetts, USA) was used for analyte extraction. Florisil and GCB were used for in-cell cleanup. The PLE cells were packed from bottom to top (opposite to the extraction solvent flow direction) with a cellulose filter, 5 g of Florisil, 0.6 g of GCB, a cellulose filter, leaf (0.5 g) and DE (1.5 g) homogenate, sand (to remove dead space in the cell), and a glass fiber filter. The same isotopically labeled surrogates used in the

photodegradation studies were spiked into the PLE cell before extraction to account for loss during sample workup. The solvent was 25:75 (v/v) ethyl acetate:*n*-hexane and the PLE parameters were: 5 min heat time, 10 min static time, 50% solvent flush, 3 static cycles, 120 s purge, 80 °C and 1500 psi. The percent recoveries for the full sample preparation procedure for chlorpyrifos and λ -cyhalothrin was $79 \pm 5\%$ and $100 \pm 7\%$, respectively. After extraction, extracts were concentrated to a volume of 300 μ L using a Biotage Turbovap II.

Quantification of field samples was conducted using a GC-MS-MS following the same procedures described for the photodegradation studies described in this manuscript.

4.2.4 Honeybee Risk Assessment

Honeybee risk exposure assessment was conducted for each field dissipation study using the pesticide concentrations in leaves predicted by the PeDAL model,⁹ optimized for pesticide applications to alfalfa according to the description in the Results section. The selected effect level was the lethal dose for 50% of the population (LD_{50}) for specific exposure routes (i.e. contact or oral). The LD_{50} values for each exposure route for honeybees were found in the Pesticide Properties Database (PPDB)¹⁰⁵ and ECOTOXicology Knowledgebase (ECOTOX).¹⁰⁶ When two LD_{50} values for the same compound and exposure route were listed, the smaller LD_{50} was used to represent a worst-case scenario. Bees in the field experience exposure through both contact and exposure pathways simultaneously, so the LD_{50} s for both contact and oral exposure routes were combined using the approach described by Barmaz et al.⁹⁸ The RQ was calculated with equation 4.2.

$$RQ = \frac{TDI_{\text{oral}}}{\text{Oral } LD_{50}} + \frac{TDI_{\text{contact}}}{\text{Contact } LD_{50}} \quad (4.2)$$

where TDI_{oral} is the total daily intake through the oral route and TDI_{contact} is the total daily intake through the contact exposure route. The TDI_{oral} was calculated with equation 4.3.

$$TDI_{\text{oral}} = C_{\text{plant}} \cdot M_{\text{pollen}} \quad (4.3)$$

where C_{plant} is the insecticide concentration in the plant tissue ($\mu\text{g}/\text{mg}$) and M_{pollen} is the mass of pollen consumed by honeybees daily (mg), which is 4.3 mg according to Barmaz et al.⁹⁸ The TDI_{contact} was calculated with equation 4.4.

$$TDI_{\text{contact}} = C_{\text{plant,surface}} \cdot SA_{\text{plant}} \quad (4.4)$$

where $C_{\text{plant,surface}}$ is the insecticide concentration on the leaf surface ($\mu\text{g}/\text{cm}^2$) and SA_{plant} is the surface area of plant contacted by bees daily (cm^2). The SA_{plant} for honeybees is $5 \text{ cm}^2 \text{ bee}^{-1}$ according to Barmaz et al.⁹⁸

4.3 Results and Discussion

4.3.1 Foliar Photodegradation Studies

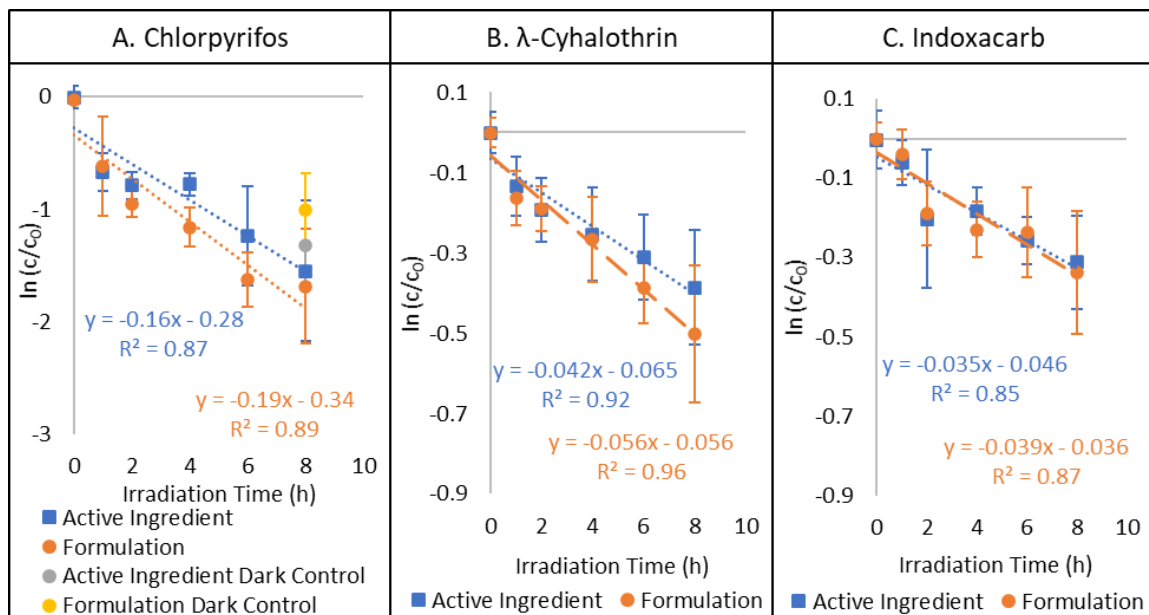


Figure 4.3 Foliar photodegradation of each compound on alfalfa leaves. Error bars represent standard deviation (n=3). c and c_0 are the concentration at the sampling time and the initial concentration, respectively.

During the photodegradation experiments for chlorpyrifos (both active ingredient and formulation) the irradiation chamber was kept at a consistent 21°C; however, this was not cool enough to prevent significant amounts of volatilization. The dark controls for the active ingredient and the formulation contained <40% of the initial chlorpyrifos (Figure 4.3A). No statistical difference was observed between the irradiated samples and the dark control removed from the solar simulator at the end of the experiment (t = 8 h). This demonstrates that photodegradation on alfalfa leaf surfaces is not a major dissipation pathway for chlorpyrifos, and that most of the dissipation is due to volatilization. This was also observed by Walia et al.,⁹¹ who observed only 30% degradation of chlorpyrifos on a soft-shield fern (*Polystichum setiferum*) after receiving 9 hours per day of simulated

sunlight at a constant 1000 W m^{-2} for 25 days (dark control still had 95% of initial chlorpyrifos mass present).⁹¹ Due to the lack of significant difference between the dark control and irradiated samples at the end of the experiment, no photodegradation rate was calculated. In extreme scenarios in which photodegradation may be an important process, such as conditions of unusually strong sunlight and unusually low temperatures, preventing volatilization, the photodegradation rates measured by Walia et al.⁹¹ should be used.

Table 4.9 Pseudo-first order foliar photodegradation rates for λ -cyhalothrin and indoxacarb on alfalfa leaves with 95% confidence intervals.

Chemical	Pseudo-first order foliar photodegradation rate constants (h^{-1})	
	Active ingredient	Formulation
λ -Cyhalothrin	0.042 ± 0.017	0.056 ± 0.018
Indoxacarb	0.035 ± 0.018	0.037 ± 0.021

The photodegradation rate constant for λ -cyhalothrin active ingredient was 0.042 h^{-1} (Table 4.9). The change in concentration over time during the photodegradation experiments suggests that the λ -cyhalothrin in formulation photodegraded slightly faster than the active ingredient (Figure 4.3B) with a rate constant of 0.056 h^{-1} (Table 4.9); however, these rates are not statistically different. The photodegradation rate constant for indoxacarb active ingredient was 0.035 h^{-1} (Table 4.9). The change in concentration over time during the photodegradation experiments suggests that the indoxacarb in formulation photodegraded at a similar rate to the active ingredient (Figure 4.3C) with a rate constant of 0.037 h^{-1} (Table 4.9). There was no statistical difference between the rate of photodegradation for the active ingredient when compared to the commercial formulation. For both λ -cyhalothrin and indoxacarb, the concentrations in the dark controls were $>90\%$ of those in samples that received no irradiation ($t = 0 \text{ h}$) indicating that the losses experienced in the irradiated samples can be predominantly attributed to

photodegradation. This was an expected result due to λ -cyhalothrin and indoxacarb's low vapor pressures (Table 4.9).

For all pesticides there was no statistically significant difference in the photodegradation rate of the pure active ingredient and the commercial formulation. While this has been observed for other pesticide active ingredient and formulations tested, formulation effects have also been shown to significantly increase photodegradation rate in some cases.^{100,107} Due to the uncertain effects of the additives in formulations, future experiments should be conducted with formulated pesticides to ensure the results are more useful for environmental modeling.

4.3.2 Field Dissipation Studies and Model Optimization

4.3.2.1 Chlorpyrifos

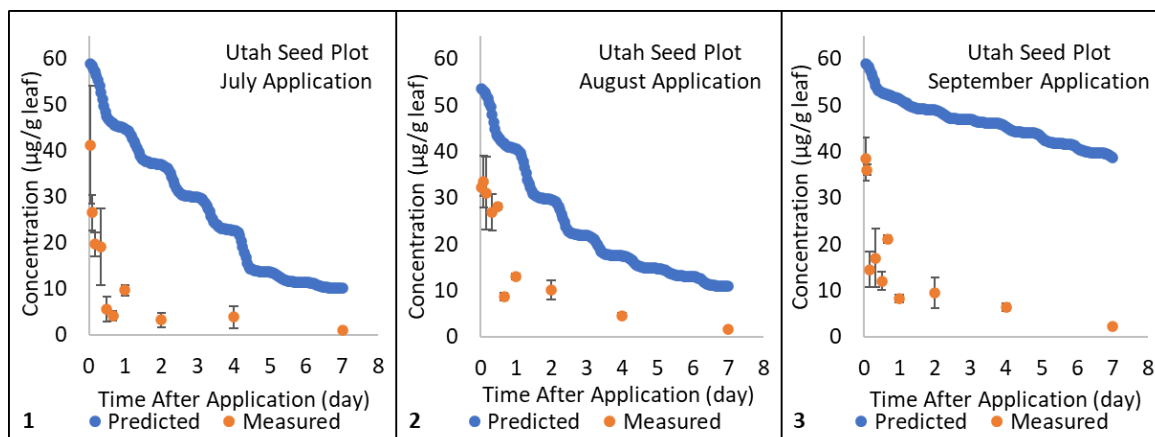


Figure 4.4 Predicted and measured chlorpyrifos concentrations in leaves for each trial when using the scenario-specific inputs shown in Table 4.6 and weather inputs from the appendix along with the plant intercept percentage set to 95%, soil density set to 2.4 kg/L, and the fraction of organic carbon set to 0.2 g/g. The numbers in the bottom left corner of each plot indicate the field trial number. For each scenario, the plant-air partition coefficient ($K_{\text{plant-air}}$) was calculated using the predictive equation for clover from Komp and McLachlan.²⁸ Error bars indicate standard deviation (n=3).

The PeDAL pesticide fate model was used to predict chlorpyrifos concentrations in leaves over a week for each field trial (Figure 4.4). The model did not accurately depict the dissipation shown by the measured concentrations when using default model inputs. The two obvious differences between the measured and predicted concentrations are the predicted initial concentration was higher than the measured concentration and the measured data shows a much faster decrease in concentration than the predicted data. Therefore, we had to optimize the model. The PeDAL model was previously shown to have good agreement between predicted and measured values of DT_{50} values,⁹ but has not been evaluated over a longer period of time. To produce predicted initial concentrations that were closer, we changed the plant intercept percentage. This input value specifies the amount of pesticide that is modeled to deposit on plants in the field rather than the soil. Whole number percentages were tested for each chlorpyrifos scenario to get good agreement between the predicted and measured initial concentrations for the three scenarios. An average value of 63% for the plant intercept percentage led to the best agreement between predicted and measured data. The predicted initial concentrations may have required adjustments due to the volatility of chlorpyrifos, which led to more volatilization during spraying, reducing the amount that landed on the target plants.

To better match the rate of dissipation observed in the chlorpyrifos studies, the plant-air partition coefficient ($K_{\text{plant-air}}$) was also changed. The $K_{\text{plant-air}}$ value due to the impact this factor has on volatilization, which is the main loss process for chlorpyrifos. In Chapter 3, it was noted that the lack of plant- and chemical-specific measured $K_{\text{plant-air}}$ values was likely a source of error in the model.⁹ In Chapter 3, the $K_{\text{leaf-air}}$ values were measured for the formulation we used in this work. The $K_{\text{plant-air}}$ values, though, varied

between months. In an attempt to optimize the model and make it most applicable for future chlorpyrifos studies on alfalfa fields, we used an equation to predict the temperature-specific $K_{\text{plant-air}}$ for each chlorpyrifos scenario. The trendline is given in equation 4.5.

$$y = -0.0051x + 7.1 \quad (4.5)$$

where x is the input for temperature in Kelvin and y is the $\log K_{\text{plant-air}}$ value. This equation was the trendline for the plot of the average $K_{\text{plant-air}}$ values at both 10 °C and 25 °C vs the temperature they were measured at in Kelvin. The predicted concentrations and measured concentrations after modifying the PeDAL model are shown in Figure 4.5.

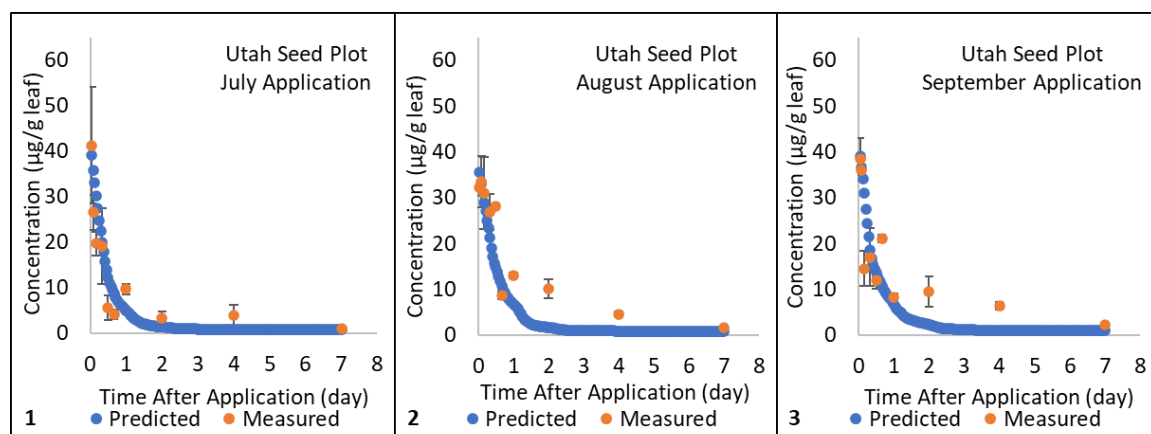


Figure 4.5. Predicted and measured chlorpyrifos concentrations in leaves for each trial after modifying the PeDAL model and when using the scenario-specific inputs shown in Table 4.6 and weather inputs from the appendix along with the soil density set to 2.4 kg/L, and the fraction of organic carbon set to 0.2 g/g. The numbers in the bottom left corner of each plot indicate the field trial number. Error bars indicate standard deviation (n=3).

Using the measured leaf concentrations (Figure 4.5), CPL_{24} and the DT_{50} values were calculated (Table 4.10). The chlorpyrifos trials were conducted in different months to evaluate the model over a range of meteorological conditions. Trial 1 and trial 3 showed similar measured CPL_{24} and DT_{50} values (77%, 78% and 0.31, 0.25 days,

respectively.) This was a surprising result because the meteorological conditions were most similar for chlorpyrifos trials 1 and 2 (average temperatures throughout the study was 22.2 °C and 22.8 °C, respectively) compared to trial 3 (average temperature was 13.0 °C). The plant parameters leaf area index and leaf thickness, though, were more similar between trial 1 and 3 compared to trial 2 (Table 4.6). This suggests that the plant parameters, which likely impact leaf processes, has a strong effect on pesticide dissipation. Trials 1 and 2 had warmer temperatures throughout the study, which is expected to lead to more volatilization. However, the CPL_{24} and DT_{50} values calculated using measured data show the trial with the fastest pesticide dissipation was trial 3 (the September application) and the slowest dissipation was trial 2 (the August application).

Table 4.10 Cumulative percentage lost in 24 hours from plants (CPL_{24}) and time to reach 50% of the initial plant concentration (DT_{50}) in days calculated using both the predicted concentrations and the measured chlorpyrifos concentrations.

	CPL_{24} (%)			DT_{50} (day)		
	Predicted	Measured	%Difference	Predicted	Measured	%Difference
Chlorpyrifos Trial 1	88%	77%	13%	0.30	0.31	3.3%
Chlorpyrifos Trial 2	81%	71%	13%	0.37	0.59	46%
Chlorpyrifos Trial 3	84%	78%	7.4%	0.28	0.25	11%

The leaf concentrations predicted by the optimized PeDAL model were also used to calculate the CPL_{24} and DT_{50} values (Table 4.10). The CPL_{24} and DT_{50} values from both the predicted and measured data were compared. Both values are similar for the chlorpyrifos trials, with all but one value having less than 15% difference between the values. For chlorpyrifos trial 2, though, the DT_{50} percent difference was 46%. The predicted and measured data for trial 2 (Figure 4.5), specifically the measured and predicted concentrations at Day 2, show the dissipation predicted by the model is faster

compared to the measured data. This difference in behavior is likely due to the $K_{\text{plant-air}}$ value used since Chapter 3 showed that this value can vary by more than one log unit based on the plant growth stage. This hypothesis is supported due to the different leaf properties recorded for trial 2 compared to trials 1 and 3 (Table 4.6). Chlorpyrifos trial 2 had similar leaf lengths to the other two trials, but leaves were not as thick for trial 2 and the leaf area index was higher for trial 2 than the other trials. This indicates that leaves were likely in different growth stages, which led to different volatilization behavior. However, the $K_{\text{plant-air}}$ value used in the PeDAL model still produced similar predicted CPL_{24} and DT_{50} values for the other two trials (completed in July and September), so the $K_{\text{plant-air}}$ value used is applicable for most of the trials. Also, even though percent difference was high for the DT_{50} of trial 2, the CPL_{24} had good agreement between the predicted and measured values, further indicating that PeDAL model is accurately describing the pesticide behavior after application, even when the application occurs in different months of the year.

4.3.2.2 λ -Cyhalothrin

The PeDAL pesticide fate model was used to predict λ -cyhalothrin concentrations in leaves over a week for each field trial (Figure 4.6). The model did not accurately depict the dissipation shown by the measured concentrations. For λ -cyhalothrin, the predicted concentrations were closer to the measured concentrations than for chlorpyrifos, but after ~2 days the measured concentrations were higher than the predicted concentrations. The main loss process for λ -cyhalothrin is photodegradation, so to reduce the loss due to this

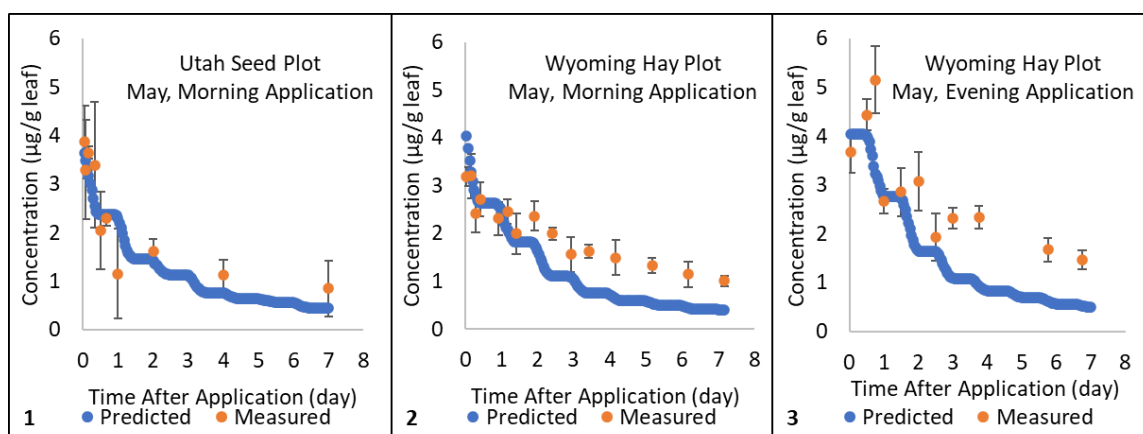


Figure 4.6 Predicted and measured λ -cyhalothrin concentrations in leaves for each trial when using the scenario-specific inputs shown in Table S7 and weather inputs from the appendix along with the plant intercept percentage set to 95%, soil density set to 2.4 kg/L, and the fraction of organic carbon set to 0.2 g/g. The numbers in the bottom left corner of each plot indicate the field trial number. For each scenario, the plant-air partition coefficient ($K_{\text{plant-air}}$) was calculated using the predictive equation for clover from Komp and McLachlan.²⁸ Error bars indicate standard deviation (n=3).

process and predict higher concentrations later in the modeled scenario using the PeDAL model, the leaf penetration rate was investigated. The PeDAL model considers any pesticide that has penetrated into the leaf unavailable for volatilization or photodegradation.⁹ This parameter was set in the model as a generic value of 0.002 h⁻¹,⁸⁹ but this process is likely chemical- and plant-specific so it is unsurprising that this value is a source of error in the PeDAL model. Leaf penetration rates from 0.002-0.010 h⁻¹

were tested for each scenario to find the rate that creates the best agreement between predicted and measured concentrations at the last sampling time. An average value of 0.008 h^{-1} for the leaf penetration rate led to the best agreement between predicted and measured data for λ -cyhalothrin. The predicted concentrations and measured concentrations after modifying the PeDAL model are shown in Figure 4.7.

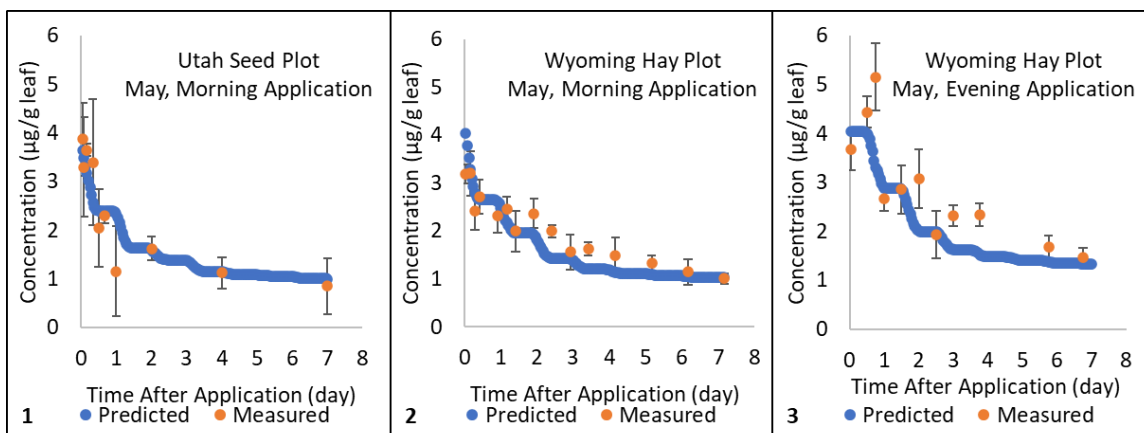


Figure 4.7 Predicted and measured λ -cyhalothrin concentrations in leaves for each trial after modifying the PeDAL model and when using the scenario-specific inputs shown in Table S6 and weather inputs from the appendix along with the soil density set to 2.4 kg/L , and the fraction of organic carbon set to 0.2 g/g . The numbers in the bottom left corner of each plot indicate the field trial number. Error bars indicate standard deviation ($n=3$).

Using the measured leaf concentrations (Figure 4.7), CPL_{24} and the DT_{50} were calculated (Table 4.11). For the λ -cyhalothrin trials, calculating the CPL_{24} and DT_{50} using the measured values were complicated due to several time points that had an increase in pesticide concentration over time. The main loss process for λ -cyhalothrin predicted by the model is photodegradation, so during the evening the model predicts very little loss. This minimal loss over time predicted as well as the variability in concentration may correspond to the measured pesticide concentration increases. This increase may also be due to other factors such as morning dew on the plants.

The λ -cyhalothrin trials were all completed in May, but were conducted on different alfalfa plot types (a seed plot and a hay plot), in different locations (Utah and Wyoming), and using different application times (morning and evening). The fastest dissipation occurred for trial 1, followed by trial 2 and the slowest dissipation study was trial 3. Comparing trial 1 and 2 (both were morning applications), trial 1 showed the fastest dissipation rate. This result could be due to several factors including the alfalfa plot type, the location of the study, or the leaf characteristics for this study (Table 4.7) since all of these factors vary between studies. Comparing trials 2 and 3 (both were conducted in Wyoming on hay plots), trial 2 showed faster dissipation. Trial 2 had an application time of 9:00am and trial 3 had an application time of 8:00pm. Trials 2 and 3 were conducted on the same day on fields that were near each other so the meteorological conditions as well as leaf characteristics were all the same, indicating that the difference in dissipation behavior is due to the difference in application timing. The PeDAL model predicts that the main loss process for λ -cyhalothrin is photodegradation, so we hypothesized that an evening application would reduce degradation immediately after application, prolonging the efficacy time. The observed results support this hypothesis. This is an important result because many farmers do not plan spraying with the intent of avoiding photodegradation directly after application. However, it is unclear whether spraying at night would be detrimental to the efficacy (if pests are not on plants until middle of day).

Using the optimized PeDAL model data (Figure 4.7), CPL₂₄ and the DT₅₀ were calculated from the predicted leaf concentrations and compared to the CPL₂₄ and the DT₅₀ values calculated from measured values (Table 4.11). For several trials, the percent difference is ~20%. The CPL₂₄ had better agreement between predicted and measured values for trial 2 and 3 when compared to the DT₅₀ values, but trial 3 had better agreement for the DT₅₀ values. Overall, based on the percent differences, the PeDAL model accurately predicted the pesticide concentration over time after application for all λ -cyhalothrin trials.

Table 4.11 Cumulative percentage lost in 24 hours from plants (CPL₂₄) and time to reach 50% of the initial plant concentration (DT₅₀) in days calculated using both the predicted concentrations and the measured λ -cyhalothrin concentrations.

	CPL ₂₄ (%)			DT ₅₀ (day)		
	Predicted	Measured	%Difference	Predicted	Measured	%Difference
λ -Cyhalothrin Trial 1	38%	46%	19%	1.2	1.1	8.7%
λ -Cyhalothrin Trial 2	40%	33%	19%	1.3	1.6	21%
λ -Cyhalothrin Trial 3	29%	27%	7.1%	1.9	2.2	15%

4.3.3 Honeybee Risk Quotients

Using the optimized model inputs for each scenario, the RQ was modeled based on predicted leaf concentrations over time (Figure 4.8). A RQ of one (Figure 4.8, red line) indicates that the field concentrations lead to bee exposure equal to the LD₅₀ concentration. The RQ graphs for the chlorpyrifos trials show that the predicted RQ drops below the threshold of one quickly but shows a consistent risk for the remainder of the seven days modeled. The RQ graphs for λ -cyhalothrin show that even for trial 1 and 2, which drop below the threshold of one, the predicted RQ remains very close to one even after seven days. In contrast to the other scenarios, λ -cyhalothrin trial 3 is predicted to not

reach a RQ of one during the seven days modeled. This supports the hypothesis that an evening application leads to higher pesticide concentrations compared to a morning application. However, this higher concentration over time is concerning because many farmers spray at night because they believe this is safer for bees. While this may be true in the sense that bees are not foraging during the evening, if the pesticide concentration poses a risk to honeybees longer than a morning application it overall would be more detrimental to bees to apply pesticide at night.

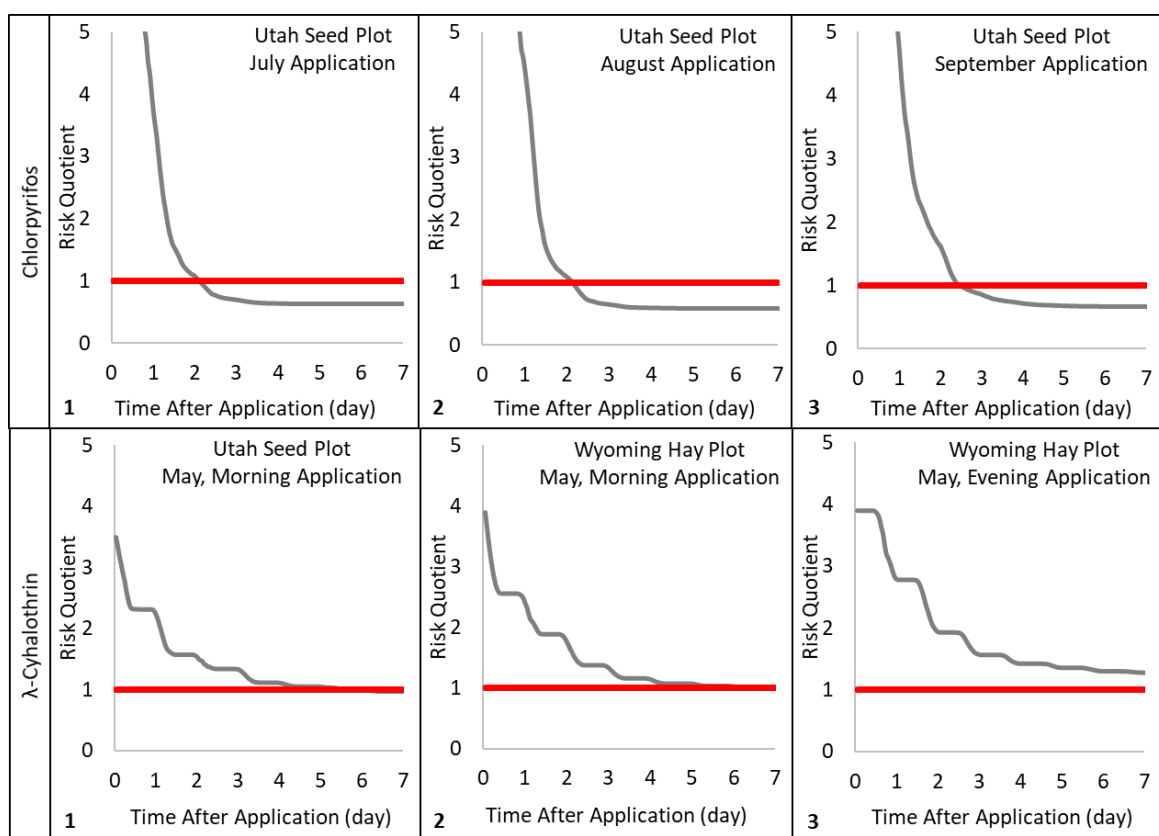


Figure 4.8 RQs over time based on the predicted plant concentration. The red line shows when the RQ equals one and the gray link indicates the RQ based on field conditions. The numbers in the bottom left corner of each plot indicate the field trial number.

In this work we only calculate RQs for honeybees, but alfalfa leaf-cutting bees (*M. rotundata*) are generally used to pollinate alfalfa fields. Because LD₅₀ values are not readily available for alfalfa leaf-cutting bees, we are unable to calculate a RQ using the method used in this work. However, alfalfa leaf-cutting bees are expected to be more vulnerable to pesticides than honeybees,¹⁰⁸ so the time for a RQ to reach one would likely be even longer than our predicted values for the honeybee.

Table 4.12 Leaf concentration seven days after pesticide application and the time when the RQ equals one (in days) when using predicted leaf concentrations from the PeDAL model as well as the measured leaf concentrations.

	Leaf Concentration at 7 days After Application ($\mu\text{g/g}$ leaf)			Time when Risk Quotient Equals 1 (day)		
	Predicted	Measured	%Difference	Predicted	Measured	%Difference
Chlorpyrifos Trial 1	0.83	1.0	19%	2.1	6.9	110%
Chlorpyrifos Trial 2	0.91	1.8	66%	2.1	6.8	110%
Chlorpyrifos Trial 3	0.96	2.3	82%	2.4	>7	NA
λ -Cyhalothrin Trial 1	1.0	0.85	16%	6.0	5.4	11%
λ -Cyhalothrin Trial 2	1.0	0.94	6.2%	6.3	6.5	3.1%
λ -Cyhalothrin Trial 3	1.3	1.4	7.4%	>7	>7	NA

To evaluate the optimized PeDAL model inputs, the time when the RQ equals one and the insecticide concentration in leaves at seven days after application was calculated using both the predicted and measured concentrations (Table 4.12). For chlorpyrifos trials the leaf concentration at seven days as well as the time when the RQ equals one do not agree for the predicted and measured data. For λ -cyhalothrin, though, there is good agreement between the predicted and measured data. We attribute the large percent differences for the chlorpyrifos trials to an incorrect penetration rate. While this rate has minimal effect on the initial decrease of pesticide, which is described using the CPL₂₄

and DT_{50} , the predicted pesticide concentrations during the later days of the field trial is strongly affected by the penetration rate. The agreement of the predicted and measured values for λ -cyhalothrin are likely due to the optimization of the penetration rate to match the measured values. This finding emphasizes the need to have accurate penetration rates, especially if we want to accurately predict pesticide behavior for longer periods of time, which is required when predicting RQs to inform decisions about pollinator management.

Chapter 5. Conclusion

5.1 General Conclusions

Pesticide is critical to protect crops from insects, weeds, and diseases, which would decrease the crop yield. Although pesticide use is necessary, it still carries risks due to the concern for non-target organisms. Therefore, understanding how a pesticide moves through an environment after it is applied is necessary to determine the most efficient application practices.

In chapter 2, I described the development of an extraction method for extracting 20 pesticides from both alfalfa and citrus leaves using the Accelerated Solvent Extractor (ASE). This method was modified for use with the Energized Dispersive Guided Extraction (EDGE) system. A comparison of extraction methods was conducted when packing the extraction cells with layered sorbent and leaf matrix as well as when the sorbents and leaf matrix was mixed before being added to the cell. The methods were compared in terms of lipid mass extracted, UV-Vis spectra of extract, percent recovery of pesticides, field concentrations measured, and extraction parameters such as extraction time and solvent volume used. There were no significant differences in the residual lipid mass extracted with each method. The UV-Vis data showed that while Florisil decreased the absorbance of the sample, GCB was required to remove most of the pigment from the samples.

The layered sorbent ASE method had significantly higher percent recoveries than the layered sorbent EDGE method for alfalfa and the mixed sorbent ASE method had significantly higher percent recoveries than the mixed sorbent EDGE method for both alfalfa and citrus tests when considering the average recovery of all pesticides. This

indicates that the ASE has better recoveries of spiked pesticides. Even with these results, though, only a handful of individual pesticides had significantly different percent recoveries when considering the pesticides individually. The field concentrations calculated when extracting leaves using each method showed no significant difference between any methods. This suggests the ASE and EDGE produce similar pesticide concentration in leaf extracts. The use of labelled surrogates to account for any loss during the extraction process may have contributed to the lack of significant differences. The extraction time for the ASE was ~45 minutes, while the EDGE only required ~10 minutes. This difference in extraction time can lead more efficient sample processing when using the EDGE. The ASE used slightly less solvent per extraction compared to the EDGE, but because no method development was performed on the EDGE the extra solvent may not be required to get the same percent recoveries.

The results presented show that the methods developed for each instrument are adequate to use for pesticide extraction from leaves. However, for other sample matrices that require deeper solvent penetration for extraction the high pressures used by the ASE may be necessary. This work was the first to quantitatively compare the new EDGE instrument to a previously used, trusted extraction instrument. This work provided future researchers details about using the EDGE that can guide the extraction method chosen as well as give insight into what drawbacks this new instrument may have.

In chapter 3, I measured the leaf-air partition coefficients ($K_{\text{leaf-air}}$) for chlorpyrifos (both as active ingredient alone and in a formulation) on alfalfa leaves using different experimental conditions. At the end of each experiment, leaves were sequentially extracted to investigate the foliar penetration at the different conditions. The $K_{\text{leaf-air}}$

values decreased with increasing temperature, which was the expected result based the theory that an increase in temperature leads to an increase in the movement of molecules, which allows them to break the bonds on the surface of the leaf more easily and can more readily volatilize. The active ingredient alone, though showed more sensitivity to temperature change than the formulation. The added components of a formulation are often added to increase the residency time of the pesticide on the leaf, so it is likely that these also work to offset the expected increase in volatilization with increasing temperature.

The foliar penetration was also affected by temperature. An increase in temperature led to more penetration, shown by a decrease in percentage on the leaf surface and an increase in the deeper leaf layers. This is expected because an increase in temperature results in more diffusion due to the increase in movement of the leaf waxes, which creates more space for pesticide to penetrate through. The results show that with increasing temperature, both volatilization and penetration increase. These two processes likely offset each other (more penetration means less pesticide on the surface to volatilize, but more volatilization reduces the amount of pesticide on the leaf available for penetration). For the active ingredient and formulation, the importance of these processes seems to be different since we observe different trends for the compounds. These trends were also different depending on the leaf growth stage, which is just another factor that complicates the measurement of $K_{\text{leaf-air}}$ values.

$K_{\text{leaf-air}}$ and foliar penetration was tested for leaves that were collected during different months to assess the influence of leaf age/plant growth stage on these processes. Both processes were affected by the leaf collection date, but no noticeable trends were

observed. Leaf growth stage could have impacted the leaf size, thickness, and accumulation of different foliar tissues, causing the differences in measured values between months.

The results from this work highlighted how complicated the interaction between pesticide and leaf surfaces are. This work can be used to guide researchers about what experimental conditions need to be investigated more using a broad range of chemicals (temperature and leaf age) and which should not be a high priority to evaluate (humidity). In future work researchers should do an in-depth study of the leaf properties that are affected by changing leaf stage such as the type of wax that is in the leaf cuticle.

In chapter 4, foliar photodegradation rates for two pesticides (both as active ingredients alone and as formulations) were measured and the formulation photodegradation rates were incorporated into a pesticide dissipation model. This model was then used to predict the pesticide concentration in plants after application to an alfalfa field for six field studies and compared to measured values from these studies. The chlorpyrifos tests were executed to evaluate the dissipation behavior in different months as well as evaluate the model predictions for different weather and crop conditions. The λ -cyhalothrin studies were conducted to evaluate the model at two different locations as well as evaluate the implications of applying a pesticide in the evening compared to the morning.

After comparing the model-predicted pesticide concentrations in the leaves and the measured concentrations, the model was optimized to improve the agreement between the values. For the chlorpyrifos studies, the model's plant-intercept percentage was adjusted to 63% to better match the starting measured concentrations. The volatilization

behavior predicted by the model showed improvement when the measured $K_{\text{leaf-air}}$ values for chlorpyrifos formulation from chapter 3 were incorporated into the model. These changes led to good agreement between the predicted and measured pesticide concentrations for the chlorpyrifos field studies. The chlorpyrifos studies completed in July and September showed similar dissipation behavior, which was surprising because the temperatures were most similar between the July and August studies. The plant properties were similar for the July and September studies, so this may indicate that the leaf properties have more effect on the dissipation behavior than the meteorological conditions.

The λ -cyhalothrin predicted concentration did not originally match the measured concentration after ~day 2 of the study. To adjust the model to better match the measured data, the foliar penetration rate was changed from 0.002 h^{-1} to 0.008 h^{-1} . This led to good agreement between data. The agreement of data for all trials suggest that the model accurately predicts pesticide concentration at multiple locations. Comparing the Wyoming morning and evening application trials, we see that the morning application has a faster dissipation from the field. This supports the hypothesis that spraying λ -cyhalothrin at night reduces the photodegradation of the compound, therefore decreasing the dissipation and extending the efficacy time. This information can give farmers insight about how spray timing can impact the efficacy time of the pesticide depending on the main loss process expected for the pesticide.

Using the optimized model for each pesticide, risk quotients were calculated for honeybees. The chlorpyrifos data did not show good agreement between the predicted and measured data. λ -cyhalothrin, however, showed good agreement. This is likely due to

using the optimized foliar penetration rate for λ -cyhalothrin while the chlorpyrifos model used a generic penetration rate. This optimized penetration rate is critical to accurately predict pesticide fate when modeling for more than ~ 2 days. This highlights the need for more compound- and plant-specific penetration rates to accurately predict pesticide fate as well as accurately assess the risk pesticides pose to honeybees. Even if the fate model is not perfect, though, it can still guide farmer application choices because it allows them to compare different spray scenarios and find the best option based on meteorological conditions as well as pesticide being applied.

In Chapter 3, it was shown that leaf properties have a strong impact on pesticide-leaf interactions and different plant growth stage leads to different leaf-air partitioning behavior. In Chapter 4, it was shown that the $K_{\text{leaf-air}}$ can greatly impact modelling results, and therefore impact risk quotient estimates made by the pesticide fate model. This work highlights some areas that need to be further investigated to accurately predict pesticide behavior after application to an alfalfa field.

5.2 Future Recommendations

The ASE generally had better percent recoveries than the EDGE. However, no work was conducted to optimize the EDGE method. If the EDGE method had been optimized, the results may have been different. Therefore, future work evaluating the EDGE should also optimize the EDGE method to allow a more accurate comparison. Method optimization could be done by testing several different method parameters such as: extraction solvent, extraction time, or the number of extraction cycles used. Even without method optimization, the EDGE was shown to be an acceptable extraction instrument. However, it is still unknown whether the instrument can extract compounds

when they are more tightly bound (such as in fish or soil matrices). Future work should also evaluate the EDGE instrument using these matrices.

The $K_{\text{leaf-air}}$ values measured as well as the foliar penetration showed a difference in behavior for both the active ingredient alone and the formulation as well as when the leaves were at a different growth stage. The difference in volatilization and penetration behavior for the active ingredient and formulation suggest that both processes are chemical-specific, and when multiple chemicals are applied to leaves together the interaction of the chemicals likely affect both processes. This emphasizes the need for more $K_{\text{leaf-air}}$ values as well as foliar penetration data to be measured for a broad range of compounds, especially in the formulations since that is what is applied by farmers and what is most important for pesticide fate modeling. The differences in results based on the leaf growth stage suggests that these processes are growth stage specific. This suggests more studies on plant growth stage are needed, paying careful attention to leaf characteristics such as the type of waxes that make up the cuticle, leaf water content, leaf thickness, and leaf length. The type of waxes in the cuticle would be more difficult to measure compared to the other characteristics listed, but the types of waxes influence the interaction a pesticide has with the leaf as well as affect the penetration behavior, so this may be the most important characteristic to monitor. If leaf characteristics can be actively monitored over time while conducting volatilization and penetration studies, it may be possible to use the leaf characteristics to relate data from one plant species to another based on these measurable characteristics. Improvements in our ability to predict of $K_{\text{leaf-air}}$ values could greatly improve fate models.

The optimization of the pesticide fate models emphasized the importance of several processes: volatilization (predicted from the $K_{\text{leaf-air}}$) and pesticide penetration rates. As discussed previously, more plant-and chemical-specific $K_{\text{leaf-air}}$ values are needed if we hope to accurately predict the pesticide behavior after application on an agricultural field. Previously in the fate model, the penetration rate was set at a generic value. It is not surprising that this is a source of error due to penetration being a diffusion process that is affected by chemical properties. The work presented in Chapter 3 with foliar penetration did not measure penetration over time, rather it focused more on how the pesticide equilibrates over a 16-h experiment. To measure pesticide penetration, leaves would need to be sampled over time to get the change in concentration in each leaf layer. More measurements of pesticide penetration rates when using chemicals with a broad range of chemical properties may allow for a predictive equation to be made that would better model the pesticide penetration rate based on the chemical. While this work did predict risk to honeybees based on pesticide concentrations, there was no comparison to measured pesticide concentrations in honeybees. Future work is needed to evaluate pesticide uptake for a foraging honeybee. Also, honeybees are not the only pollinator that is used by farmers. More bee species need to be considered in risk assessments to give those who manage bees the best information to reduce dangerous pesticide exposure to the bees they manage. More data is needed to accomplish this, though, such as the lethal dose for 50% of the population (LD_{50}) for more bee species for more pesticides. The LD_{50} s for alfalfa leaf-cutting bees are currently being measured for several pesticides by our collaborators to help expand the risk assessments that we can do.

References

- (1) Rezende-Teixeira, P.; Dusi, R. G.; Jimenez, P. C.; Espindola, L. S.; Costa-Lotufo, L. V. What Can We Learn from Commercial Insecticides? Efficacy, Toxicity, Environmental Impacts, and Future Developments. *Environ. Pollut.* **2022**, *300* (January), 118983. <https://doi.org/10.1016/j.envpol.2022.118983>.
- (2) Aktar, W.; Sengupta, D.; Chowdhury, A. Impact of Pesticides Use in Agriculture: Their Benefits and Hazards. *Interdiscip. Toxicol.* **2009**, *2* (1), 1–12. <https://doi.org/10.2478/v10102-009-0001-7>.
- (3) Achee, N. L.; Grieco, J. P.; Vatandoost, H.; Seixas, G.; Pinto, J.; Ching-Ng, L.; Martins, A. J.; Juntarajumnong, W.; Corbel, V.; Gouagna, C.; David, J. P.; Logan, J. G.; Osborne, J.; Marois, E.; Devine, G. J.; Vontas, J. Alternative Strategies for Mosquito-Borne Arbovirus Control. *PLoS Negl. Trop. Dis.* **2019**, *13* (1), 1–22. <https://doi.org/10.1371/journal.pntd.0006822>.
- (4) Cooper, J.; Dobson, H. The Benefits of Pesticides to Mankind and the Environment. *Crop Prot.* **2007**, *26* (9), 1337–1348. <https://doi.org/10.1016/j.cropro.2007.03.022>.
- (5) Parra-Arroyo, L.; González-González, R. B.; Castillo-Zacarías, C.; Melchor Martínez, E. M.; Sosa-Hernández, J. E.; Bilal, M.; Iqbal, H. M. N.; Barceló, D.; Parra-Saldívar, R. Highly Hazardous Pesticides and Related Pollutants: Toxicological, Regulatory, and Analytical Aspects. *Sci. Total Environ.* **2022**, *807*, 18–26. <https://doi.org/10.1016/j.scitotenv.2021.151879>.
- (6) Serrão, J. E.; Plata-Rueda, A.; Martínez, L. C.; Zanuncio, J. C. Side-Effects of Pesticides on Non-Target Insects in Agriculture: A Mini-Review. *Sci. Nat.* **2022**,

- 109 (2), 1–11. <https://doi.org/10.1007/s00114-022-01788-8>.
- (7) Mdeni, N. L.; Adeniji, A. O.; Okoh, A. I.; Okoh, O. O. Analytical Evaluation of Carbamate and Organophosphate Pesticides in Human and Environmental Matrices: A Review. *Molecules* **2022**, *27* (3), 1–21. <https://doi.org/10.3390/molecules27030618>.
- (8) Fu, H.; Tan, P.; Wang, R.; Li, S.; Liu, H.; Yang, Y.; Wu, Z. Advances in Organophosphorus Pesticides Pollution: Current Status and Challenges in Ecotoxicological, Sustainable Agriculture, and Degradation Strategies. *J. Hazard. Mater.* **2022**, *424* (PB), 127494. <https://doi.org/10.1016/j.jhazmat.2021.127494>.
- (9) Lyons, S. M.; Hageman, K. J. Foliar Photodegradation in Pesticide Fate Modeling: Development and Evaluation of the Pesticide Dissipation from Agricultural Land (PeDAL) Model. *Environ. Sci. Technol.* **2021**, *55* (55), 4842–4850. <https://doi.org/10.1021/acs.est.0c07722>.
- (10) Rodríguez-Solana, R.; Salgado, J. M.; Domínguez, J. M.; Cortés-Diéguez, S. Comparison of Soxhlet, Accelerated Solvent and Supercritical Fluid Extraction Techniques for Volatile (GC-MS and GC/FID) and Phenolic Compounds (HPLC-ESI/MS/MS) from Lamiaceae Species. *Phytochem. Anal.* **2015**, *26* (1), 61–71. <https://doi.org/10.1002/pca.2537>.
- (11) Madej, K.; Kalenik, T. K.; Piekoszewski, W. Sample Preparation and Determination of Pesticides in Fat-Containing Foods. *Food Chem.* **2018**, *269* (April 2017), 527–541. <https://doi.org/10.1016/j.foodchem.2018.07.007>.
- (12) Nascimento, M. M.; Da Rocha, G. O.; De Andrade, J. B. Pesticides in the Atmospheric Environment: An Overview on Their Determination Methodologies.

- Anal. Methods* **2018**, *10* (37), 4484–4504. <https://doi.org/10.1039/c8ay01327f>.
- (13) Raynie, D. E., Qui, C. Improving Extraction Processes and Sample Preparation in Food Analysis. *LCGC North Am.* **2017**, *35* (3), 158–169.
- (14) Parrilla Vázquez, P.; Ferrer, C.; Martínez Bueno, M. J.; Fernández-Alba, A. R. Pesticide Residues in Spices and Herbs: Sample Preparation Methods and Determination by Chromatographic Techniques. *TrAC - Trends Anal. Chem.* **2019**, *115*, 13–22. <https://doi.org/10.1016/j.trac.2019.03.022>.
- (15) Barchanska, H.; Danek, M.; Sajdak, M.; Turek, M. Review of Sample Preparation Techniques for the Analysis of Selected Classes of Pesticides in Plant Matrices. *Crit. Rev. Anal. Chem.* **2018**, *48* (6), 467–491. <https://doi.org/10.1080/10408347.2018.1451297>.
- (16) Hoff, R. B.; Pizzolato, T. M. Combining Extraction and Purification Steps in Sample Preparation for Environmental Matrices: A Review of Matrix Solid Phase Dispersion (MSPD) and Pressurized Liquid Extraction (PLE) Applications. *TrAC - Trends Anal. Chem.* **2018**, *109*, 83–96. <https://doi.org/10.1016/j.trac.2018.10.002>.
- (17) Ali, I.; Suhail, M.; Alharbi, O. M. L.; Hussain, I. Advances in Sample Preparation in Chromatography for Organic Environmental Pollutants Analyses. *J. Liq. Chromatogr. Relat. Technol.* **2019**, *0* (0), 1–24. <https://doi.org/10.1080/10826076.2019.1579739>.
- (18) Subedi, B.; Aguilar, L.; Robinson, E. M.; Hageman, K. J.; Björklund, E.; Sheesley, R. J.; Usenko, S. Selective Pressurized Liquid Extraction as a Sample-Preparation Technique for Persistent Organic Pollutants and Contaminants of Emerging Concern. *TrAC - Trends Anal. Chem.* **2015**, *68*, 119–132.

<https://doi.org/10.1016/j.trac.2015.02.011>.

- (19) Luque de Castro, M. D.; Priego-Capote, F. Soxhlet Extraction: Past and Present Panacea. *J. Chromatogr. A* **2010**, *1217* (16), 2383–2389.
<https://doi.org/10.1016/j.chroma.2009.11.027>.
- (20) Perestrelo, R.; Silva, P.; Porto-Figueira, P.; Pereira, J. A. M.; Silva, C.; Medina, S.; Câmara, J. S. QuEChERS - Fundamentals, Relevant Improvements, Applications and Future Trends. *Anal. Chim. Acta* **2019**, *1070*, 1–28.
<https://doi.org/10.1016/j.aca.2019.02.036>.
- (21) Kim, L.; Lee, D.; Cho, H. K.; Choi, S. D. Review of the QuEChERS Method for the Analysis of Organic Pollutants: Persistent Organic Pollutants, Polycyclic Aromatic Hydrocarbons, and Pharmaceuticals. *Trends Environ. Anal. Chem.* **2019**, *22*, e00063. <https://doi.org/10.1016/j.teac.2019.e00063>.
- (22) Richter, B. E.; Jones, B. A.; Ezzell, J. L.; Porter, N. L.; Avdalovic, N.; Pohl, C. Accelerated Solvent Extraction: A Technique for Sample Preparation. *Anal. Chem.* **1996**, *68* (6), 1033–1039. <https://doi.org/10.1021/ac9508199>.
- (23) C.E.M Corporation. Automated Extraction System EDGE <http://cem.com/edge/> (accessed Sep 1, 2019).
- (24) C.E.M Corporation. Application Notes http://cem.com/en/literature?application=Extraction&literature_type=Application_Notes (accessed Sep 1, 2019).
- (25) Kinross, A. D.; Hageman, K. J.; Doucette, W. J.; Foster, A. L. Comparison of Accelerated Solvent Extraction (ASE) and Energized Dispersive Guided Extraction (EDGE) for the Analysis of Pesticides in Leaves. *J. Chromatogr. A*

- 2020**, 1627. <https://doi.org/10.1016/j.chroma.2020.461414>.
- (26) Nizzetto, L.; Pastore, C.; Liu, X.; Camporini, P.; Stroppiana, D.; Herbert, B.; Boschetti, M.; Zhang, G.; Brivio, P. A.; Jones, K. C.; Di Guardo, A. Accumulation Parameters and Seasonal Trends for PCBs in Temperate and Boreal Forest Plant Species. *Environ. Sci. Technol.* **2008**, 42 (16), 5911–5916.
<https://doi.org/10.1021/es800217m>.
- (27) Kömp, P.; McLachlan, M. S. Influence of Temperature on the Plant/Air Partitioning of Semivolatile Organic Compounds. *Environ. Sci. Technol.* **1997**, 31 (3), 886–890. <https://doi.org/10.1021/es960590u>.
- (28) Kömp, P.; McLachlan, M. S. Interspecies Variability of the Plant/Air Partitioning of Polychlorinated Biphenyls. *Environ. Sci. Technol.* **1997**, 31 (10), 2944–2948.
<https://doi.org/10.1021/es970141+>.
- (29) Bolinius, D. J.; Macleod, M.; McLachlan, M. S.; Mayer, P.; Jahnke, A. A Passive Dosing Method to Determine Fugacity Capacities and Partitioning Properties of Leaves. *Environ. Sci. Process. Impacts* **2016**, 18 (10), 1325–1332.
<https://doi.org/10.1039/c6em00423g>.
- (30) Bacci, E.; Calamari, D.; Gaggi, C.; Vighi, M. Bioconcentration of Organic Chemical Vapors in Plant Leaves: Experimental Measurements and Correlation. *Environ. Sci. Technol.* **1990**, 24 (6), 885–889.
<https://doi.org/10.1021/es00076a015>.
- (31) Bacci, E.; Gaggi, C. Chlorinated Hydrocarbon Vapours and Plant Foliage: Kinetics and Applications. *Chemosphere* **1987**, 16, 2515–2522.
- (32) Hull, H. M. Leaf Structure as Related to Absorption of Pesticides and Other

- Compounds. *Residue Rev.* **1970**, 1–150. https://doi.org/10.1007/978-3-662-39818-0_1.
- (33) Schlegel, T. K.; Schönherr, J.; Schreiber, L. Size Selectivity of Aqueous Pores in Stomatous Cuticles of *Vicia Faba* Leaves. *Planta* **2005**, *221* (5), 648–655. <https://doi.org/10.1007/s00425-005-1480-1>.
- (34) Schönherr, J. Characterization of Aqueous Pores in Plant Cuticles and Permeation of Ionic Solutes. *J. Exp. Bot.* **2006**, *57* (11), 2471–2491. <https://doi.org/10.1093/jxb/erj217>.
- (35) Buchholz, A. Characterization of the Diffusion of Non-Electrolytes across Plant Cuticles: Properties of the Lipophilic Pathway. *J. Exp. Bot.* **2006**, *57* (11), 2501–2513. <https://doi.org/10.1093/jxb/erl023>.
- (36) Valeska Zeisler-Diehl, V.; Migdal, B.; Schreiber, L. Quantitative Characterization of Cuticular Barrier Properties: Methods, Requirements, and Problems. *J. Exp. Bot.* **2017**, *68* (19), 5281–5291. <https://doi.org/10.1093/jxb/erx282>.
- (37) Riederer, M.; Schönherr, J. Thermodynamic Analysis of Nonelectrolyte Sorption in Plant Cuticles: The Effects of Concentration and Temperature on Sorption of 4-Nitrophenol. *Planta* **1986**, *169*, 69–80.
- (38) Baur, P.; Schönherr, J. Temperature Dependence of the Diffusion of Organic Compounds across Plant Cuticles. *Chemosphere* **1995**, *30* (7), 1331–1340.
- (39) Davie-Martin, C. L.; Hageman, K. J.; Chin, Y. P. An Improved Screening Tool for Predicting Volatilization of Pesticides Applied to Soils. *Environ. Sci. Technol.* **2013**, *47* (2), 868–876. <https://doi.org/10.1021/es3020277>.
- (40) Taylor, M.; Lyons, S. M.; Davie-Martin, C. L.; Geoghegan, T. S.; Hageman, K. J.

- Understanding Trends in Pesticide Volatilization from Agricultural Fields Using the Pesticide Loss via Volatilization Model. *Environ. Sci. Technol.* **2020**, *54* (4), 2202–2209. <https://doi.org/10.1021/acs.est.9b04762>.
- (41) Sharp, D.; Eskenazi, B.; Harrison, R.; Callas, P.; Smith, A. H. Delayed Health Hazards of Pesticide Exposure. *Annu. Rev. Public Health* **1986**, *7* (1), 441–471. <https://doi.org/10.1146/annurev.publhealth.7.1.441>.
- (42) Corporation, C. E. M. EDGE Automated Pressurized Fluid Extraction for USEPA 3545. **2017**.
- (43) Lavin, K. S.; Hageman, K. J. Selective Pressurised Liquid Extraction of Halogenated Pesticides and Polychlorinated Biphenyls from Pine Needles. *J. Chromatogr. A* **2012**, *1258*, 30–36. <https://doi.org/10.1016/j.chroma.2012.08.042>.
- (44) Pérez, R. A.; Tadeo, J. L.; Albero, B.; Miguel, E.; Sánchez-Brunete, C. Gas Chromatography-Triple-Quadrupole Mass Spectrometry for Analysis of Selected Polyhalogenated Pollutants in Plants. Comparison of Extraction Methods. *Anal. Bioanal. Chem.* **2013**, *405* (1), 389–400. <https://doi.org/10.1007/s00216-012-6465-x>.
- (45) Corporation, C. E. M. Extraction of Pesticides from Difficult Matrices. **2018**, 2–4.
- (46) Banerjee, K.; Oulkar, D. P.; Patil, S. H. S. B.; Jadhav, M. R.; Dasgupta, S.; Patil, S. H. S. B.; Bal, S.; Adsule, P. G. Multiresidue Determination and Uncertainty Analysis of 87 Pesticides in Mango by Liquid Chromatography-Tandem Mass Spectrometry. *J. Agric. Food Chem.* **2009**, *57* (10), 4068–4078. <https://doi.org/10.1021/jf900358r>.
- (47) Karbiwnyk, C. M.; Miller, K. E. A Review of Current Analytical Applications

- Employing Graphitized Carbon Black. In *Carbon Black: Production, Properties and Uses*; Sanders, I. J., Peeten, T. L., Eds.; Nova Science Publishers, Inc., 2011; pp 69–91.
- (48) Li, L.; Li, W.; Qin, D.; Jiang, S.; Liu, F. Application of Graphitized Carbon Black to the QuEChERS Method for Pesticide Multiresidue Analysis in Spinach. *J. AOAC Int.* **2009**, *92* (2), 538–547.
- (49) Walorczyk, S. Application of Gas Chromatography/Tandem Quadrupole Mass Spectrometry to the Multi-Residue Analysis of Pesticides in Green Leafy Vegetables. *Rapid Commun. Mass Spectrom.* **2008**, *22* (23), 3791–3801. <https://doi.org/10.1002/rcm.3800>.
- (50) Schenck, F. J.; Lehotay, S. J.; Vega, V. Comparison of Solid-Phase Extraction Sorbents for Cleanup in Pesticide Residue Analysis of Fresh Fruits and Vegetables. *J. Sep. Sci.* **2002**, *25* (14), 883–890. [https://doi.org/10.1002/1615-9314\(20021001\)25:14<883::AID-JSSC883>3.0.CO;2-7](https://doi.org/10.1002/1615-9314(20021001)25:14<883::AID-JSSC883>3.0.CO;2-7).
- (51) Łozowicka, B.; Mojsak, P.; Kaczyński, P.; Konecki, R.; Borusiewicz, A. The Fate of Spirotetramat and Dissipation Metabolites in Apiaceae and Brassicaceae Leaf-Root and Soil System under Greenhouse Conditions Estimated by Modified QuEChERS/LC–MS/MS. *Sci. Total Environ.* **2017**, *603–604*, 178–184. <https://doi.org/10.1016/j.scitotenv.2017.06.046>.
- (52) Siebers, J.; Binner, R.; Wittich, K. P. Investigation on Downwind Short-Range Transport of Pesticides after Application in Agricultural Crops. *Chemosphere* **2003**, *51* (5), 397–407. [https://doi.org/10.1016/S0045-6535\(02\)00820-2](https://doi.org/10.1016/S0045-6535(02)00820-2).
- (53) Klöppel, H.; Kördel, W. Pesticide Volatilization and Exposure of Terrestrial

- Ecosystems. *Chemosphere* **1997**, *35* (6), 1271–1289.
- (54) McLachlan, M. S. Framework for the Interpretation of Measurements of SOCs in Plants. *Environ. Sci. Technol.* **1999**, *33* (11), 1799–1804.
<https://doi.org/10.1021/es980831t>.
- (55) van den Berg, F.; Tiktak, A.; Boesten, J. J. T. I.; van der Linden, A. M. A. PEARL Model for Pesticide Behaviour and Emissions in Soil-Plant System: Description of Processes. *Wageningen UR* **2016**, *61* (February), 134.
- (56) Wolters, A.; Leistra, M.; Linnemann, V.; Klein, M.; Schäffer, A.; Vereecken, H. Pesticide Volatilization from Plants: Improvement of the PEC Model PELMO Based on a Boundary-Layer Concept. *Environ. Sci. Technol.* **2004**, *38* (10), 2885–2893. <https://doi.org/10.1021/es035061m>.
- (57) Scholtz, M. T.; Voldner, E.; McMillan, A. C.; Van Heyst, B. J. A Pesticide Emission Model (PEM) Part I: Model Development. *Atmos. Environ.* **2002**, *36*, 5005–5013.
- (58) Schreiber, L.; Skrabs, M.; Hartmann, K. D.; Diamantopoulos, P.; Simanova, E.; Santrucek, J. Effect of Humidity on Cuticular Water Permeability of Isolated Cuticular Membranes and Leaf Disks. *Planta* **2001**, *214* (2), 274–282.
<https://doi.org/10.1007/s004250100615>.
- (59) Barber, J. L.; Thomas, G. O.; Kerstiens, G.; Jones, K. C. Current Issues and Uncertainties in the Measurement and Modelling of Air-Vegetation Exchange and within-Plant Processing of POPs. *Environ. Pollut.* **2004**, *128*, 99–138.
<https://doi.org/10.1016/j.envpol.2003.08.024>.
- (60) Baur, P.; Marzouk, H.; Schönherr, J.; Grayson, B. T. Partition Coefficients of

Active Ingredients between Plant Cuticle and Adjuvants as Related to Rates of Foliar Uptake. *J. Agric. Food Chem.* **1997**, *45* (9), 3659–3665.

<https://doi.org/10.1021/jf970233i>.

- (61) Grotkopp, E.; Rejmánek, M.; Rost, T. L. Toward a Causal Explanation of Plant Invasiveness: Seedling Growth and Life-History Strategies of 29 Pine (*Pinus*) Species. *Am. Nat.* **2002**, *159* (4), 396–419. <https://doi.org/10.1086/338995>.
- (62) Poorter, H.; De Jong, R. A Comparison of Specific Leaf Area, Chemical Composition and Leaf Construction Costs of Field Plants from 15 Habitats Differing in Productivity. *New Phytol.* **1999**, *143* (1), 163–176. <https://doi.org/10.1046/j.1469-8137.1999.00428.x>.
- (63) McCall, P. J.; Stafford, L. E.; Zorner, P. S.; Gavit, P. D. Modeling the Foliar Behavior of Atrazine with and without Crop Oil Concentrate on Giant Foxtail and the Effect of Tridiphane on the Model Rate Constants. *J. Agric. Food Chem.* **1986**, *34* (2), 235–238. <https://doi.org/10.1021/jf00068a020>.
- (64) Baur, P.; Buchholz, A.; Schönherr, J. Diffusion in Plant Cuticles as Affected by Temperature and Size of Organic Solutes: Similarity and Diversity among Species. *Plant, Cell Environ.* **1997**, *20* (8), 982–994. <https://doi.org/10.1111/j.1365-3040.1997.tb00675.x>.
- (65) Lichiheb, N.; Bedos, C.; Personne, E.; Benoit, P.; Bergheaud, V.; Fanucci, O.; Bouhleb, J.; Barriuso, E. Measuring Leaf Penetration and Volatilization of Chlorothalonil and Epoxiconazole Applied on Wheat Leaves in a Laboratory-Scale Experiment. *J. Environ. Qual.* **2015**, *44* (6), 1782–1790. <https://doi.org/10.2134/jeq2015.03.0165>.

- (66) Dereumeaux, C.; Fillol, C.; Quenel, P.; Denys, S. Pesticide Exposures for Residents Living Close to Agricultural Lands: A Review. *Environ. Int.* **2020**, *134* (November 2019), 105210. <https://doi.org/10.1016/j.envint.2019.105210>.
- (67) Wang, S.; Salamova, A.; Hites, R. A.; Venier, M. Spatial and Seasonal Distributions of Current Use Pesticides (CUPs) in the Atmospheric Particulate Phase in the Great Lakes Region. *Environ. Sci. Technol.* **2018**, *52* (11), 6177–6186. <https://doi.org/10.1021/acs.est.8b00123>.
- (68) Wang, S.; Salamova, A.; Venier, M. Occurrence, Spatial, and Seasonal Variations, and Gas-Particle Partitioning of Atmospheric Current-Use Pesticides (CUPs) in the Great Lakes Basin. *Environ. Sci. Technol.* **2021**, *55* (6), 3539–3548. <https://doi.org/10.1021/acs.est.0c06470>.
- (69) US Federal Regulations. Tolerance Revocations: Chlorpyrifos <https://www.regulations.gov/document/EPA-HQ-OPP-2021-0523-0001> (accessed Dec 10, 2021).
- (70) European Commission. Chlorpyrifos & Chlorpyrifos-methyl https://ec.europa.eu/food/plants/pesticides/approval-active-substances/renewal-approval/chlorpyrifos-chlorpyrifos-methyl_en (accessed Mar 28, 2022).
- (71) Pesticide Action Network (PAN) International. Consolidated List of Banned Pesticides <https://pan-international.org/pan-international-consolidated-list-of-banned-pesticides/> (accessed Mar 28, 2022).
- (72) Environmental Protection Authority. First step towards reassessing controversial insecticide <https://www.epa.govt.nz/news-and-alerts/latest-news/first-step-towards-reassessing-controversial-insecticide/#:~:text=Chlorpyrifos is currently>

- approved in, vineyards%2C vegetable and cereal crops. (accessed Mar 28, 2022).
- (73) CIRS. List of Banned and Restricted Pesticide Products in China <https://www.cirs-group.com/en/agrochemicals/list-of-banned-and-restricted-pesticide-products-in-china> (accessed Mar 28, 2022).
- (74) Anvisa: Agência Nacional de Vigilância Sanitária. Chlorpyrifos http://antigo.anvisa.gov.br/resultado-de-busca?x=0&y=0&_3_keywords=chlorpyrifos&_3_formDate=1441824476958&p_p_id=3&p_p_lifecycle=0&p_p_state=normal&p_p_mode=view&_3_groupId=0&_3_struts_action=%2Fsearch%2Fsearch&_3_cur=1&_3_format= (accessed Mar 28, 2022).
- (75) Clough, S. R. Petroleum Distillates. *Encyclopedia of Toxicology*; Elsevier, 2005; pp 372–375. <https://doi.org/10.1016/B0-12-369400-0/00741-9>.
- (76) Das, S.; Hageman, K. J. Influence of Adjuvants on Pesticide Soil–Air Partition Coefficients: Laboratory Measurements and Predicted Effects on Volatilization. *Environ. Sci. Technol.* **2020**, *54* (12), 7302–7308. <https://doi.org/10.1021/acs.est.0c00964>.
- (77) Buschhaus, C.; Herz, H.; Jetter, R. Chemical Composition of the Epicuticular and Intracuticular Wax Layers on Adaxial Sides of *Rosa Canina* Leaves. *New Phytol.* **2007**, *176*, 311–316. <https://doi.org/10.1093/aob/mcm255>.
- (78) Jetter, R.; Schäffer, S.; Riederer, M. Leaf Cuticular Waxes Are Arranged in Chemically and Mechanically Distinct Layers: Evidence from *Prunus Laurocerasus* L. *Plant, Cell Environ.* **2000**, *23* (6), 619–628. <https://doi.org/10.1046/j.1365-3040.2000.00581.x>.

- (79) Bergman, D. K.; Dillwith, J. W.; Zarrabi, A. A.; Caddel, J. L.; Berberet, R. C. Epicuticular Lipids of Alfalfa Relative to Its Susceptibility to Spotted Alfalfa Aphids (Homoptera: Aphididae). *Environ. Entomol.* **1991**, *20* (3), 781–785.
- (80) Rüdel, H. Volatilisation of Pesticides from Soil and Plant Surfaces. *Chemosphere* **1997**, *35*, 143–152.
- (81) Castro, M. J. L.; Ojeda, C.; Cirelli, A. F. Advances in Surfactants for Agrochemicals. *Environ. Chem. Lett.* **2014**, *12* (1), 85–95.
<https://doi.org/10.1007/s10311-013-0432-4>.
- (82) Houbraken, M.; Senaeve, D.; Fevery, D.; Spanoghe, P. Influence of Adjuvants on the Dissipation of Fenpropimorph, Pyrimethanil, Chlorpyrifos and Lindane on the Solid/Gas Interface. *Chemosphere* **2015**, *138*, 357–363.
<https://doi.org/10.1016/j.chemosphere.2015.06.040>.
- (83) Schwarzenbach, R. P.; Gschwend, P. M.; Imboden, D. M. *Environmental Organic Chemistry*, 2nd ed.; John Wiley and Sons, Inc.: Hoboken, NJ, 2003.
<https://doi.org/10.1002/0471649643>.
- (84) Christensen, K.; Harper, B.; Luukinen, B.; Buhl, K.; Stone, D. Chlorpyrifos Technical Fact Sheet <http://npic.orst.edu/factsheets/archive/chlorptech.html> (accessed Jul 4, 2022).
- (85) Davie-Martin, C. L.; Hageman, K. J.; Chin, Y. P.; Rougé, V.; Fujita, Y. Influence of Temperature, Relative Humidity, and Soil Properties on the Soil-Air Partitioning of Semivolatile Pesticides: Laboratory Measurements and Predictive Models. *Environ. Sci. Technol.* **2015**, *49* (17), 10431–10439.
<https://doi.org/10.1021/acs.est.5b02525>.

- (86) Hippelein, M.; McLachlan, M. S. Soil/Air Partitioning of Semivolatile Organic Compounds. 2. Influence of Temperature and Relative Humidity. *Environ. Sci. Technol.* **2000**, *34* (16), 3521–3526. <https://doi.org/10.1021/es991421n>.
- (87) Goss, K. U. Effects of Temperature and Relative Humidity on the Sorption of Organic Vapors on Clay Minerals. *Environ. Sci. Technol.* **1993**, *27* (10), 2127–2132. <https://doi.org/10.1021/es00047a019>.
- (88) van den Berg, F.; Jacobs, C. M. J.; Butler Ellis, M. C.; Spanoghe, P.; Doan Ngoc, K.; Fragkoulis, G. Modelling Exposure of Workers, Residents and Bystanders to Vapour of Plant Protection Products after Application to Crops. *Sci. Total Environ.* **2016**, *573*, 1010–1020. <https://doi.org/10.1016/j.scitotenv.2016.08.180>.
- (89) Houbraken, M.; Doan Ngoc, K.; van den Berg, F.; Spanoghe, P. Modelling Pesticides Volatilisation in Greenhouses: Sensitivity Analysis of a Modified PEARL Model. *Sci. Total Environ.* **2017**, *599–600*, 1408–1416. <https://doi.org/10.1016/j.scitotenv.2017.05.027>.
- (90) Lichiheb, N.; Personne, E.; Bedos, C.; Van den Berg, F.; Barriuso, E. Implementation of the Effects of Physicochemical Properties on the Foliar Penetration of Pesticides and Its Potential for Estimating Pesticide Volatilization from Plants. *Sci. Total Environ.* **2016**, *550*, 1022–1031. <https://doi.org/10.1016/j.scitotenv.2016.01.058>.
- (91) Walia, S.; Dureja, P.; Mukerjee, S. K. New Photodegradation Products of Chlorpyrifos and Their Detection on Glass, Soil, and Leaf Surfaces. *Arch. Environ. Contam. Toxicol.* **1988**, *17*, 183–188.
- (92) Anderson, S. C.; Chu, L.; Bouma, C.; Beukelman, L.; McLouth, R.; Larson, E.;

- Nienow, A. M. Comparison of the Photodegradation of Imazethapyr in Aqueous Solution, on Epicuticular Waxes, and on Intact Corn (*Zea Mays*) and Soybean (*Glycine Max*) Leaves. *J. Environ. Sci. Heal. - Part B Pestic. Food Contam. Agric. Wastes* **2018**, *54* (2), 129–137. <https://doi.org/10.1080/03601234.2018.1511400>.
- (93) Su, L.; Sivey, J. D.; Dai, N. Emerging Investigator Series: Sunlight Photolysis of 2,4-D Herbicides in Systems Simulating Leaf Surfaces. *Environ. Sci. Process. Impacts* **2018**, *20* (8), 1123–1135. <https://doi.org/10.1039/c8em00186c>.
- (94) Eyheraguibel, B.; Richard, C.; Ledoigt, G.; Ter Halle, A. Photoprotection by Plant Extracts: A New Ecological Means to Reduce Pesticide Photodegradation. *J. Agric. Food Chem.* **2010**, *58* (17), 9692–9696. <https://doi.org/10.1021/jf101792h>.
- (95) Monadjemi, S.; El Roz, M.; Richard, C.; Ter Halle, A. Photoreduction of Chlorothalonil Fungicide on Plant Leaf Models. *Environ. Sci. Technol.* **2011**, *45* (22), 9582–9589. <https://doi.org/10.1021/es202400s>.
- (96) Fukushima, M.; Katagi, T. Photodegradation of Fenitrothion and Parathion in Tomato Epicuticular Waxes. *J. Agric. Food Chem.* **2006**, *54* (2), 474–479. <https://doi.org/10.1021/jf052113d>.
- (97) Cabras, P.; Angioni, A.; Garau, V. L.; Melis, M.; Pirisi, F. M.; Minelli, E. V. Effect of Epicuticular Waxes of Fruits on the Photodegradation of Fenthion. *J. Agric. Food Chem.* **1997**, *45* (9), 3681–3683. <https://doi.org/10.1021/jf970102h>.
- (98) Barmaz, S.; Potts, S. G.; Vighi, M. A Novel Method for Assessing Risks to Pollinators from Plant Protection Products Using Honeybees as a Model Species. *Ecotoxicology* **2010**, *19* (7), 1347–1359. <https://doi.org/10.1007/s10646-010-0521-0>.

- (99) Delphine, L.; Alexandra, T. H.; Bussiere, P. O.; Claire, R. Effect of a Spreading Adjuvant on Mesotrione Photolysis on Wax Films. *J. Agric. Food Chem.* **2009**, *57* (20), 9624–9628. <https://doi.org/10.1021/jf901996d>.
- (100) Eyheraguibel, B.; ter Halle, A.; Richard, C.; Halle, A. Ter; Richard, C. Photodegradation of Bentazon, Clopyralid, and Triclopyr on Model Leaves: Importance of a Systematic Evaluation of Pesticide Photostability on Crops. *J. Agric. Food Chem.* **2009**, *57* (5), 1960–1966. <https://doi.org/10.1021/jf803282f>.
- (101) Ultraviolet (UV) Radiation | UCAR Center for Science Education.
- (102) Weber, J.; Halsall, C. J.; Wargent, J. J.; Paul, N. D. A Comparative Study on the Aqueous Photodegradation of Two Organophosphorus Pesticides under Simulated and Natural Sunlight. *J. Environ. Monit.* **2009**, *11* (3), 654–659. <https://doi.org/10.1039/b811387d>.
- (103) Laszakovits, J. R.; Berg, S. M.; Anderson, B. G.; O'Brien, J. E.; Wammer, K. H.; Sharpless, C. M. P-Nitroanisole/Pyridine and p-Nitroacetophenone/Pyridine Actinometers Revisited: Quantum Yield in Comparison to Ferrioxalate. *Environ. Sci. Technol. Lett.* **2017**, *4* (1), 11–14. <https://doi.org/10.1021/acs.estlett.6b00422>.
- (104) Logan, S. R. Does a Photochemical Reaction Have a Kinetic Order? *J. Chem. Educ.* **1997**, *74* (11), 1303. <https://doi.org/10.1021/ed082p37.2>.
- (105) Lewis, K. A.; Tzilivakis, J.; Warner, D. J.; Green, A. An International Database for Pesticide Risk Assessments and Management. *Hum. Ecol. Risk Assess. An Int. J.* **2016**, *22* (4), 1050–1064.
- (106) U.S. Environmental Protection Agency. ECOTOX User Guide: ECOTOXicology Knowledgebase System. Version 5.3 <http://www.epa.gov/ecotox/> (accessed Jan 9,

2021).

- (107) Lavieille, D.; Ter Halle, A.; Richard, C. Understanding Mesotrione Photochemistry When Applied on Leaves. *Environ. Chem.* **2008**, *5* (6), 420–425. <https://doi.org/10.1071/EN08073>.
- (108) Schmolke, A.; Galic, N.; Feken, M.; Thompson, H.; Sgolastra, F.; Pitts-Singer, T.; Elston, C.; Pamminger, T.; Hinarejos, S. Assessment of the Vulnerability to Pesticide Exposures Across Bee Species. *Environ. Toxicol. Chem.* **2021**, *40* (9), 2640–2651. <https://doi.org/10.1002/etc.5150>.
- (109) Prah, S. Chlorophyll a <https://omlc.org/spectra/PhotochemCAD/html/123.html> (accessed Dec 4, 2019).
- (110) Prah, S. Chlorophyll b <https://omlc.org/spectra/PhotochemCAD/html/125.html> (accessed Dec 4, 2019).
- (111) US EPA. Estimation Programs Interface Suite™ for Microsoft® Windows, v 4.11. United States Environmental Protection Agency: Washington, DC, USA 2012.

Appendix

Table A1. Weather conditions for pesticide dissipation studies.

Chlorpyrifos Field Dissipation Trial 1				Chlorpyrifos Field Dissipation Trial 2			
Date, Time	Air Temp. (°C)	Wind Speed (m/s)	Solar Intensity (W*m ⁻²)	Date, Time	Air Temp. (°C)	Wind Speed (m/s)	Solar Intensity (W*m ⁻²)
7/13/2020 9:00	19.8	0.939	491	8/11/2020 9:00	21.1	1.028	627
7/13/2020 10:00	21.8	0.849	790	8/11/2020 10:00	22.5	0.849	579
7/13/2020 11:00	23.5	0.983	861	8/11/2020 11:00	25.4	0.983	889
7/13/2020 12:00	25.4	0.939	1024	8/11/2020 12:00	27	0.715	643
7/13/2020 13:00	26.5	1.073	1004	8/11/2020 13:00	28.4	1.118	509
7/13/2020 14:00	27.5	1.028	935	8/11/2020 14:00	28.8	0.671	467
7/13/2020 15:00	28.2	1.341	812	8/11/2020 15:00	30.6	1.565	723
7/13/2020 16:00	28.6	1.207	654	8/11/2020 16:00	31.3	1.699	590
7/13/2020 17:00	28.6	1.386	471	8/11/2020 17:00	30.9	1.654	398
7/13/2020 18:00	27.8	1.609	273	8/11/2020 18:00	30.1	1.252	174
7/13/2020 19:00	25.6	2.012	97	8/11/2020 19:00	25.6	0.76	11
7/13/2020 20:00	24.1	1.654	5	8/11/2020 20:00	24.1	1.073	0
7/13/2020 21:00	21.4	0.849	0	8/11/2020 21:00	23.3	1.162	0
7/13/2020 22:00	19.8	0.671	0	8/11/2020 22:00	22.3	1.52	0
7/13/2020 23:00	18.6	1.118	0	8/11/2020 23:00	21.1	1.922	0
7/14/2020 0:00	18.3	1.699	0	8/12/2020 0:00	21.3	1.743	0
7/14/2020 1:00	18	1.207	0	8/12/2020 1:00	18.6	1.073	0
7/14/2020 2:00	15.8	0.894	0	8/12/2020 2:00	18.3	1.654	0
7/14/2020 3:00	13.9	0.402	0	8/12/2020 3:00	16.8	0.671	0
7/14/2020 4:00	13.6	1.028	0	8/12/2020 4:00	15.9	0.715	0

7/14/2020 5:00	11.7	0.447	9	8/12/2020 5:00	15.4	1.252	2
7/14/2020 6:00	13.2	1.118	123	8/12/2020 6:00	13.8	0.268	48
7/14/2020 7:00	16.3	1.162	338	8/12/2020 7:00	16.7	0.581	237
7/14/2020 8:00	18.6	0.76	535	8/12/2020 8:00	19.9	0.805	445
7/14/2020 9:00	20.2	0.671	717	8/12/2020 9:00	22.6	0.983	633
7/14/2020 10:00	21.3	1.431	867	8/12/2020 10:00	25	1.028	767
7/14/2020 11:00	22.8	1.475	975	8/12/2020 11:00	27.2	2.056	887
7/14/2020 12:00	23.8	1.52	1021	8/12/2020 12:00	28.2	2.414	936
7/14/2020 13:00	24.6	1.52	1008	8/12/2020 13:00	28.9	3.129	933
7/14/2020 14:00	25.7	1.118	939	8/12/2020 14:00	29.1	3.532	869
7/14/2020 15:00	26.2	1.386	822	8/12/2020 15:00	29.7	3.442	759
7/14/2020 16:00	26.6	1.386	650	8/12/2020 16:00	28.1	2.235	580
7/14/2020 17:00	26.8	1.073	479	8/12/2020 17:00	28.9	1.609	390
7/14/2020 18:00	26.5	0.983	279	8/12/2020 18:00	28.9	2.906	194
7/14/2020 19:00	25	0.402	101	8/12/2020 19:00	26.9	1.743	23
7/14/2020 20:00	21.8	0.358	5	8/12/2020 20:00	23.8	1.252	0
7/14/2020 21:00	19.6	0.581	0	8/12/2020 21:00	22.5	1.162	0
7/14/2020 22:00	18.1	0.76	0	8/12/2020 22:00	20.2	0.983	0
7/14/2020 23:00	16.8	1.162	0	8/12/2020 23:00	18	0.939	0
7/15/2020 0:00	15.7	1.162	0	8/13/2020 0:00	17.2	0.76	0
7/15/2020 1:00	14.1	0.536	0	8/13/2020 1:00	17.6	0.894	0
7/15/2020 2:00	13.1	0.536	0	8/13/2020 2:00	15.8	0.402	0
7/15/2020 3:00	11.8	0.536	0	8/13/2020 3:00	15.1	0.358	0

7/15/2020 4:00	11.2	0.402	0	8/13/2020 4:00	14.5	0.581	0
7/15/2020 5:00	10.5	0.447	8	8/13/2020 5:00	13.8	0.626	2
7/15/2020 6:00	10.4	0.089	122	8/13/2020 6:00	13.3	0.268	60
7/15/2020 7:00	13.8	0.447	343	8/13/2020 7:00	16.2	0.492	254
7/15/2020 8:00	16.1	0.671	542	8/13/2020 8:00	18.8	0.536	432
7/15/2020 9:00	18.1	0.983	724	8/13/2020 9:00	20.8	0.715	652
7/15/2020 10:00	20.2	0.849	875	8/13/2020 10:00	25.6	0.894	819
7/15/2020 11:00	22.4	0.76	978	8/13/2020 11:00	27.4	1.386	641
7/15/2020 12:00	24.6	0.805	1014	8/13/2020 12:00	27.3	1.878	470
7/15/2020 13:00	26.6	1.296	1010	8/13/2020 13:00	28.7	2.235	885
7/15/2020 14:00	27.5	1.296	943	8/13/2020 14:00	29.7	2.906	894
7/15/2020 15:00	28.3	1.52	826	8/13/2020 15:00	30.3	2.459	754
7/15/2020 16:00	28.6	1.699	668	8/13/2020 16:00	30.7	2.593	592
7/15/2020 17:00	28.5	1.475	481	8/13/2020 17:00	30.7	3.398	397
7/15/2020 18:00	28.3	0.626	282	8/13/2020 18:00	29.4	2.772	193
7/15/2020 19:00	26.3	0.268	101	8/13/2020 19:00	27.6	1.743	33
7/15/2020 20:00	23.5	1.207	5	8/13/2020 20:00	24.3	1.162	0
7/15/2020 21:00	21.7	0.939	0	8/13/2020 21:00	22.1	0.581	0
7/15/2020 22:00	19.7	0.671	0	8/13/2020 22:00	20	0.715	0
7/15/2020 23:00	17.9	0.536	0	8/13/2020 23:00	19.2	1.207	0
7/16/2020 0:00	17	0.626	0	8/14/2020 0:00	19.1	1.788	0
7/16/2020 1:00	15.7	0.447	0	8/14/2020 1:00	16.9	1.341	0
7/16/2020 2:00	14.9	0.268	0	8/14/2020 2:00	15.7	0.76	0

7/16/2020 3:00	13.4	0.268	0	8/14/2020 3:00	14.2	0.536	0
7/16/2020 4:00	12.9	0.447	0	8/14/2020 4:00	13.5	0.671	0
7/16/2020 5:00	11.7	0.358	9	8/14/2020 5:00	13.3	0.805	2
7/16/2020 6:00	12.9	0.447	119	8/14/2020 6:00	13.5	0.805	61
7/16/2020 7:00	15.9	0.581	334	8/14/2020 7:00	14.7	0.358	255
7/16/2020 8:00	17.3	0.805	531	8/14/2020 8:00	17.4	0.894	453
7/16/2020 9:00	19.4	0.715	713	8/14/2020 9:00	20	1.475	642
7/16/2020 10:00	21.7	0.76	864	8/14/2020 10:00	23.3	0.805	799
7/16/2020 11:00	23.9	0.894	964	8/14/2020 11:00	26.1	1.028	906
7/16/2020 12:00	25.9	1.118	1008	8/14/2020 12:00	27.3	1.341	948
7/16/2020 13:00	27.7	1.207	1001	8/14/2020 13:00	28.1	1.922	893
7/16/2020 14:00	29.3	1.162	930	8/14/2020 14:00	28.9	2.101	862
7/16/2020 15:00	30.4	1.073	808	8/14/2020 15:00	29.8	2.861	735
7/16/2020 16:00	30.9	1.475	652	8/14/2020 16:00	29.8	2.727	577
7/16/2020 17:00	31	1.207	467	8/14/2020 17:00	29.8	2.593	388
7/16/2020 18:00	30.7	0.983	273	8/14/2020 18:00	28.7	2.369	191
7/16/2020 19:00	28.7	0.447	100	8/14/2020 19:00	26.5	0.849	34
7/16/2020 20:00	25.9	1.52	4	8/14/2020 20:00	23.6	0.805	0
7/16/2020 21:00	24.2	1.52	0	8/14/2020 21:00	21.8	0.849	0
7/16/2020 22:00	23.2	1.296	0	8/14/2020 22:00	19.9	0.894	0
7/16/2020 23:00	21.7	1.609	0	8/14/2020 23:00	19.4	0.671	0
7/17/2020 0:00	18.9	0.492	0	8/15/2020 0:00	18.1	0.805	0
7/17/2020 1:00	18.2	0.805	0	8/15/2020 1:00	16.7	0.581	0

7/17/2020 2:00	17.5	0.671	0	8/15/2020 2:00	15.5	0.447	0
7/17/2020 3:00	16.4	0.626	0	8/15/2020 3:00	14.6	0.581	0
7/17/2020 4:00	15.7	0.76	0	8/15/2020 4:00	13.8	0.626	0
7/17/2020 5:00	15.9	1.028	9	8/15/2020 5:00	13	0.313	2
7/17/2020 6:00	15.3	0.581	113	8/15/2020 6:00	12.5	0.224	57
7/17/2020 7:00	18.2	0.536	322	8/15/2020 7:00	15.4	0.224	251
7/17/2020 8:00	20.6	0.447	518	8/15/2020 8:00	16.9	0.939	450
7/17/2020 9:00	23.3	0.536	702	8/15/2020 9:00	19.3	0.76	642
7/17/2020 10:00	26.8	0.536	851	8/15/2020 10:00	21.8	0.581	805
7/17/2020 11:00	30.5	1.699	959	8/15/2020 11:00	24.6	0.805	913
7/17/2020 12:00	31.9	4.068	1008	8/15/2020 12:00	27.3	0.849	946
7/17/2020 13:00	32.4	4.202	1009	8/15/2020 13:00	29.6	0.849	795
7/17/2020 14:00	32.9	3.979	859	8/15/2020 14:00	30.7	0.983	875
7/17/2020 15:00	33.8	4.292	834	8/15/2020 15:00	31.5	0.805	736
7/17/2020 16:00	34.1	3.934	661	8/15/2020 16:00	31.6	1.341	578
7/17/2020 17:00	33.8	3.085	462	8/15/2020 17:00	31.8	0.715	385
7/17/2020 18:00	32.1	1.743	166	8/15/2020 18:00	30.7	0.671	190
7/17/2020 19:00	28.7	0.447	81	8/15/2020 19:00	27.1	0.76	35
7/17/2020 20:00	26.1	1.118	3	8/15/2020 20:00	24.2	1.162	0
7/17/2020 21:00	25.1	1.833	0	8/15/2020 21:00	23.1	1.207	0
7/17/2020 22:00	24	0.76	0	8/15/2020 22:00	21.6	1.073	0
7/17/2020 23:00	22.7	0.849	0	8/15/2020 23:00	19.7	0.536	0
7/18/2020 0:00	21.3	0.402	0	8/16/2020 0:00	18.8	0.805	0

7/18/2020 1:00	19.6	0.626	0	8/16/2020 1:00	17.4	0.536	0
7/18/2020 2:00	18.2	0.626	0	8/16/2020 2:00	15.9	0.671	0
7/18/2020 3:00	17.4	0.492	0	8/16/2020 3:00	15.6	0.671	0
7/18/2020 4:00	16.9	0.581	0	8/16/2020 4:00	14.6	0.76	0
7/18/2020 5:00	16.6	0.492	8	8/16/2020 5:00	13.8	0.671	2
7/18/2020 6:00	16.8	0.224	111	8/16/2020 6:00	13.1	0.536	63
7/18/2020 7:00	19.7	0.671	319	8/16/2020 7:00	16.1	0.134	263
7/18/2020 8:00	20.9	0.849	514	8/16/2020 8:00	18.2	0.581	414
7/18/2020 9:00	23.8	0.849	695	8/16/2020 9:00	20.1	0.894	562
7/18/2020 10:00	26.4	1.207	847	8/16/2020 10:00	22.7	0.76	723
7/18/2020 11:00	27.9	1.475	952	8/16/2020 11:00	24.7	0.76	797
7/18/2020 12:00	28.9	1.296	998	8/16/2020 12:00	26.7	0.76	861
7/18/2020 13:00	29.6	1.431	988	8/16/2020 13:00	28.6	0.805	822
7/18/2020 14:00	30.1	1.341	916	8/16/2020 14:00	30.6	0.894	776
7/18/2020 15:00	30.7	1.341	799	8/16/2020 15:00	31.6	0.76	616
7/18/2020 16:00	31	1.073	643	8/16/2020 16:00	31.9	0.715	455
7/18/2020 17:00	30.9	1.207	459	8/16/2020 17:00	30.7	0.134	284
7/18/2020 18:00	30.3	0.76	260	8/16/2020 18:00	28.9	0.447	174
7/18/2020 19:00	28.6	0.536	85	8/16/2020 19:00	26.2	0.894	17
7/18/2020 20:00	25.8	0.492	4	8/16/2020 20:00	25.8	0.805	0
7/18/2020 21:00	24.3	0.805	0	8/16/2020 21:00	24.3	0.671	0
7/18/2020 22:00	22.7	1.743	0	8/16/2020 22:00	22.3	0.626	0
7/18/2020 23:00	21.7	2.056	0	8/16/2020 23:00	20.8	0.671	0

7/19/2020 0:00	19.9	0.581	0	8/17/2020 0:00	20.1	0.536	0
7/19/2020 1:00	19.1	0.447	0	8/17/2020 1:00	18.8	0.76	0
7/19/2020 2:00	17.8	0.268	0	8/17/2020 2:00	17.5	0.581	0
7/19/2020 3:00	16.7	0.492	0	8/17/2020 3:00	16.7	0.447	0
7/19/2020 4:00	15.7	0.671	0	8/17/2020 4:00	15.9	0.671	0
7/19/2020 5:00	14.8	0.492	9	8/17/2020 5:00	15.6	0.805	1
7/19/2020 6:00	15.5	0.358	111	8/17/2020 6:00	15	0.492	56
7/19/2020 7:00	18.2	0.268	317	8/17/2020 7:00	17.6	0.313	246
7/19/2020 8:00	19.5	0.671	516	8/17/2020 8:00	20.3	0.626	444
7/19/2020 9:00	21.3	0.536	700	8/17/2020 9:00	22.9	0.76	634
7/19/2020 10:00	23.4	0.626	849	8/17/2020 10:00	24.8	1.609	785
7/19/2020 11:00	25.7	1.028	947	8/17/2020 11:00	27.2	1.431	890
7/19/2020 12:00	27.7	1.073	1000	8/17/2020 12:00	29.8	0.939	919
7/19/2020 13:00	28.6	1.431	986	8/17/2020 13:00	32.2	1.073	772
7/19/2020 14:00	29.3	1.073	921	8/17/2020 14:00	34	1.341	853
7/19/2020 15:00	30.1	1.028	806	8/17/2020 15:00	34.7	0.849	716
7/19/2020 16:00	30.6	0.983	646	8/17/2020 16:00	35.2	0.894	558
7/19/2020 17:00	30.4	1.475	460	8/17/2020 17:00	35.2	0.224	368
7/19/2020 18:00	29.8	1.252	265	8/17/2020 18:00	32.8	0.134	170
7/19/2020 19:00	27.2	0.313	85	8/17/2020 19:00	29.1	0.939	22
7/19/2020 20:00	23.9	0.849	4	8/17/2020 20:00	27.6	1.073	0
7/19/2020 21:00	22.4	1.296	0	8/17/2020 21:00	26.7	0.626	0
7/19/2020 22:00	20.9	1.296	0	8/17/2020 22:00	23.9	0.581	0

7/19/2020 23:00	19.8	1.341	0	8/17/2020 23:00	23.1	0.939	0
7/20/2020 0:00	19.1	1.475	0	8/18/2020 0:00	22.2	1.073	0
7/20/2020 1:00	17.3	1.207	0	8/18/2020 1:00	21.4	0.983	0
7/20/2020 2:00	15.4	0.626	0	8/18/2020 2:00	19.8	0.715	0
7/20/2020 3:00	14.6	0.447	0	8/18/2020 3:00	18.7	0.671	0
7/20/2020 4:00	14	0.581	0	8/18/2020 4:00	17.4	0.626	0
7/20/2020 5:00	13.3	0.581	8	8/18/2020 5:00	16.9	0.626	1
7/20/2020 6:00	13.8	0.492	111	8/18/2020 6:00	16.7	0.536	52
7/20/2020 7:00	16.8	0.626	324	8/18/2020 7:00	18.8	0.894	223
7/20/2020 8:00	18.2	1.028	522	8/18/2020 8:00	22.2	1.028	432
7/20/2020 9:00	20.8	0.447	709	8/18/2020 9:00	24.1	0.939	623

Chlorpyrifos Field Dissipation Trial 3				λ-Cyhalothrin Field Dissipation Trial 1			
Date, Time	Air Temp. (°C)	Wind Speed (m/s)	Solar Intensity (W*m ⁻²)	Date, Time	Air Temp. (°C)	Wind Speed (m/s)	Solar Intensity (W*m ⁻²)
9/25/2020 10:00	16.2	0.849	548	5/18/2020 9:00	23.4	5.23	566
9/25/2020 11:00	18.8	1.073	730	5/18/2020 10:00	23.9	5.543	682
9/25/2020 12:00	22	1.565	739	5/18/2020 11:00	23.9	5.677	559
9/25/2020 13:00	22.7	2.548	678	5/18/2020 12:00	24.6	5.454	673
9/25/2020 14:00	23.8	2.146	451	5/18/2020 13:00	24.9	4.873	598
9/25/2020 15:00	24.3	2.772	411	5/18/2020 14:00	26.6	4.873	841
9/25/2020 16:00	23.4	3.174	167	5/18/2020 15:00	27.4	5.946	741
9/25/2020 17:00	22.6	2.325	80	5/18/2020 16:00	27.2	5.901	643
9/25/2020 18:00	21.7	1.118	13	5/18/2020 17:00	25.7	5.052	258

9/25/2020 19:00	20.6	0.939	0	5/18/2020 18:00	24.1	2.235	64
9/25/2020 20:00	17.3	0.805	0	5/18/2020 19:00	23.7	2.146	25
9/25/2020 21:00	16	0.894	0	5/18/2020 20:00	22.5	1.341	0
9/25/2020 22:00	14.7	0.894	0	5/18/2020 21:00	21.6	1.073	0
9/25/2020 23:00	14.1	0.581	0	5/18/2020 22:00	19.4	1.654	0
9/26/2020 0:00	13.3	1.073	0	5/18/2020 23:00	14.6	1.699	0
9/26/2020 1:00	14.5	1.073	0	5/19/2020 0:00	12.2	1.565	0
9/26/2020 2:00	15.1	1.118	0	5/19/2020 1:00	11.1	1.922	0
9/26/2020 3:00	16.9	0.849	0	5/19/2020 2:00	10.5	1.743	0
9/26/2020 4:00	17.1	0.76	0	5/19/2020 3:00	9.8	1.654	0
9/26/2020 5:00	16.9	0.581	0	5/19/2020 4:00	9.1	0.983	0
9/26/2020 6:00	15.6	0.447	1	5/19/2020 5:00	8.4	0.358	12
9/26/2020 7:00	16.4	1.252	28	5/19/2020 6:00	8.6	0.268	138
9/26/2020 8:00	16.3	1.207	58	5/19/2020 7:00	10.9	0.894	341
9/26/2020 9:00	15.6	2.056	70	5/19/2020 8:00	12.4	0.671	535
9/26/2020 10:00	15.7	1.609	235	5/19/2020 9:00	14.1	1.207	707
9/26/2020 11:00	16.3	1.743	281	5/19/2020 10:00	16.2	1.073	848
9/26/2020 12:00	16.1	0.849	146	5/19/2020 11:00	18.7	1.341	935
9/26/2020 13:00	16.6	0.894	213	5/19/2020 12:00	21.1	1.922	979
9/26/2020 14:00	17.7	1.654	586	5/19/2020 13:00	22.7	1.609	873
9/26/2020 15:00	17.4	1.699	331	5/19/2020 14:00	22.4	4.649	559
9/26/2020 16:00	17.3	1.431	189	5/19/2020 15:00	20.9	5.186	350
9/26/2020 17:00	16.4	0.939	53	5/19/2020 16:00	19.4	4.917	237

9/26/2020 18:00	15.2	0.76	8	5/19/2020 17:00	17.7	5.588	258
9/26/2020 19:00	14.5	0.76	0	5/19/2020 18:00	16.3	4.336	135
9/26/2020 20:00	13.3	0.313	0	5/19/2020 19:00	13.7	2.638	20
9/26/2020 21:00	12	0.402	0	5/19/2020 20:00	12.4	1.431	0
9/26/2020 22:00	10.3	0.492	0	5/19/2020 21:00	11.6	1.296	0
9/26/2020 23:00	9.2	0.626	0	5/19/2020 22:00	11.1	0.581	0
9/27/2020 0:00	9	0.805	0	5/19/2020 23:00	11.1	0.671	0
9/27/2020 1:00	7.9	0.849	0	5/20/2020 0:00	10.9	0.715	0
9/27/2020 2:00	7.4	0.447	0	5/20/2020 1:00	10.6	1.296	0
9/27/2020 3:00	7.2	0.76	0	5/20/2020 2:00	8.8	1.386	0
9/27/2020 4:00	6.6	0.715	0	5/20/2020 3:00	6.9	0.313	0
9/27/2020 5:00	5.6	0.492	0	5/20/2020 4:00	6.1	0.492	0
9/27/2020 6:00	5.2	0.626	6	5/20/2020 5:00	6.1	0.492	11
9/27/2020 7:00	5.4	0.492	72	5/20/2020 6:00	7.3	0.536	145
9/27/2020 8:00	8.9	0.313	322	5/20/2020 7:00	11.2	2.325	334
9/27/2020 9:00	11.3	1.341	507	5/20/2020 8:00	12.6	3.621	548
9/27/2020 10:00	12.2	1.386	653	5/20/2020 9:00	12.1	3.666	346
9/27/2020 11:00	13.5	1.699	744	5/20/2020 10:00	10.8	3.666	202
9/27/2020 12:00	14.9	2.638	769	5/20/2020 11:00	11.6	4.157	771
9/27/2020 13:00	15.9	2.772	755	5/20/2020 12:00	10.8	4.157	262
9/27/2020 14:00	16.5	2.906	668	5/20/2020 13:00	11.8	4.157	529
9/27/2020 15:00	16.8	2.593	546	5/20/2020 14:00	9.9	3.219	104
9/27/2020 16:00	16.9	1.967	372	5/20/2020 15:00	9.6	1.654	268

9/27/2020 17:00	16.4	2.056	167	5/20/2020 16:00	10.4	1.922	248
9/27/2020 18:00	14.6	1.609	25	5/20/2020 17:00	8.1	3.04	100
9/27/2020 19:00	11.6	0.313	0	5/20/2020 18:00	8.3	1.341	125
9/27/2020 20:00	10.3	0.536	0	5/20/2020 19:00	8.2	0.447	15
9/27/2020 21:00	10.1	0.671	0	5/20/2020 20:00	7.3	2.235	0
9/27/2020 22:00	8.4	0.626	0	5/20/2020 21:00	6.9	1.967	0
9/27/2020 23:00	6.9	0.715	0	5/20/2020 22:00	7.7	2.414	0
9/28/2020 0:00	6.2	0.581	0	5/20/2020 23:00	6.4	0.671	0
9/28/2020 1:00	5.6	0.536	0	5/21/2020 0:00	6.2	0.849	0
9/28/2020 2:00	4.4	0.626	0	5/21/2020 1:00	6.9	3.576	0
9/28/2020 3:00	4	0.402	0	5/21/2020 2:00	7.2	3.219	0
9/28/2020 4:00	3.7	0.671	0	5/21/2020 3:00	7	2.503	0
9/28/2020 5:00	2.9	0.447	0	5/21/2020 4:00	7.5	1.565	0
9/28/2020 6:00	2.6	0.447	7	5/21/2020 5:00	7.9	1.699	10
9/28/2020 7:00	3.3	0.402	72	5/21/2020 6:00	7.6	0.402	48
9/28/2020 8:00	5.9	0.983	317	5/21/2020 7:00	7.8	0.447	75
9/28/2020 9:00	8.3	1.118	505	5/21/2020 8:00	9.4	0.805	436
9/28/2020 16:00	18	0.849	350	5/21/2020 9:00	10.4	1.028	413
9/28/2020 17:00	17.8	0.715	159	5/21/2020 10:00	11.4	1.341	738
9/28/2020 18:00	14.9	0.671	18	5/21/2020 11:00	13.1	1.922	826
9/28/2020 19:00	13.3	1.296	0	5/21/2020 12:00	14.2	2.503	910
9/28/2020 20:00	12.7	1.386	0	5/21/2020 13:00	14.8	3.532	986
9/28/2020 21:00	10.9	0.626	0	5/21/2020 14:00	15.3	3.71	742

9/28/2020 22:00	9.4	0.715	0	5/21/2020 15:00	16.1	3.621	737
9/28/2020 23:00	8.4	0.402	0	5/21/2020 16:00	16.9	3.576	534
9/29/2020 0:00	7.3	0.671	0	5/21/2020 17:00	17.3	3.353	359
9/29/2020 1:00	6.9	0.492	0	5/21/2020 18:00	17.4	2.369	233
9/29/2020 2:00	5.5	0.447	0	5/21/2020 19:00	16.3	0.983	55
9/29/2020 3:00	5.3	0.894	0	5/21/2020 20:00	13.8	1.341	1
9/29/2020 4:00	4.8	0.581	0	5/21/2020 21:00	12.9	0.671	0
9/29/2020 5:00	3.9	0.492	0	5/21/2020 22:00	11.3	0.76	0
9/29/2020 6:00	3.4	0.268	4	5/21/2020 23:00	10.6	0.983	0
9/29/2020 7:00	3.6	0.358	61	5/22/2020 0:00	8.9	0.76	0
9/29/2020 8:00	7.3	0.492	321	5/22/2020 1:00	8.6	1.431	0
9/29/2020 9:00	9.7	0.805	504	5/22/2020 2:00	7.8	2.325	0
9/29/2020 10:00	12.2	0.894	653	5/22/2020 3:00	7.3	2.325	0
9/29/2020 11:00	14.9	0.983	748	5/22/2020 4:00	6.8	1.967	0
9/29/2020 12:00	17.4	0.983	782	5/22/2020 5:00	7.2	2.325	11
9/29/2020 13:00	19.1	0.805	756	5/22/2020 6:00	7.7	2.056	76
9/29/2020 14:00	20.4	0.894	668	5/22/2020 7:00	8.2	0.715	150
9/29/2020 15:00	21.6	0.76	532	5/22/2020 8:00	8.9	1.162	268
9/29/2020 16:00	22.1	0.715	351	5/22/2020 9:00	10.1	0.939	320
9/29/2020 17:00	21.8	0.313	160	5/22/2020 10:00	11.4	1.296	446
9/29/2020 18:00	17.7	0.805	17	5/22/2020 11:00	12.4	0.849	544
9/29/2020 19:00	16.8	1.028	0	5/22/2020 12:00	15.5	1.52	607
9/29/2020 20:00	14.6	0.626	0	5/22/2020 13:00	16.2	3.353	310

9/29/2020 21:00	13.5	1.118	0	5/22/2020 14:00	15.9	2.638	326
9/29/2020 22:00	12.2	0.671	0	5/22/2020 15:00	14.8	3.353	399
9/29/2020 23:00	10.1	0.76	0	5/22/2020 16:00	11.4	4.605	181
9/30/2020 0:00	9.7	0.626	0	5/22/2020 17:00	8.8	3.308	70
9/30/2020 1:00	8.3	0.671	0	5/22/2020 18:00	7.3	2.772	23
9/30/2020 2:00	7.3	0.402	0	5/22/2020 19:00	6.1	2.146	7
9/30/2020 3:00	6.6	0.626	0	5/22/2020 20:00	5.3	1.922	0
9/30/2020 4:00	5.9	0.447	0	5/22/2020 21:00	4.7	1.654	0
9/30/2020 5:00	5.4	0.492	0	5/22/2020 22:00	4.4	0.402	0
9/30/2020 6:00	4.9	0.492	4	5/22/2020 23:00	4.5	0.089	0
9/30/2020 7:00	4.9	0.313	59	5/23/2020 0:00	4.9	0.76	0
9/30/2020 8:00	8.8	0.536	314	5/23/2020 1:00	4.6	1.609	0
9/30/2020 9:00	11	1.028	496	5/23/2020 2:00	2.1	2.325	0
9/30/2020 10:00	13.7	1.162	645	5/23/2020 3:00	0.3	0	0
9/30/2020 11:00	16.4	0.849	739	5/23/2020 4:00	0.7	0	0
9/30/2020 12:00	19.2	0.626	774	5/23/2020 5:00	1.3	0	10
9/30/2020 13:00	21.6	0.805	750	5/23/2020 6:00	1.9	0.268	66
9/30/2020 14:00	23	0.894	663	5/23/2020 7:00	2.7	0.849	194
9/30/2020 15:00	23.8	0.983	517	5/23/2020 8:00	4.4	0.894	441
9/30/2020 16:00	24.2	0.715	335	5/23/2020 9:00	5.7	0.939	362
9/30/2020 17:00	23.2	0.179	129	5/23/2020 10:00	5.7	0.849	127
9/30/2020 18:00	19.2	1.028	12	5/23/2020 11:00	5.6	1.296	129
9/30/2020 19:00	17.2	1.028	0	5/23/2020 12:00	5.9	2.28	126

9/30/2020 20:00	16.4	1.073	0	5/23/2020 13:00	6.4	0.894	169
9/30/2020 21:00	14.4	0.939	0	5/23/2020 14:00	6.6	0.671	197
9/30/2020 22:00	12.6	0.939	0	5/23/2020 15:00	7.4	0.715	292
9/30/2020 23:00	12.2	1.073	0	5/23/2020 16:00	8.1	0.983	411
10/1/2020 0:00	10.9	0.76	0	5/23/2020 17:00	9	1.296	438
10/1/2020 1:00	9.9	0.671	0	5/23/2020 18:00	9.3	0.76	229
10/1/2020 2:00	9.1	0.805	0	5/23/2020 19:00	8.7	0.715	62
10/1/2020 3:00	8.1	0.715	0	5/23/2020 20:00	6.4	1.386	1
10/1/2020 4:00	6.9	0.849	0	5/23/2020 21:00	5.7	1.565	0
10/1/2020 5:00	6.5	0.894	0	5/23/2020 22:00	4.6	0.849	0
10/1/2020 6:00	5.8	0.76	4	5/23/2020 23:00	4.2	1.296	0
10/1/2020 7:00	5.9	0.402	59	5/24/2020 0:00	3.2	0.402	0
10/1/2020 8:00	9.6	0.268	304	5/24/2020 1:00	3.5	0.313	0
10/1/2020 9:00	12.1	0.983	484	5/24/2020 2:00	4	0.313	0
10/1/2020 10:00	14.5	0.671	631	5/24/2020 3:00	4	0.402	0
10/1/2020 11:00	17.1	0.671	712	5/24/2020 4:00	4.1	0.179	0
10/1/2020 12:00	19.6	0.402	756	5/24/2020 5:00	4.4	0.179	4
10/1/2020 13:00	21.9	0.671	715	5/24/2020 6:00	5	1.073	146
10/1/2020 14:00	23.4	0.581	638	5/24/2020 7:00	6.3	0.715	239
10/1/2020 15:00	24.6	0.581	489	5/24/2020 8:00	7.6	0.849	535
10/1/2020 16:00	24.7	0.402	286	5/24/2020 9:00	9.3	1.252	602
10/1/2020 17:00	22.3	0.134	116	5/24/2020 10:00	10.4	1.699	809
10/1/2020 18:00	18.9	1.073	8	5/24/2020 11:00	11.6	1.922	983

10/1/2020 19:00	17.7	1.162	0	5/24/2020 12:00	13.2	2.012	1073
10/1/2020 20:00	16.3	1.475	0	5/24/2020 13:00	13.6	2.548	873
10/1/2020 21:00	14.9	1.207	0	5/24/2020 14:00	13.7	2.772	661
10/1/2020 22:00	13.6	0.671	0	5/24/2020 15:00	14.1	2.101	481
10/1/2020 23:00	12.8	0.492	0	5/24/2020 16:00	14.5	2.235	562
10/2/2020 0:00	10.9	0.536	0	5/24/2020 17:00	14.4	1.341	318
10/2/2020 1:00	9.8	0.671	0	5/24/2020 18:00	14.3	1.833	203
10/2/2020 2:00	9.1	0.581	0	5/24/2020 19:00	13.1	0.983	72
10/2/2020 3:00	8.7	0.626	0	5/24/2020 20:00	10.8	0.983	2
10/2/2020 4:00	7.9	0.626	0	5/24/2020 21:00	9.6	1.252	0
10/2/2020 5:00	6.7	0.313	0	5/24/2020 22:00	8.3	0.939	0
10/2/2020 6:00	6.7	0.536	3	5/24/2020 23:00	7.9	0.715	0
10/2/2020 7:00	7.4	0.536	63	5/25/2020 0:00	6.7	0.626	0
10/2/2020 8:00	8.4	0.492	166	5/25/2020 1:00	5.6	0.447	0
10/2/2020 9:00	10.4	0.715	267	5/25/2020 2:00	4.7	0.447	0
10/2/2020 10:00	12.4	0.671	344	5/25/2020 3:00	4.2	0.358	0
10/2/2020 11:00	14.5	0.671	631	5/25/2020 4:00	3.6	0.581	0
10/2/2020 12:00	17.1	0.671	712	5/25/2020 5:00	3.1	0.492	12
10/2/2020 13:00	19.6	0.402	756	5/25/2020 6:00	4.2	0.492	147
10/2/2020 14:00	21.9	0.671	715	5/25/2020 7:00	6.6	0.849	354
10/2/2020 15:00	23.4	0.581	638	5/25/2020 8:00	9.1	1.073	541
10/2/2020 16:00	24.6	0.581	489	5/25/2020 9:00	11.1	1.028	721

λ -Cyhalothrin Field Dissipation Trial 2				λ -Cyhalothrin Field Dissipation Trial 3			
Date, Time	Air Temp. (°C)	Wind Speed (m/s)	Solar Intensity (W*m ⁻²)	Date, Time	Air Temp. (°C)	Wind Speed (m/s)	Solar Intensity (W*m ⁻²)
5/25/2021 10:00	19.69	3.487	787.8	5/25/2021 20:00	15.74	0.424	3.265
5/25/2021 11:00	20.87	3.299	892	5/25/2021 21:00	11.9	0.697	0.114
5/25/2021 12:00	21.61	2.99	953	5/25/2021 22:00	10.42	0.368	0.085
5/25/2021 13:00	22.19	3.014	923	5/25/2021 23:00	9.37	0.216	0.031
5/25/2021 14:00	22.89	2.652	846	5/26/2021 0:00	9.68	0.683	0.015
5/25/2021 15:00	23.34	2.127	737.1	5/26/2021 1:00	10.3	1.094	0.014
5/25/2021 16:00	23.84	1.638	623.1	5/26/2021 2:00	9.74	0.494	0.031
5/25/2021 17:00	24.04	1.271	429.5	5/26/2021 3:00	9.67	0.762	0.014
5/25/2021 18:00	23.92	0.9	261.1	5/26/2021 4:00	9.31	0.88	0.025
5/25/2021 19:00	20.83	0.824	69.13	5/26/2021 5:00	9.19	0.99	18.27
5/25/2021 20:00	15.74	0.424	3.265	5/26/2021 6:00	10.45	1.681	84.7
5/25/2021 21:00	11.9	0.697	0.114	5/26/2021 7:00	11.52	2.912	153.6
5/25/2021 22:00	10.42	0.368	0.085	5/26/2021 8:00	13.56	3.172	281.2
5/25/2021 23:00	9.37	0.216	0.031	5/26/2021 9:00	16.15	3.716	532.4
5/26/2021 0:00	9.68	0.683	0.015	5/26/2021 10:00	17.22	4.163	477.2
5/26/2021 1:00	10.3	1.094	0.014	5/26/2021 11:00	20.32	4.378	832
5/26/2021 2:00	9.74	0.494	0.031	5/26/2021 12:00	22.75	6.434	645.1
5/26/2021 3:00	9.67	0.762	0.014	5/26/2021 13:00	22.22	5.576	284.5
5/26/2021 4:00	9.31	0.88	0.025	5/26/2021 14:00	22.43	3.437	375.9
5/26/2021 5:00	9.19	0.99	18.27	5/26/2021 15:00	23.67	2.881	475.7

5/26/2021 6:00	10.45	1.681	84.7	5/26/2021 16:00	25.19	3.732	483.3
5/26/2021 7:00	11.52	2.912	153.6	5/26/2021 17:00	25.76	4.108	376.6
5/26/2021 8:00	13.56	3.172	281.2	5/26/2021 18:00	23	5.285	142.9
5/26/2021 9:00	16.15	3.716	532.4	5/26/2021 19:00	18.64	4.354	45.67
5/26/2021 10:00	17.22	4.163	477.2	5/26/2021 20:00	16.58	1.611	4.789
5/26/2021 11:00	20.32	4.378	832	5/26/2021 21:00	13.57	1.613	0.081
5/26/2021 12:00	22.75	6.434	645.1	5/26/2021 22:00	11.62	2.197	0.116
5/26/2021 13:00	22.22	5.576	284.5	5/26/2021 23:00	10.6	2.152	0.105
5/26/2021 14:00	22.43	3.437	375.9	5/27/2021 0:00	9.82	1.48	0.078
5/26/2021 15:00	23.67	2.881	475.7	5/27/2021 1:00	8.01	0.564	0.038
5/26/2021 16:00	25.19	3.732	483.3	5/27/2021 2:00	5.665	0.509	0.037
5/26/2021 17:00	25.76	4.108	376.6	5/27/2021 3:00	5.184	0.505	0.113
5/26/2021 18:00	23	5.285	142.9	5/27/2021 4:00	4.87	1.122	0.102
5/26/2021 19:00	18.64	4.354	45.67	5/27/2021 5:00	4.944	0.686	12.91
5/26/2021 20:00	16.58	1.611	4.789	5/27/2021 6:00	7.032	1.643	122.1
5/26/2021 21:00	13.57	1.613	0.081	5/27/2021 7:00	9.32	2.218	281.9
5/26/2021 22:00	11.62	2.197	0.116	5/27/2021 8:00	11.57	2.671	473.4
5/26/2021 23:00	10.6	2.152	0.105	5/27/2021 9:00	13.84	2.717	650.8
5/27/2021 0:00	9.82	1.48	0.078	5/27/2021 10:00	15.55	3.376	810
5/27/2021 1:00	8.01	0.564	0.038	5/27/2021 11:00	16.72	3.535	896
5/27/2021 2:00	5.665	0.509	0.037	5/27/2021 12:00	17.85	3.563	773.8
5/27/2021 3:00	5.184	0.505	0.113	5/27/2021 13:00	19.46	3.35	957
5/27/2021 4:00	4.87	1.122	0.102	5/27/2021 14:00	20.73	3.735	874

5/27/2021 5:00	4.944	0.686	12.91	5/27/2021 15:00	21.41	2.782	725.8
5/27/2021 6:00	7.032	1.643	122.1	5/27/2021 16:00	21.1	2.64	497.4
5/27/2021 7:00	9.32	2.218	281.9	5/27/2021 17:00	20.62	3.349	445.7
5/27/2021 8:00	11.57	2.671	473.4	5/27/2021 18:00	17.63	4.792	261.1
5/27/2021 9:00	13.84	2.717	650.8	5/27/2021 19:00	13.95	4.567	94.1
5/27/2021 10:00	15.55	3.376	810	5/27/2021 20:00	10.03	2.452	4.044
5/27/2021 11:00	16.72	3.535	896	5/27/2021 21:00	7.959	2.004	0.056
5/27/2021 12:00	17.85	3.563	773.8	5/27/2021 22:00	6.41	1.459	0.061
5/27/2021 13:00	19.46	3.35	957	5/27/2021 23:00	5.186	0.165	0.09
5/27/2021 14:00	20.73	3.735	874	5/28/2021 0:00	4.655	0.377	0.112
5/27/2021 15:00	21.41	2.782	725.8	5/28/2021 1:00	5.414	0.251	0.115
5/27/2021 16:00	21.1	2.64	497.4	5/28/2021 2:00	5.923	1.61	0.121
5/27/2021 17:00	20.62	3.349	445.7	5/28/2021 3:00	6.589	1.957	0.022
5/27/2021 18:00	17.63	4.792	261.1	5/28/2021 4:00	6.928	3.381	0.05
5/27/2021 19:00	13.95	4.567	94.1	5/28/2021 5:00	6.878	3.026	4.902
5/27/2021 20:00	10.03	2.452	4.044	5/28/2021 6:00	7.24	3.254	49.42
5/27/2021 21:00	7.959	2.004	0.056	5/28/2021 7:00	7.954	3.347	166.3
5/27/2021 22:00	6.41	1.459	0.061	5/28/2021 8:00	9.34	3.277	344.7
5/27/2021 23:00	5.186	0.165	0.09	5/28/2021 9:00	11.14	2.972	604.1
5/28/2021 0:00	4.655	0.377	0.112	5/28/2021 10:00	13.76	2.14	766.7
5/28/2021 1:00	5.414	0.251	0.115	5/28/2021 11:00	16.24	1.925	887
5/28/2021 2:00	5.923	1.61	0.121	5/28/2021 12:00	18.76	1.752	939
5/28/2021 3:00	6.589	1.957	0.022	5/28/2021 13:00	21.38	2.027	869

5/28/2021 4:00	6.928	3.381	0.05	5/28/2021 14:00	23.32	2.278	747.6
5/28/2021 5:00	6.878	3.026	4.902	5/28/2021 15:00	24.61	3.077	756.9
5/28/2021 6:00	7.24	3.254	49.42	5/28/2021 16:00	24.17	3.17	447.9
5/28/2021 7:00	7.954	3.347	166.3	5/28/2021 17:00	23.94	3.035	299.8
5/28/2021 8:00	9.34	3.277	344.7	5/28/2021 18:00	23.95	3.547	259.1
5/28/2021 9:00	11.14	2.972	604.1	5/28/2021 19:00	21.58	2.639	27.61
5/28/2021 10:00	13.76	2.14	766.7	5/28/2021 20:00	19.51	3.205	2.611
5/28/2021 11:00	16.24	1.925	887	5/28/2021 21:00	17.98	3.179	0.058
5/28/2021 12:00	18.76	1.752	939	5/28/2021 22:00	15.92	2.397	0.016
5/28/2021 13:00	21.38	2.027	869	5/28/2021 23:00	14.15	1.953	0.046
5/28/2021 14:00	23.32	2.278	747.6	5/29/2021 0:00	13.05	2.306	0.114
5/28/2021 15:00	24.61	3.077	756.9	5/29/2021 1:00	12.91	2.687	0.113
5/28/2021 16:00	24.17	3.17	447.9	5/29/2021 2:00	12.14	2.767	0.115
5/28/2021 17:00	23.94	3.035	299.8	5/29/2021 3:00	10.72	2.03	0.099
5/28/2021 18:00	23.95	3.547	259.1	5/29/2021 4:00	10.14	1.335	0.054
5/28/2021 19:00	21.58	2.639	27.61	5/29/2021 5:00	10.78	1.361	1.64
5/28/2021 20:00	19.51	3.205	2.611	5/29/2021 6:00	11.38	1.374	27.62
5/28/2021 21:00	17.98	3.179	0.058	5/29/2021 7:00	12.45	2.228	132.8
5/28/2021 22:00	15.92	2.397	0.016	5/29/2021 8:00	13.52	3.437	260.1
5/28/2021 23:00	14.15	1.953	0.046	5/29/2021 9:00	15.34	2.941	466.2
5/29/2021 0:00	13.05	2.306	0.114	5/29/2021 10:00	16.22	2.675	605.5
5/29/2021 1:00	12.91	2.687	0.113	5/29/2021 11:00	17.84	1.992	892
5/29/2021 2:00	12.14	2.767	0.115	5/29/2021 12:00	19.4	2.29	837

5/29/2021 3:00	10.72	2.03	0.099	5/29/2021 13:00	20.57	2.792	719.1
5/29/2021 4:00	10.14	1.335	0.054	5/29/2021 14:00	20.67	2.948	547.6
5/29/2021 5:00	10.78	1.361	1.64	5/29/2021 15:00	21.17	2.438	471.9
5/29/2021 6:00	11.38	1.374	27.62	5/29/2021 16:00	21	2.758	413.2
5/29/2021 7:00	12.45	2.228	132.8	5/29/2021 17:00	19.46	4.178	211.2
5/29/2021 8:00	13.52	3.437	260.1	5/29/2021 18:00	14.24	4.3	56.24
5/29/2021 9:00	15.34	2.941	466.2	5/29/2021 19:00	13	1.834	49.76
5/29/2021 10:00	16.22	2.675	605.5	5/29/2021 20:00	13.12	1.264	2.838
5/29/2021 11:00	17.84	1.992	892	5/29/2021 21:00	12.56	0.472	0.108
5/29/2021 12:00	19.4	2.29	837	5/29/2021 22:00	12.88	1.435	0.114
5/29/2021 13:00	20.57	2.792	719.1	5/29/2021 23:00	12.74	0.966	0.114
5/29/2021 14:00	20.67	2.948	547.6	5/30/2021 0:00	12.72	0.573	0.109
5/29/2021 15:00	21.17	2.438	471.9	5/30/2021 1:00	12.74	1.69	0.111
5/29/2021 16:00	21	2.758	413.2	5/30/2021 2:00	12.31	2.225	0.113
5/29/2021 17:00	19.46	4.178	211.2	5/30/2021 3:00	11.94	2.684	0.112
5/29/2021 18:00	14.24	4.3	56.24	5/30/2021 4:00	11.34	2.758	0.1
5/29/2021 19:00	13	1.834	49.76	5/30/2021 5:00	9.16	3.947	2.321
5/29/2021 20:00	13.12	1.264	2.838	5/30/2021 6:00	8.93	2.955	7.576
5/29/2021 21:00	12.56	0.472	0.108	5/30/2021 7:00	8.78	1.602	14.77
5/29/2021 22:00	12.88	1.435	0.114	5/30/2021 8:00	8.93	0.271	62.7
5/29/2021 23:00	12.74	0.966	0.114	5/30/2021 9:00	9.65	0.782	172.2
5/30/2021 0:00	12.72	0.573	0.109	5/30/2021 10:00	10.98	0.805	366.2
5/30/2021 1:00	12.74	1.69	0.111	5/30/2021 11:00	12.7	0.534	590.5

5/30/2021 2:00	12.31	2.225	0.113	5/30/2021 12:00	14.47	0.873	745.2
5/30/2021 3:00	11.94	2.684	0.112	5/30/2021 13:00	15.08	1.393	532.1
5/30/2021 4:00	11.34	2.758	0.1	5/30/2021 14:00	15.98	1.946	846
5/30/2021 5:00	9.16	3.947	2.321	5/30/2021 15:00	16.78	1.884	670.1
5/30/2021 6:00	8.93	2.955	7.576	5/30/2021 16:00	16.59	2.777	370.2
5/30/2021 7:00	8.78	1.602	14.77	5/30/2021 17:00	15.79	2.799	149.6
5/30/2021 8:00	8.93	0.271	62.7	5/30/2021 18:00	15.59	2.577	143.4
5/30/2021 9:00	9.65	0.782	172.2	5/30/2021 19:00	14.57	1.689	38.22
5/30/2021 10:00	10.98	0.805	366.2	5/30/2021 20:00	12.87	1.706	4.509
5/30/2021 11:00	12.7	0.534	590.5	5/30/2021 21:00	11.52	1.19	0.109
5/30/2021 12:00	14.47	0.873	745.2	5/30/2021 22:00	9.61	0.14	0.043
5/30/2021 13:00	15.08	1.393	532.1	5/30/2021 23:00	8.31	0.054	0.02
5/30/2021 14:00	15.98	1.946	846	5/31/2021 0:00	6.942	0.124	0.119
5/30/2021 15:00	16.78	1.884	670.1	5/31/2021 1:00	6.419	0.054	0.114
5/30/2021 16:00	16.59	2.777	370.2	5/31/2021 2:00	5.18	0.002	0.11
5/30/2021 17:00	15.79	2.799	149.6	5/31/2021 3:00	5.287	0.55	0.099
5/30/2021 18:00	15.59	2.577	143.4	5/31/2021 4:00	4.183	0.045	0.119
5/30/2021 19:00	14.57	1.689	38.22	5/31/2021 5:00	3.92	0.031	13.09
5/30/2021 20:00	12.87	1.706	4.509	5/31/2021 6:00	6.087	0.201	135.5
5/30/2021 21:00	11.52	1.19	0.109	5/31/2021 7:00	9.31	0.349	303.3
5/30/2021 22:00	9.61	0.14	0.043	5/31/2021 8:00	12.94	0.551	480.2
5/30/2021 23:00	8.31	0.054	0.02	5/31/2021 9:00	15.41	3.247	648.5
5/31/2021 0:00	6.942	0.124	0.119	5/31/2021 10:00	16.77	3.592	712.1

5/31/2021 1:00	6.419	0.054	0.114	5/31/2021 11:00	17.9	3.77	768.9
5/31/2021 2:00	5.18	0.002	0.11	5/31/2021 12:00	18.64	3.584	809
5/31/2021 3:00	5.287	0.55	0.099	5/31/2021 13:00	19.43	3.368	941
5/31/2021 4:00	4.183	0.045	0.119	5/31/2021 14:00	20	3.411	883
5/31/2021 5:00	3.92	0.031	13.09	5/31/2021 15:00	20.42	2.982	769.7
5/31/2021 6:00	6.087	0.201	135.5	5/31/2021 16:00	20.61	3.353	624.1
5/31/2021 7:00	9.31	0.349	303.3	5/31/2021 17:00	20.55	3.407	453.6
5/31/2021 8:00	12.94	0.551	480.2	5/31/2021 18:00	19.81	3.268	273.8
5/31/2021 9:00	15.41	3.247	648.5	5/31/2021 19:00	17.84	2.402	101.7
5/31/2021 10:00	16.77	3.592	712.1	5/31/2021 20:00	13.78	2.052	4.006
5/31/2021 11:00	17.9	3.77	768.9	5/31/2021 21:00	11.76	1.979	0.106
5/31/2021 12:00	18.64	3.584	809	5/31/2021 22:00	11.07	2.213	0.088
5/31/2021 13:00	19.43	3.368	941	5/31/2021 23:00	10.18	1.079	0.054
5/31/2021 14:00	20	3.411	883	6/1/2021 0:00	8.89	0.775	0.033
5/31/2021 15:00	20.42	2.982	769.7	6/1/2021 1:00	7.744	0.551	0.023
5/31/2021 16:00	20.61	3.353	624.1	6/1/2021 2:00	7.667	1.335	0.009
5/31/2021 17:00	20.55	3.407	453.6	6/1/2021 3:00	7.507	1.066	0.003
5/31/2021 18:00	19.81	3.268	273.8	6/1/2021 4:00	7.77	1.296	0.029
5/31/2021 19:00	17.84	2.402	101.7	6/1/2021 5:00	8.22	1.077	2.03
5/31/2021 20:00	13.78	2.052	4.006	6/1/2021 6:00	9.1	1.511	11.68
5/31/2021 21:00	11.76	1.979	0.106	6/1/2021 7:00	10.96	2.323	215.1
5/31/2021 22:00	11.07	2.213	0.088	6/1/2021 8:00	12.96	2.053	425.3
5/31/2021 23:00	10.18	1.079	0.054	6/1/2021 9:00	15.12	1.626	549.7

6/1/2021 0:00	8.89	0.775	0.033	6/1/2021 10:00	18.28	1.227	778.4
6/1/2021 1:00	7.744	0.551	0.023	6/1/2021 11:00	20.53	1.207	774.3
6/1/2021 2:00	7.667	1.335	0.009	6/1/2021 12:00	21.66	1.809	614.7
6/1/2021 3:00	7.507	1.066	0.003	6/1/2021 13:00	22.97	2.99	742.5
6/1/2021 4:00	7.77	1.296	0.029	6/1/2021 14:00	23.96	3.525	830
6/1/2021 5:00	8.22	1.077	2.03				
6/1/2021 6:00	9.1	1.511	11.68				
6/1/2021 7:00	10.96	2.323	215.1				
6/1/2021 8:00	12.96	2.053	425.3				
6/1/2021 9:00	15.12	1.626	549.7				
6/1/2021 10:00	18.28	1.227	778.4				
6/1/2021 11:00	20.53	1.207	774.3				
6/1/2021 12:00	21.66	1.809	614.7				
6/1/2021 13:00	22.97	2.99	742.5				
6/1/2021 14:00	23.96	3.525	830				

Curriculum Vitae

Ashlie D. Kinross

Department of Chemistry and Biochemistry

ashliepender@gmail.com

(435) 310-1041

Education

Utah State University

2017- 2022 PhD Candidate in Analytical Chemistry and Research/Teaching Assistant. Department of Chemistry and Biochemistry. Projects focus on evaluating extraction methods for pesticides from leaves and gaining a better understanding of how pesticides move through an agricultural field after application and related the predicted pesticide fate to pollinator exposure risk assessment. Degree expected to be completed by May 2022.
Supervisor: Kimberly Hageman

Southern Utah University

2017 Bachelor of Science, Chemistry. Southern Utah University, Utah. Participated in undergraduate research that investigated the novel formation of copper nanoparticles.
Undergraduate Research Supervisor: Chris Monson

Teaching

- Instructor of record for General Chemistry Lab I and II (CHEM 1215 and CHEM 1225), Summer 2021.
- Teaching Assistant for Instrumental Analysis lab (CHEM 5650), Spring 2021.
- Teaching Assistant for General Chemistry II lab (CHEM 1225), Spring 2021.
- Supervising Teaching Assistant for General and Organic Chemistry labs, Spring 2019-Spring 2021 semesters. In this role I supervised teaching assistants and answered questions and assisted them if any accidents occurred in the labs.
- Teaching Assistant for Quantitative Analysis lab (CHEM 3005), Fall 2020 semester.
- Teaching Assistant for Organic Chemistry I lab (CHEM 2315), Fall 2019 semester.
- Guest Lecturer for two class periods of Instrumental Analysis (CHEM 5640), Spring 2019.
- Teaching Assistant for General Chemistry I lab (CHEM 1215), Fall 2017-Spring 2018 and Spring 2020 semesters.
- Undergraduate Teaching Assistant for General Chemistry lab and class (CHEM 1210/1215), Spring 2017 semester.

Publications

- Kinross, A., Hageman, K. J., Doucette, W., and Foster, A. (2020). "Comparison of Accelerated Solvent Extraction (ASE) and Energized Dispersive Guided Extraction (EDGE) for the analysis of pesticides in leaves," *Journal of Chromatography A* 1627.

- Kinross, A., and Hageman, K. J. (2019). “Air Analysis: Sampling,” In Worsford, P., Townsend, A., Poole, C., Miró, M. (Eds), *Encyclopedia of Analytical Science*, 3rd Edition, Amsterdam, Netherlands: Elsevier.
- Rao, Y., Qian, Y., Deng, G.-H., Kinross, A., Turro, N.J., and Eisenthal, K.B. (2019). “Molecular rotation in 3 dimensions at an air/water interface using femtosecond time resolved sum frequency generation,” *Journal of Chemical Physics* 150, 094709.
- Ding, S., Kinross, A., Wang, X., Yang, H., Zhang, Q., Liu, W., and Sun, D. (2018). “Experiment and density functional theory analyses of GdTaO₄ single crystal,” *Solid State Communications* 273, 5-10.

Manuscripts in Progress

- Kinross, A., Hageman, K. J., Luu, C. (manuscript submitted 2021). “Understanding the effects of temperature and relative humidity on insecticide plant-air partitioning and foliar penetration.”
- Kinross, A., Hageman, K. J. “Predicting bee exposure using the Alfalfa Insecticide Management (AIM) toolkit.”
- Heath, S. M., Hageman, K. J., Kinross, A. “Development of a method to extract pesticides from several bee species.”

Presentations

- 2021 “Combining insecticide fate modeling and insect toxicity thresholds for improved pesticide management” Ashlie D. Kinross, Kimberly J. Hageman, Sean M. Lyons at Fall American Chemical Society (ACS) 2021 Meeting.
- 2021 “Development of the Pesticide Dissipation from Agricultural Land (PeDAL) Model for Improved Pollinator and Beneficial Insect Risk Assessment” Kimberly J. Hageman, Sean M. Lyons, Ashlie D. Kinross at the Society of Environmental Toxicology and Chemistry (SETAC) Europe Annual Meeting.
- 2020 “Plant-Air Partitioning of Semivolatile Pesticides on Citrus and Alfalfa Leaves with Varied Temperature and Relative Humidity” Calvin Luu, Ashlie D. Kinross, Kimberly J. Hageman at the Utah State University’s Student Research Symposium.
- 2019 “Pesticide Extraction from Leaves: Comparing Accelerated Solvent Extraction (ASE) and Energized Dispersive Guided Extraction (EDGE)” Ashlie D. Kinross, Kimberly J. Hageman, William J. Doucette, and Alexandria L. Foster at the SETAC North America Annual Meeting.
- 2017 “Copper Nanoparticle Synthesis from Bulk Copper Metal” Ashlie Pender, Emily Pehrson, at the Utah Conference of Undergraduate Research.
- 2016 “Copper Nanoparticle Synthesis from Bulk Copper Metal” Ashlie Pender, Emily Pehrson, at Southern Utah University’s College of Science and Engineering Research Symposium.

Scholarships and Awards

- 2021 USU Graduate Student Travel Award: presented by USU Graduate School used to help fund attendance at the Fall ACS conference

- 2020 Marjorie H. Gardner Teaching Award: presented by USU Department of Chemistry and Biochemistry to an outstanding teaching assistant
- 2019 SETAC Student Travel Award: presented by SETAC to help fund attendance at the SETAC North America Annual Meeting
- 2019 USU Graduate Student Travel Award: presented by USU Graduate School used to help fund attendance at the SETAC North America Annual Meeting
- 2016 Skaggs Research Foundation Grant: presented by SUU College of Science to fund undergraduate research projects
- 2012 President's Scholarship: an academic scholarship presented by SUU to incoming students to cover tuition
- 2012 New Century Scholarship: presented by Utah System of Higher education to students who completed an associate degree while in high school

Service

- 2020-2021 Serving on the Mental Health Committee for Department of Chemistry and Biochemistry. The Mental Health Committee made surveys for graduate students to assess the mental health of the department. It also planned activities to help graduate students stay connected with each other.
- 2019-2021 Serving on the Joint Safety Committee for Department of Chemistry and Biochemistry. The Joint Safety Committee visited the research labs in the department to ensure all safety protocols were being followed.
- 2020 Volunteered at the Utah Conference on Undergraduate Research (UCUR)
- 2017 Student Group Supervisor for You Be the Chemist (Chemical Education Foundation sponsored, grades 5-8 competition)
- 2016 Student Group Supervisor for The Chemical Olympics (ACS-sponsored high school competition)